

AD-A124 696

IMPROVED SIGNAL CONTROL: AN ANALYSIS OF THE EFFECTS OF
AUTOMATIC GAIN CON..(U) AIR FORCE INST OF TECH

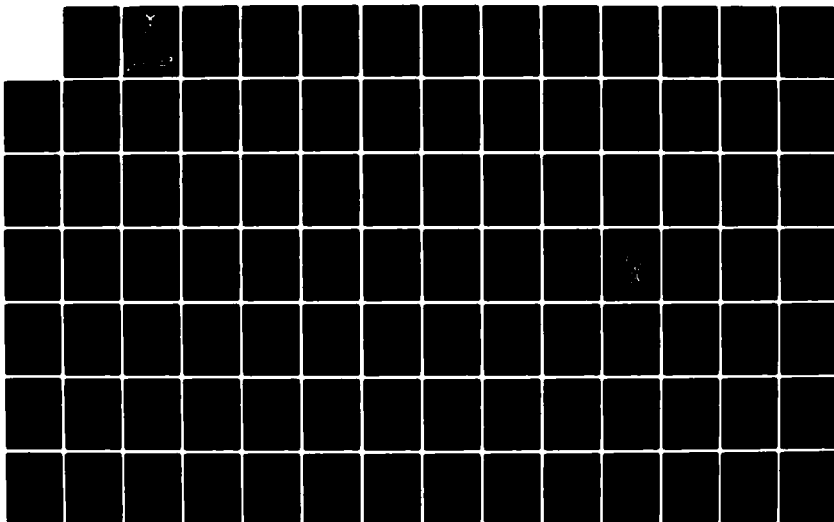
1/2

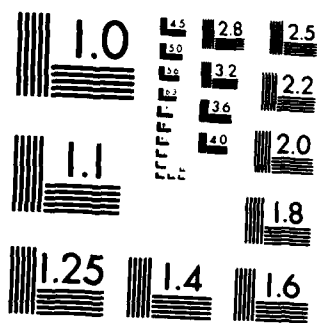
WRIGHT-PATTERSON AFB OH SCHOOL OF ENGI... K L FISHER

UNCLASSIFIED DEC 82 AFIT/GEO/EE/82D-3

F/G 17/2

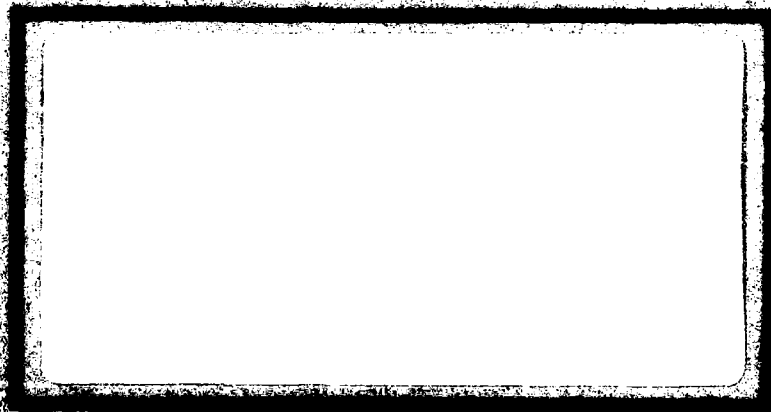
NL





MICROCOPY RESOLUTION TEST CHART
NATIONAL BUREAU OF STANDARDS-1963-A

ADA 124696



THIS DOCUMENT HAS BEEN APPROVED
FOR RELEASE AND SALE TO
THE PUBLIC BY THE AIR FORCE

RESEARCH AND DEVELOPMENT COMMAND
WASHINGTON, D.C.

DTIC
ELECTE
FEB 22 1962

S D

INSTITUTE OF TECHNOLOGY

AFIT/GEO/EE/82D-3

IMPROVED SIGNAL CONTROL: AN
ANALYSIS OF THE EFFECTS OF
AUTOMATIC GAIN CONTROL FOR OPTICAL
SIGNAL DETECTION

THESIS

AFIT/GEO/EE/82D-3

Kirk L. Fisher
Lt USAF

DTIC
ELECTE
FEB 22 1983
A

Approved for public release; distribution unlimited

AFIT/GEO/EE/82D-3

IMPROVED SIGNAL CONTROL: AN ANALYSIS OF THE EFFECTS
OF AUTOMATIC GAIN CONTROL FOR OPTICAL SIGNAL DETECTION

THESIS

Presented to the Faculty of the School of Engineering
of the Air Force Institute of Technology

Air University

in Partial Fulfillment of the
Requirements for the Degree of
Master of Science

by

Kirk L. Fisher, B.S.

Lt USAF

Graduate Electro-optics

December 1982

RECEIVED
12 17 82
GEOGRAPHIC
SUBSISTENCE
By
Distribution
Availability
Date



Approved for public release; distribution unlimited.

Preface

Currently, research is being conducted by the Air Force Wright Aeronautical Laboratories to replace copper wire data links on board aircraft with an optical fiber system. The optical fibers are to be used to transmit information from sensors, which are placed throughout the aircraft, to a central receiver. Because of the attenuation in the cable and the optical to electrical conversion process, the signal incurs variations causing the detection accuracy to decrease. This report is to analyze the effects of adding an automatic gain control (AGC) circuit to provide amplification of the signal and control to the signal variations.

I would like to thank my advisor, LtCol R. J. Carpinella, of the Air Force Institute of Technology, for his guidance towards the completion of this study. I would also like to express my gratitude to my fellow classmates, family, and my fiancée, Lynette Pray, for their support and inspiration throughout the extent of this study. And finally, I wish to acknowledge my thanks to my typist, Mrs Ruth Walker.

Kirk L. Fisher

Contents

	<u>Page</u>
Preface	ii
List of Figures	v
List of Tables	vii
List of Symbols	viii
Abstract	x
I. Introduction	1
Background	1
Problem	2
Scope	4
Assumptions	5
Approach and Presentation	5
II. Performance Parameters	7
Optimum Decision Criteria	7
Objective of Adding an AGC	12
III. Receiver Model	13
Photodetector Model	13
Ideal Photodetector	14
Non-Ideal Photodetector	16
AGC Model	17
VGA	18
GCP	19
Basic Configurations	19
Steady-State Analysis	21
IV. Computer Simulation	25
Photodetector Algorithm	25
Simulation of a Poisson Counting Process	25
Simulation of the Photodetector Output Voltage	27
AGC Algorithm	32
Simulation of the AGC	33
Steady-State Response Curve	34
Test Signal Response	35
Receiver Algorithm	37
V. Results	43
Receiver with an IAGC	43

Simulation Parameters	43
Analysis	45
Receiver with an AGC	56
Simulation Parameters	56
Analysis	57
Receiver with a Dual AGC	63
VI. Conclusions and Recommendations	72
Bibliography	71
Appendix A: Graphs of Various AGC Responses	72
Appendix B: Computer Program	85
Vita	93

List of Figures

Figure		Page
1	Received Optical Signal	3
2	Deterministic Binary Signal of the Photodetector	8
3	Photodetector Configuration	14
4	VGA	18
5	Single Loop AGC Configuration	20
6	Complex AGC Configurations	21
7	Single Loop AGC	22
8	Steady State Response Curve	24
9	Block Diagram of the Counting Process Algorithm	27
10	Simulation of the Poisson Counting Process . . .	28
11	Photodetector with Switch Impementation	29
12	Block Diagram of the AGC Algorithm	34
13	Simulated Steady State Response Curve	36
14	Steady-State Graphic Analysis of the Test Signal	38
15	AGC Input Test Signal	39
16	AGC Output with Test Signal Input	40
17	Input Optical Signal for a Receiver with an IAGC	45
18	Graphic Analysis of the IAGC Response	46
19	IAGC Input	49
20	IAGC Output	50
21	Improvement of the SNR by the IAGC	52
22	Worst Case Signal	54
23	Approximation to Describe Signal Fluctuations .	56

24	Graphic Analysis of the AGC Response	58
25	Input Optical Signal for a Receiver with an AGC	59
26	AGC Input	60
27	AGC Output	61
28	Dual AGC Output	64

List of Tables

<u>Table</u>		<u>Page</u>
1	Example of Photodetector Simulation Parameters for Various Data Rates	31
2	Estimate of the Probability of a Bit Error for an Initial Signal (binary one) Using an IAGC . . .	53
3	Estimate of the Probability of a Bit Error for the "Worst Case" Signal Using an IAGC	55
4	Estimate of the Probability of a Bit Error for the "Worst Case" Signal Using an AGC	62
5	Estimate of the Probability of a Bit Error for the "Worst Case" Signal Using a Dual AGC ($\lambda_s=10000$)	66
6	Estimate of the Probability of a bit Error for the "Worst Case" Signal Using a Dual AGC ($\lambda_s=5000$)	67

List of Symbols

A	-	effective area of the photodetector
A	-	constant gain amplification factor
b	-	bias voltage
B_N	-	bandwidth of counting process
C	-	capacitance
f_o	-	optical frequency
f_s	-	sampling frequency
G_o	-	AGC gain parameter
hf_o	-	energy per photon
q	-	charge of an electron
R	-	resistance
T_B	-	bit period
T_f	-	frame period
T_s	-	switching period
a	-	AGC control parameter
η	-	quantum efficiency of photon to electron conversions
λ_1	-	binary "one" given in terms of the rate of electron emissions
λ_0	-	binary "zero" given in terms of the rate of electron emissions
λ_D	-	constant rate of thermally emitted electrons
λ_S	-	constant rate of photon to electron conversions
λ_{SD}	-	$\lambda_S + \lambda_D$
$h(t)$	-	impulse response
$H(f)$	-	Fourier transform of $h(t)$

$U(\vec{r}, t)$ - spatial and time representation of optical signal

$P(t)$ - optical power

$p(t)$ - power density

$\lambda_p(t)$ - rate of photons striking the detector surface

$\lambda(t)$ - rate of electrons emitted from the detector

$N(t)$ - count process

\vec{k} - counting vector

$i(t)$ - photodetector output current

$x(t)$ - photodetector output voltage of AGC input voltage

$y(t)$ - AGC output voltage

$g(t)$ - AGC gain

$v_c(t)$ - AGC control voltage

$\delta(t)$ - unit delta function

$u(t)$ - unit step function

$\text{Pr}(\text{error})$ - probability of bit error

$\begin{matrix} D \\ \geq 1 \\ D \end{matrix}$ - decision criteria [Ref 6]

$\prod_{i=1}^N (x_i)$ - product of x_i terms

$*$ - indicates convolution

Abstract

-4
This paper is to analyze the effects of an automatic gain control (AGC) in an optical receiver system. The intent of using an AGC is to improve the performance of the receiver.

The received signal is Manchester encoded and contains fluctuations caused by transmission attenuation. In the conversion from an optical signal to an electrical signal, the photodetector produces shot noise. The purpose of the AGC will be to amplify the photodetector signal, control signal fluctuations, reduce shot noise, and improve detection accuracy.

Using this criteria, the effects of the AGC in the receiver was examined. But because of the non-linearities associated with an AGC, an analytical analysis can not be conducted. Therefore, the receiver was simulated on the computer. This paper describes the models and algorithms used to analyze the receiver. Through the simulations, the receiver's performance with an AGC is compared to the performance without an AGC.

Because of the limited time for the analysis, only three specific AGC's were examined. The first AGC studied is classified as an instantaneous AGC (IAGC) followed by an analysis of a common AGC. The final AGC to be investigated is a dual AGC which is an AGC cascaded to an IAGC.

IMPROVED SIGNAL CONTROL: AN ANALYSIS OF THE EFFECTS OF
AUTOMATIC GAIN CONTROL FOR OPTICAL SIGNAL DETECTION

I. Introduction

Background

In recent years the application of optical fibers in communication systems has increased significantly. Technological developments have enabled low loss optical fibers to replace copper wire communication links. Improvements were made in laser diodes and LED's to achieve higher optical power outputs. Because of the higher output powers and low loss cables, the distance between repeaters can be increased, thereby, reducing construction cost. Construction costs were also decreased and the construction simplified by improved techniques and hardware for the interfacing and the splicing of optical fibers. These are just a few of the advancements which have contributed to the feasibility of an optical fiber communication system and to its resultant growth.

The practicality of an optical fiber communication system explains the current growth and increased usage, but the inherent advantages of the system prompted the initial interest and research. The most important attribute is that more information can be transmitted through optical fibers than through copper wire. Currently, Gigabit data rates have been

obtained by using single mode fibers. Optical cables are also immune to electromagnetic radiation. No special shielding is required to protect them against high electric or magnetic fields. The fibers are lightweight and pose no hazard to fire or electrical shock. Because of these advantages and the technological developments, optical fibers have become a cost-effective replacement for copper wire; and optical fiber communication systems are being implemented in many new projects.

Problem

One such project is to implement an optical fiber data link on board an aircraft. The optical cables would carry information from several sensors to a central receiver. The sensors are placed at various positions throughout the aircraft. Each sensor will transmit a Manchester encoded optical signal via an optical fiber. Because the signals must travel different path lengths to reach the receiver, the attenuation losses will cause the optical power level to fluctuate between the signals. At the receiver several bits of information from each signal will be observed for one frame period (T_f). Thus, the received signal (see Figure 1) will be a Manchester encoded optical signal with fluctuations in the power level depending on which sensor is being observed.

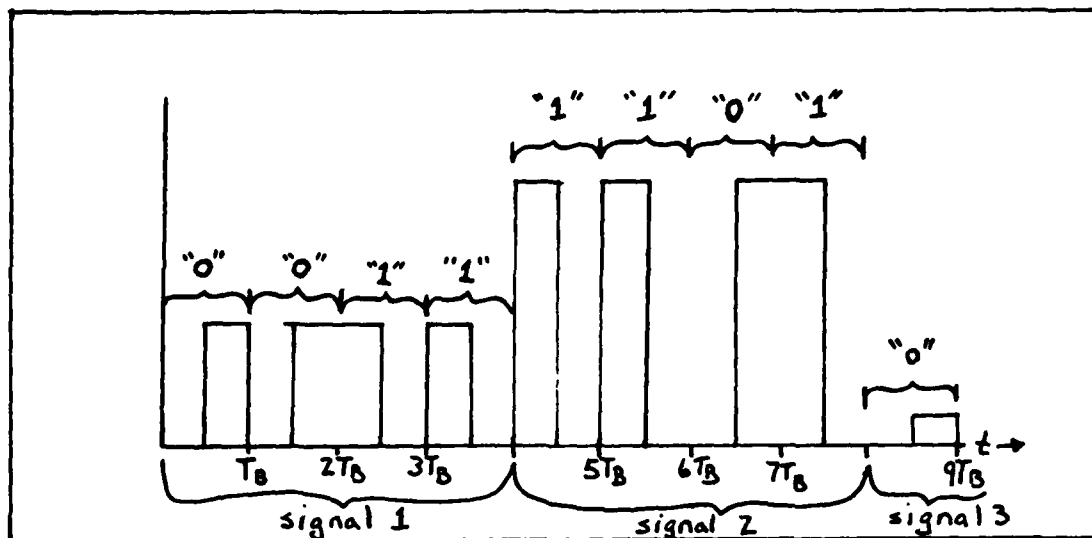


Figure 1. Received Optical Signal

The received optical signal is then converted into an electrical signal by a photodetector. Because of the fluctuations in the received signal, the detector's output signal will vary over a wide dynamic range. The photodetector signal will also incur variations caused by the dark current and shot noise which are inherent to the photodetectors. The shot noise is used to describe the randomness associated with the detector's generation of an electrical signal. The dark current is a product of thermally emitted electrons flowing from the detector. The dark current, shot noise and signal fluctuations complicate the process of reconstructing the information sent.

For the particular signal being studied, the information is digitally encoded and is extracted by a decision circuit. The decision circuitry determines whether a binary "one" or

"zero" was sent based on the photodetector's output. To increase the accuracy of the decision process, an automatic gain control (AGC) circuit will be placed in between the photodetector and the decision circuitry. The purpose of the AGC will be to amplify the detector signal and to automatically adjust its gain to reduce signal variations, thereby, hopefully improving the accuracy of the reconstruction.

In this paper a detailed analysis will be conducted on the receiver to investigate the effects of an AGC in an optical receiver. Because of the non-linearities associated with an AGC, an analytical analysis of the receiver becomes very complicated. Therefore, an empirical analysis will be conducted using a computer to simulate the receiver. Through the use of the computer, the effects of the AGC on the detector signal, the signal to noise ratio, and the probability of bit errors will be examined.

Scope

Because of the limited time to conduct an analysis, only three AGC's will be studied. The first AGC to be analyzed will be an instantaneous AGC (IAGC), followed by an analysis of a common AGC. Both AGC's employ a single loop feedback configuration to provide the gain control. They both also have a gain characteristic which is an exponential function of the control voltage. The final AGC to be studied will be a dual AGC, which is a cascaded combination of an IAGC and an

AGC.

The photodetector will be a non-amplifying photodiode, such as a p-n or a p-i-n diode. The effects of avalanche photodiodes will not be considered in this analysis.

Assumptions

The photodetector will be illuminated solely by the Manchester encoded optical signal. The detector will be completely enclosed to eliminate the effects from the background radiation. The received optical signal will be undistorted except for the attenuation caused by the transmission through the optical fiber. The signal is also assumed to be spatially coherent, so that the optical power can be written as

$$P(t) = \iint_A U(\vec{r}, t) d\vec{r} = p(t) A \quad (1)$$

where

$U(\vec{r}, t)$ = spatial and time representation of the signal power density

$p(t)$ = time varying power density

A = area of the detector

All noises will be neglected except for the shot noise and dark current. The timing of the electrical circuit will be exactly synchronized with the optical signal.

Approach and Presentation

Before any analysis of the receiver is conducted, the performance parameters of the receiver will be defined. Based on the photodetector output, an optimum decision rule is developed to minimize the probability of a bit error. The

effects that the AGC has on the probability of error and the signal fluctuations will be used to assess the AGC's performance. The objective of adding an AGC will be to amplify the detector output, eliminate the signal fluctuations and to decrease the probability of a bit error.

With these objectives in mind, the mathematical models are developed to describe the receiver. These models need to represent the physical devices as accurately as possible to obtain valid results. From the mathematical models computer algorithms will be developed. Some simple simulations of the photodetector and AGC will be conducted to test the validity of the computer programs.

Using these computer programs, the effects of the three specific AGC's on the photodetector signal will be analyzed. The AGC's response to the detector's output will be obtained by plotting the first and second order statistics of the AGCs' output. The effects of the AGC on the probability of error will also be examined. From this analysis conclusions can be drawn as to the effectiveness of an AGC in an optical receiver.

II. Performance Parameters

The purpose of a receiver is to reconstruct as accurately as possible the information which was transmitted. Unfortunately, the signal becomes distorted during the transmission and the reception. The distortion introduces error in the reconstruction of the information sent. For the digitally encoded signals, the information is transmitted in binary form. Each single piece of binary information sent is referred to as a bit and is represented by a "one" or "zero". Distortion of a digital signal causes incorrect decisions or bit errors to be made. In the following section the probability of a bit error is minimized through the development of an optimal decision rule.

In the last section of this chapter the objectives of adding an AGC will be discussed. These objectives will specify the parameters to assess the performance of the AGC's.

Optimum Decision Criteria

For the digital signals which are being analyzed, the binary information is determined by the position of the pulse. This type of digital encryption is called pulse position modulation (PPM). A binary "one" will be assigned to the optical pulses which occur during the first half of a bit period (T_B), and a binary "zero" to the pulses which occur in the

second half of the bit period.

At the receiver these optical pulses are converted into an electrical signal by a photodetector. The electrical signal, that is generated by the detector, is no longer a deterministic signal; but becomes a weighted Poisson counting process (will be proven in the next chapter). Because the signal is now a random process, errors will occur in the decision process. Fortunately, the rate of the counting process is proportional to the power density of the optical signal. Thus, the binary signals can be represented by the rates of the counting processes (see Figure 2). An optimum decision rule will be developed to extract this deterministic signal from the Poisson counting process, $N(t)$.

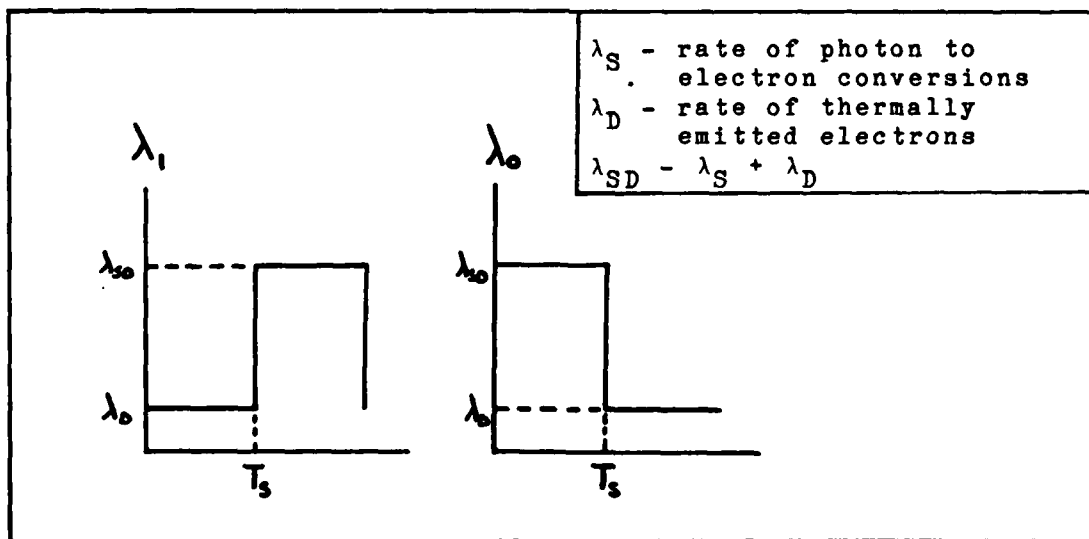


Figure 2. Deterministic Binary Signal of the Photodetector

To obtain a decision rule, the Poisson counting process is to be equivalently written in a vector form. This vec-

torization is accomplished by sampling the counting process, $N(t)$, at a rate defined by:

$$f_s \geq 2B_N \quad (2)$$

where

B_N = the bandwidth of the counting process

This sampling scheme produces a count vector given by:

$$\bar{k} = (k_1, k_2, \dots, k_J) \quad (3)$$

where

$$k_j = N(t_j) - N(t_{j-1}) \quad \text{for } j=1, 2, \dots, J$$

$$J = Tf_s$$

The probability of a count k_j occurring is defined by (Ref 3:205+):

$$\Pr(k_j/\lambda_{ij}) = [(\lambda_{ij}\Delta t)^{k_j} e^{-\lambda_{ij}\Delta t}] / k_j! \quad (4)$$

where

$$\Delta t = t_j - t_{j-1}$$

$$\lambda_{ij} = \text{rate of the } i^{\text{th}} \text{ signal during the interval } t_j - t_{j-1}$$

Since the probabilities of each sample count are independent, the probability of the count vector can be written as:

$$\Pr(\bar{k}/\lambda_i) = \prod_{j=1}^J [(\lambda_{ij}\Delta t)^{k_j} e^{-\lambda_{ij}\Delta t}] / k_j! \quad (5)$$

Based on these probabilities a decision rule can be developed.

The optimum decision rule for minimum probability of error can be derived from the maximum a posteriori (MAP) deci-

sion criteria. The MAP decision criteria is defined as:

$$\Lambda(r) = [P(\lambda_1/k)/P(\lambda_0/k)] \underset{D_0}{\overset{D_1}{\geq}} 1 \quad (6)$$

where

$\Lambda(r)$ = likelihood ratio

$P(\lambda_i/k)$ = probability that the rate is λ_i given the
observed vector \bar{k}

By applying Bayes rule, the MAP criteria can be equivalently written as:

$$\Lambda(r) = \frac{[Pr(\bar{k}/\lambda_1) Pr(\lambda_1)] / Pr(\bar{k})}{[Pr(\bar{k}/\lambda_0) Pr(\lambda_0)] / Pr(\bar{k})} \underset{D_0}{\overset{D_1}{\geq}} 1 \quad (7)$$

where

$Pr(\bar{k}/\lambda_i)$ = defined by eqn (5)

$Pr(\lambda_i)$ = priori probabilities of the given rate λ_i

$Pr(\bar{k})$ = probability of the vector \bar{k} occurring

Assuming equal priori probabilities and substituting eqn (5)

into eqn (7) produces:

$$\Lambda(r) = \frac{\prod_{j=1}^J [(\lambda_{0j} \Delta t)^{k_j} e^{-\lambda_{1j} \Delta t}] / k_j!}{\prod_{j=1}^J [(\lambda_{0j} \Delta t)^{k_j} e^{-\lambda_{0j} \Delta t}] / k_j!} \underset{D_0}{\overset{D_1}{\geq}} 1 \quad (8)$$

Since the logarithm is a monotonic increasing function, an equivalent MAP rule is:

$$\ln \Lambda(r) = \sum_{j=1}^J [k_j \ln \lambda_{1j} \Delta t - \lambda_{1j} \Delta t] - \sum_{j=1}^J [k_j \ln \lambda_{0j} \Delta t - \lambda_{0j} \Delta t] \underset{D_0}{\overset{D_1}{\geq}} 0 \quad (9)$$

By separating the summations and correctly defining the limits produces constant rates for each of the smaller summations. This causes eqn (9) to be rewritten as:

$$\sum_{j=1}^{J/2} [k_j \lambda_{SD} \Delta t - \lambda_{SD} \Delta t] + \sum_{j=J/2+1}^J [k_j \ln \lambda_D \Delta t - \lambda_D \Delta t] - \sum_{j=1}^{J/2} [k_j \lambda_D \Delta t + \lambda_D \Delta t] - \sum_{j=J/2+1}^J [k_j \ln \lambda_{SD} \Delta t - \lambda_{SD} \Delta t] \underset{D_0}{\overset{D_1}{\geq}} 0 \quad (10)$$

By rearranging the terms and simplifying, eqn (10) reduces to:

$$\sum_{j=1}^{J/2} k_j - \sum_{j=J/2+1}^J k_j \underset{D_0}{\overset{D_1}{\geq}} 0 \quad (11)$$

Thus, the optimum decision rule compares the count at the end of the first half of a bit period with the counts which occurred in the second half of the bit period. Writing this in terms of the actual counting process produces:

$$N(T/2) \underset{D_0}{\overset{D_1}{\geq}} N(T) - N(T/2) \quad (12)$$

The probability of error is given by:

$$\begin{aligned} \Pr(\text{error}) = & \Pr(N(T/2) > N(T) - N(T/2) / \lambda_0) P(\lambda_0) + \\ & 1/2 \Pr(N(T/2) = N(T) - N(T/2) / \lambda_0) P(\lambda_0) + \\ & \Pr(N(T) - N(T/2) > N(T/2) / \lambda_1) P(\lambda_1) + \\ & 1/2 \Pr(N(T) - N(T/2) = N(T/2) / \lambda_1) P(\lambda_1) \end{aligned} \quad (13)$$

Substituting in the Poisson probability densities eqn (13) becomes (Ref 3:220):

$$\Pr(\text{error}) = \sum_{i=0}^{\infty} \left[1 - \sum_{k=0}^i \left[(\lambda_D T/2)^k e^{-\lambda_D T/2} \right] / k! \right] \left[(\lambda_{SD} T/2)^i e^{-\lambda_S T/2} \right] / i! \quad (14)$$

According to the MAP decision criteria, the decision rule produces the minimum probability of error (Ref 6:42). The decision rule was developed assuming constant optical power densities of all the received pulses. But the decision rule that was derived was found to be independent of the rates. Since the rates are proportional to the optical power densities of the pulses, the decision rule will not be effected by signal fluctuations.

Objective of Adding an AGC

In the previous section an optimum decision rule was developed for the detector signal. An AGC is now added to the optical receiver. The purpose of the AGC will be to amplify the detector output, eliminate the signal fluctuations and minimize the probability of bit errors. These objectives will be the criteria from which the performance of the AGC's will be judged.

III. Receiver Model

In this chapter, the mathematical models of the receiver will be developed. These models will form the basis for the computer simulations and the analysis. Therefore, these models must accurately represent the actual physical devices. The model for the photodetector will be described in the first section of this chapter, and in the last section, models for the AGC will be presented.

Photodetector Model

The photodetector model must accurately describe optical to electrical conversion process. To accomplish this the photodetector will, at first, be described as an ideal photodetector and then as a non-ideal detector. The ideal photodetector will be defined as a detector in which electrical output is present only when the detector is being illuminated by an optical source. In reality, a small amount of electrical output will be present even when no optical power is applied; this will be considered in the non-ideal case.

For either model the detector will be followed by an RC filter (see Figure 3). R is the parallel equivalent of the internal resistance losses of the detector and an external resistor, and C is the parallel equivalent of the internal capacitance losses and an external capacitor. The detector

output current is $i(t)$ and $x(t)$ is the output voltage of the filter.

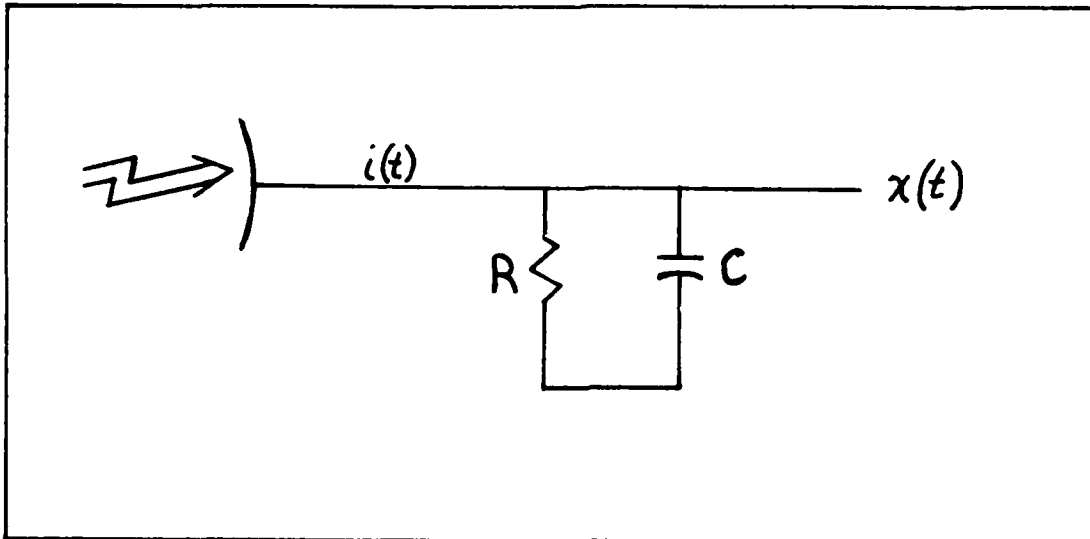


Figure 3. Photodetector Configuration

Ideal Photodetector. An ideal photodetector will produce an electrical output only when the detector is being illuminated by an optical source. The photons emitted by the source will strike the surface of the detector at a rate defined by:

$$\lambda_p(t) = p(t)A / hf_0 \quad (15)$$

where

$p(t)$ = irradiance or incident power density

A = effective area of the detector

hf_0 = energy of a photon

If a photon has sufficient energy, it will excite an electron on the surface of the detector into the conduction band. The excited electron will then be emitted out of the detector.

This process will loosely be defined as a photon to electron conversion.

As more photon to electron conversions occur, a detector output current can be described as:

$$i(t) = q \sum_{i=0}^I \delta(t-t_i) \quad (16)$$

where

q = charge of an electron

t_i = time at which a photon to electron conversion occurred

This current will flow through the filter to produce an output voltage, $x(t)$, defined by the convolution integral:

$$x(t) = \int_0^t i(\tau) h(t-\tau) d\tau \quad (17)$$

where

$h(t) = 1/C e^{-t/RC}$ = filter impulse response

or, equivalently:

$$x(t) = 1/C \int_0^t i(\tau) e^{-(t-\tau)/RC} d\tau \quad (18)$$

If the period of observation is much smaller than the RC time constant, an approximation can be made to eqn (18) which results in:

$$x(t) = 1/C \int_0^t i(\tau) d\tau \quad (19)$$

Substituting in eqn (16) for the current and integrating produces:

$$x(t) = q/C \sum_{i=0}^I u(t-t_i) = q/C N(t) \quad (20)$$

The output voltage is now modelled as a weighted counting process, counting the electrons emitted from the detector.

Because the event times (t_i 's) of these photon to electron conversions occur randomly, the counting process is Poisson distributed. The rate of occurrence of the photon to electron conversions is proportional to the rate of the photons striking the surface of the detector. This rate is defined as:

$$\lambda(t) = (\eta p(t)A) / hf_0 \quad (21)$$

where

η = quantum efficiency of the photon to electron conversions

Because the rate is time varying, the output current and voltage become inhomogeneous Poisson processes in which the statistics are known (Ref 8:432+) in terms of the rate $\lambda(t)$.

Non-ideal Photodetector. In this section the photodetector model will be expanded to take into account the dark current, which is present whether or not the detector is being illuminated. The dark current is a result of thermally excited electrons reaching the conduction band. Therefore, like the ideal model, the dark current is represented by:

$$i_d(t) = q \sum_{j=0}^J \delta(t-t_j) \quad (22)$$

where

t_j = time at which a thermally excited electron enters the conduction band

The event times (t_j 's) also occur randomly with a constant rate of occurrence λ_D (assuming no significant temperature variations).

Including dark current into the model, the current output becomes:

$$i(t) = i_s(t) + i_d(t) \quad (23)$$

where

$$i_s(t) = \text{signal current}$$

$$i_d(t) = \text{dark current}$$

Substituting eqn (16) and eqn (22) into eqn (23) produces:

$$i(t) = q \left[\sum_{i=0}^I \delta(t-t_i) + \sum_{j=0}^J \delta(t-t_j) \right] \quad (24)$$

and integrating to get the output voltage:

$$x(t) = q/C \left[\sum_{i=0}^I u(t-t_i) + \sum_{j=0}^J u(t-t_j) \right] \quad (25)$$

Again the statistics are known in terms of the rates $\lambda(t)$ and λ_D .

The output voltage given by eqn (25) will be the mathematical model used to represent an actual photodetector output. And as long as the approximation RC is greater than the observation period, this model will accurately describe the photodetector.

AGC Model

In this section several AGC models will be briefly examined and a steady state response for a specific AGC will be analyzed. For an analysis of other AGC's the reader is refer-

red to Senior [Ref 9]. Much of the analysis on AGC's presented in this section follows the same approach developed by Senior.

An AGC consists of two major components:

- 1) Variable Gain Amplifier (VGA)
- 2) Gain Control Processor (GCP)

The two components will be examined separately in the following sections. Then the various configurations which can be derived from combinations of these two components will be examined briefly. In the last section a steady state analysis will be conducted for a specific AGC.

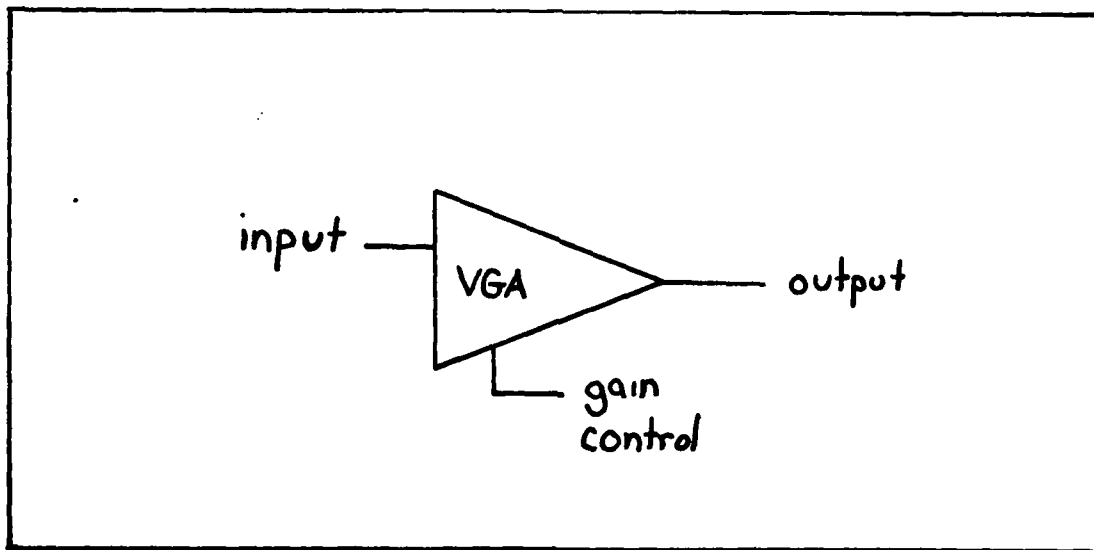


Figure 4. VGA

VGA. The VGA is a three port amplifier in which the extra port is used to control the gain of the amplifier (see Figure 4). The VGA is characterized by its gain to control voltage relationship. Virtually every VGA can be classified as either

a linear VGA where the gain is represented as a function of the $v_C(t)$ by:

$$g(t) = G_0 - v_C(t) \quad (26)$$

or an exponential VGA in which the gain is defined as:

$$g(t) = G_0 e^{-\alpha v_C(t)} \quad (27)$$

where

$$\alpha > 0$$

The discussion will be limited to these two VGA models. Other VGA's are generally designed to perform special functions and, therefore, will not be considered.

GCP. The GCP processes some portion of the signal to provide a control voltage, $v_C(t)$, to the VGA. To keep the analysis simple the GCP will be limited to the use of passive filters, constant gain amplifiers, and constant biasing. With this limitation the output control voltage, $v_{C0}(t)$, is easily defined as:

$$v_{C0}(t) = A v_{Ci}(t) * h(t) + b \quad (28)$$

where

$v_{Ci}(t)$ = input voltage

A = constant gain of amplifier

$h(t)$ = impulse response function of the passive filter

b = bias voltage

* = indicates convolution

Basic Configuration. By using various combinations of the two components (VGA and GCP), numerous AGC models can be

constructed. The simplest AGC models are classified as the single loop configurations (see Figure 5). It should be noted here that each configuration does not represent one AGC model. The configuration is used to classify a group of AGC models; the actual AGC model depends on the component characteristics.

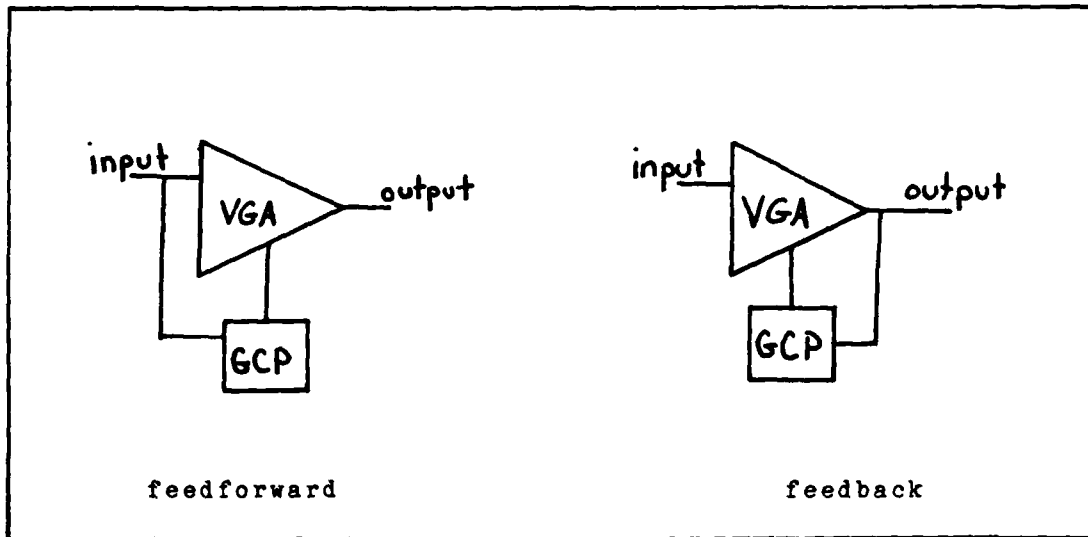


Figure 5. Single Loop AGC Configurations

The multi-loop configurations contain three or more combinations of the two AGC components. The multi-loop systems are divided into two sub-divisions:

- 1) Compound Systems
- 2) Complex Systems

A compound system is two or more single loop configurations cascaded together. A complex system includes everything which can not be classified as single loop or compound systems. Figure 6 shows two examples of complex systems.

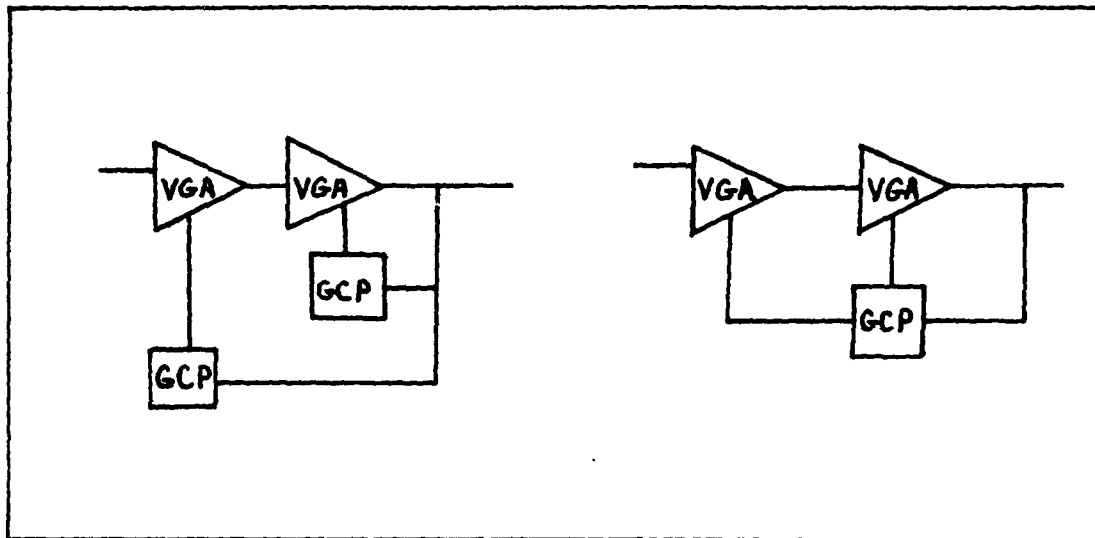


Figure 6. Complex AGC Configurations

Steady State Analysis. The steady state response curve is an important characteristic of an AGC. This curve can be used to predict an AGC's response to any input. Also, for single loop configurations, a steady-state analysis can be used to specify the AGC parameters. In this section a steady state analysis will be developed for a common AGC.

For the analysis the VGA will have an exponential gain characteristic and the GCP will be placed in a feedback configuration. The filter in the GCP will have an impulse response defined as $h(t)$. This particular system is chosen because it has a constant loop gain which provides greater stability (Ref 12). An AGC is considered stable when the output settles to a constant value after an abrupt change in the input (Ref 9:14).

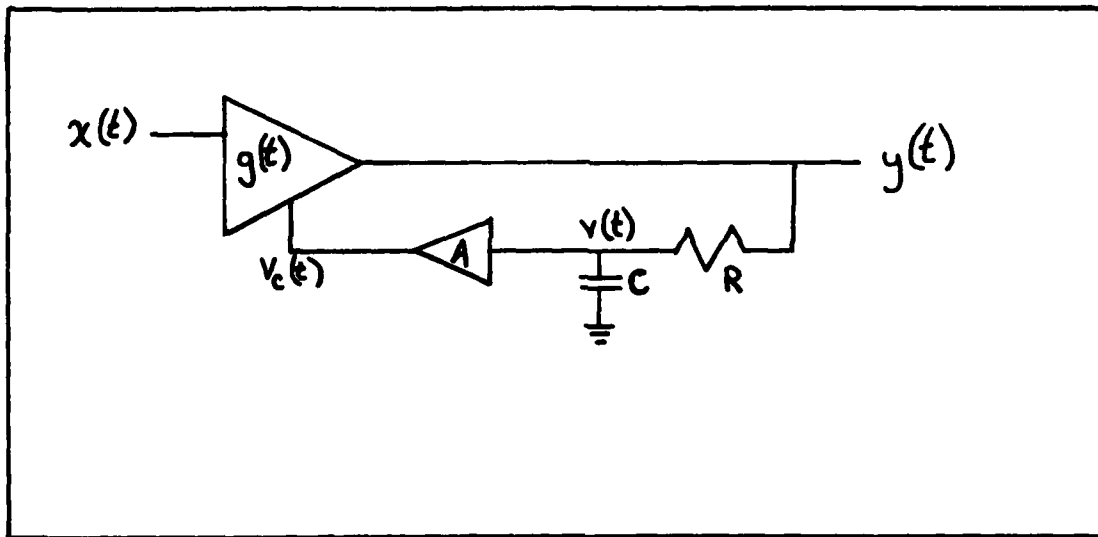


Figure 7. Single Loop AGC

Using this model (see Figure 7), a steady-state analysis of the AGC is conducted. The output of the AGC is described by:

$$y(t) = x(t) g(t) \quad (29)$$

Substituting in eqn (27) for the gain and $A v(t)$ for the control voltage produces:

$$y(t) = x(t) G_0 e^{-\alpha A v(t)} \quad (30)$$

Since the parameters A and α have the same effect on the output, the parameter α will be absorbed into the parameter A . Thus, the AGC output is given by:

$$y(t) = x(t) G_0 e^{-A v(t)} \quad (31)$$

where

$$v(t) = y(t) * h(t)$$

The steady state response is obtained by driving the AGC with a constant amplitude input, k_i . After the initial transients decay, a stable AGC will produce a constant amplitude output, k_o . For a constant output the filter response is defined as:

$$v(t) = k_o * h(t) \quad (32)$$

or, equivalently:

$$v(t) = k_o * H(0) \quad (33)$$

where

$$H(0) = \mathcal{F}\{h(t)\} \big|_{f=0}$$

Substituting in k_o for the output, k_i for the input, and $k_o H(0)$ for the control voltage, eqn (31) becomes:

$$k_o = k_i G_o e^{-Ak_o H(0)} \quad (34)$$

Eqn (34) is the steady-state response of the AGC and the response curve (see Figure 8) is obtained by plotting k_i versus k_o .

This steady-state response can serve as a useful tool to obtain the values of the AGC parameters G_o and A ; provided the input-output ranges are known. For the analysis, the input is assumed to vary between k_{i1} and k_{i2} . The output is to be limited to the range k_{o1} to k_{o2} (see Figure 8).

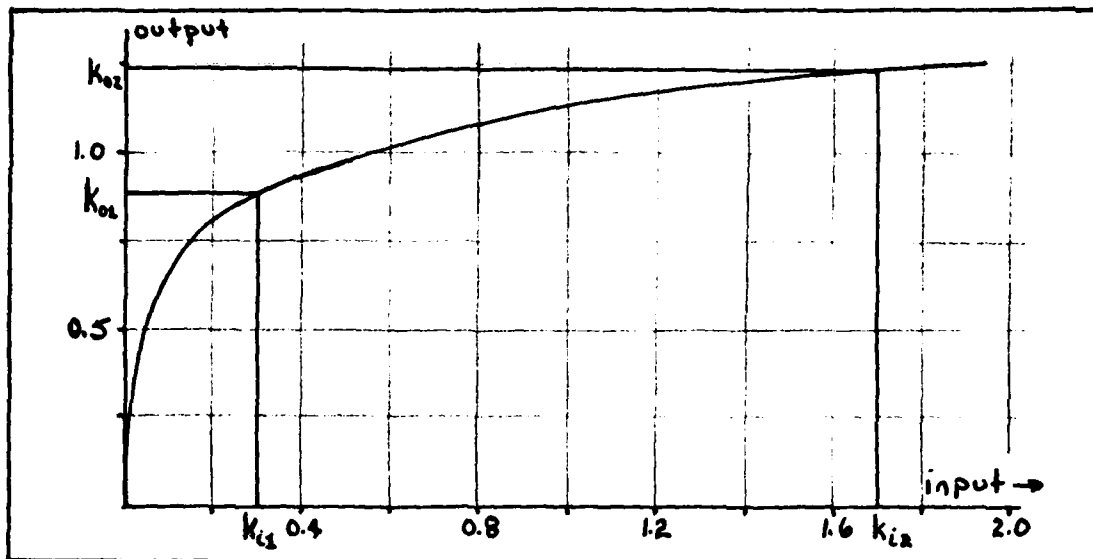


Figure 8. Steady-State Response Curve

Substituting each pair of points into eqn (34) results in:

$$k_{i1} = k_{o1} e^{AH(0)k_{o1} / G_o} \quad (35)$$

and

$$k_{i2} = k_{o2} e^{AH(0)k_{o2} / G_o} \quad (36)$$

Taking the ratio of the above equations and solving for A produces:

$$A = \ln[(k_{i2}/k_{i1}) (k_{o1}/k_{o2})] / [H(0) (k_{o2} - k_{o1})] \quad (37)$$

Once a value of A is determined, G_o can be obtained by using eqn (35) or eqn (36).

IV. Computer Simulation

Because of the non-linearities of the AGC, an accurate analytical analysis of the receiver would be very difficult and complex. Or, if approximations are made to simplify the analysis, the receiver would not be represented accurately. Therefore, an empirical analysis was conducted and the receiver simulated on the computer. This chapter describes the process used to develop a computer program to simulate the receiver.

Photodetector Algorithm

The photodetector models developed in the previous chapter easily conform to computer simulation. The first section will describe the algorithm used to simulate the counting process. The algorithm must then be modified to be able to be implemented practically and still be able to accurately represent the physical device. The last section deals with the approach used to accurately simulate the photodetector output voltage.

Simulation of a Poisson Counting Process. From the results of the previous chapter, the photodetector output voltage was mathematically modelled as a Poisson counting process. In this section an algorithm to simulate the counting process will be presented.

For a Poisson counting process, the events occur at random times. The time interval between two successive events are also random and independent of any previous time interval. To simulate the counting process, random numbers are generated by the computer to represent the random event times. Using a built-in program, random numbers which are uniformly distributed from 0 to 1 are generated. The uniform random numbers are then transformed into exponentially distributed random numbers by [Ref 10:62]:

$$\tau = -\ln(u) / \lambda \quad (38)$$

where

τ = exponentially distributed random variable

u = uniformly distributed random number (0,1)

λ = constant rate for the occurrence of events

The random number generated by eqn (38) is used to represent the length of the time interval between two successive events.

By using the above procedure to produce the random time intervals, a Poisson counting process is easily simulated. The time at which the events occur is defined by:

$$t_i = t_{i-1} + \tau_i \quad (39)$$

where t_i = arrival time of the i^{th} event

τ_i = i^{th} exponential distributed random variable

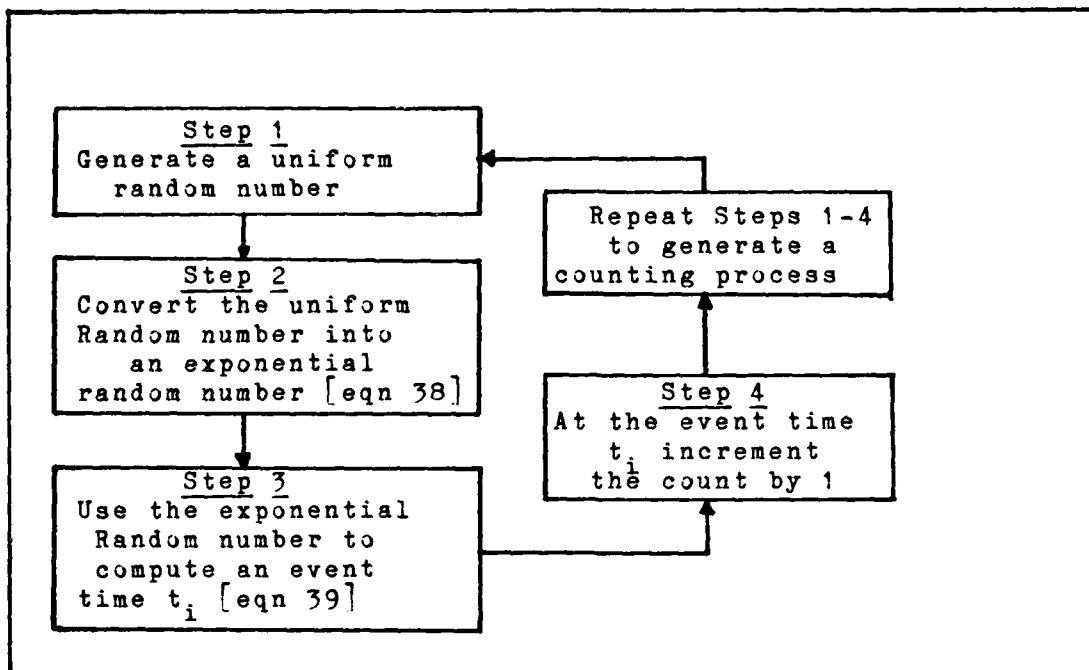


Figure 9. Block diagram of Counting Process Algorithm

The event times are continuously generated until the time exceeds a specified period of observation. The counting process is initialized to zero at the beginning of the observation period, and incremented by one at each time, t_i . A block diagram of the algorithm is shown in Figure 9 and an implementation of this algorithm for various rates is shown in Figure 10. This algorithm will be the basis for the simulation of the photodetector's output voltage.

Simulation of the Photodetector Output Voltage. The counting process algorithm is used to simulate the Poisson process, which mathematically models the detector's output voltage. This model, which was developed in the previous chapter, is defined by:

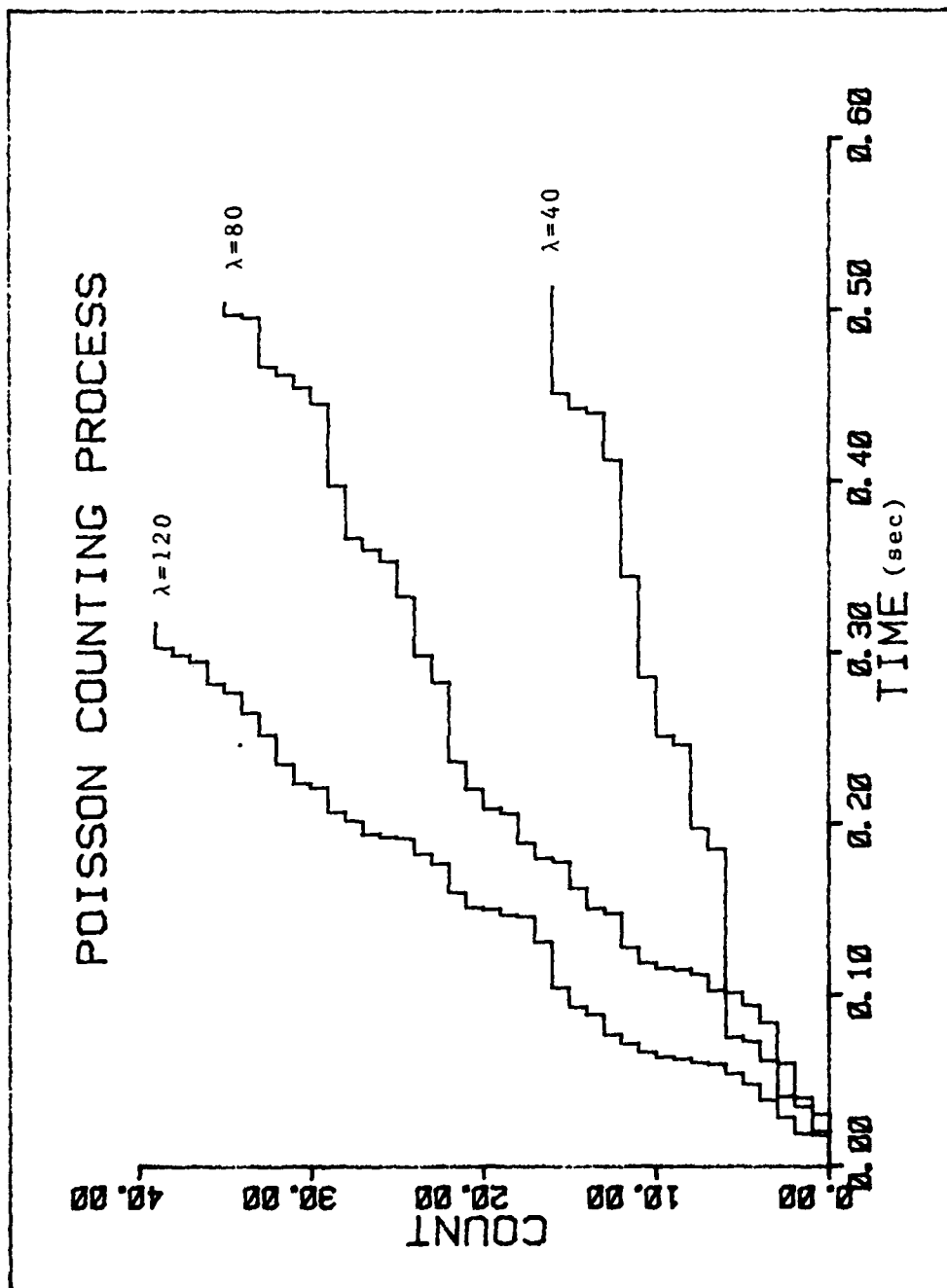


Figure 10. Simulation of the Poisson Counting Process

$$x(t) = q/C \left[\sum_{i=0}^I u(t-t_i) + \sum_{j=0}^J u(t-t_j) \right] \quad (25)$$

Each summation in eqn (25) represents a Poisson counting process. In order to conduct the simulation, both Poisson processes have to be homogeneous. The second summation in eqn (25) is considered to be a homogeneous process, but the first is inhomogeneous because of the time-varying optical signal. Fortunately, the particular optical signal being studied enables the first summation to be analyzed as a homogeneous process.

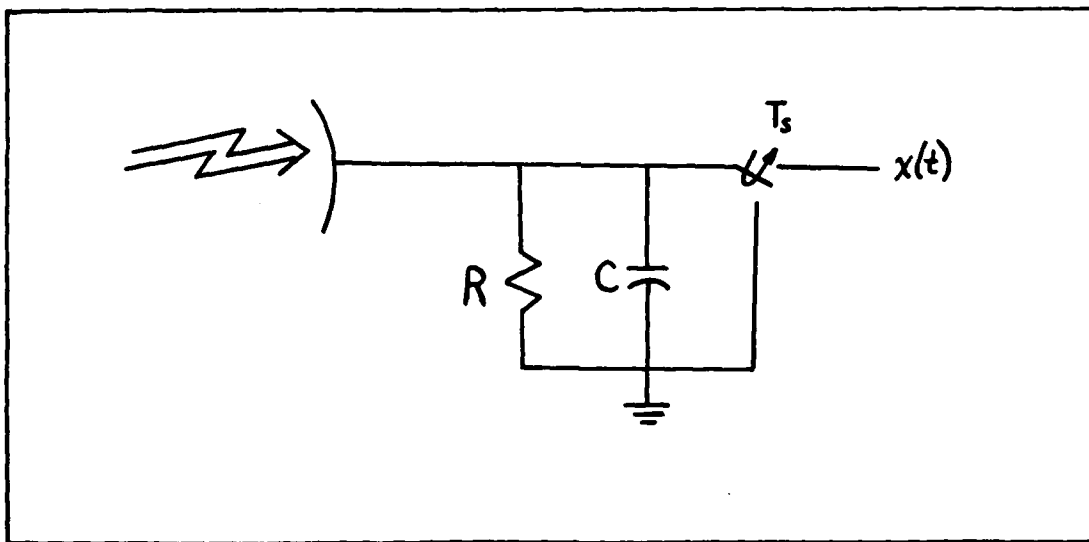


Figure 11. Photodetector with Switch Implementation

To analyze the inhomogeneous process as a homogeneous process, a switch is added to the photodetector model (see Figure 11). The clocking period (T_s) of the switch is half the bit period (T_b) of the Manchester coded optical signal. During the extent of the clock period, the output of the

detector will be observed. If the switch is synchronized with the optical signal, the power density of the received signal will remain constant during a switching period; and this will produce a homogeneous counting process at the output. At the end of a clock period the switch will temporarily short circuit the capacitor, thus, initializing a new counting process. Using this switching scheme, the output voltage is modelled as a periodic series of homogeneous Poisson processes.

To implement this model, the two counting processes are simulated by the program developed in the previous section. The two simulated processes are added and multiplied by q/C to produce the output voltage. The output is then sampled at regular time increments, Δt , so that the output will be easily integrated with the AGC simulation.

The parameters of the photodetector simulation are now specified to realistically represent the output of a physical detector. The parameter which has the most influence on an accurate simulation is the rate (λ) of the counting processes. For an accurate representation, the simulation rates are required to be the same as the actual rates of the electron emissions. For an ideal detector, the emission rates are given by:

$$\lambda = \eta P A / h f_0 \quad (21)$$

The time dependence was eliminated through the implementation of the switch. The optical power of sources generally ranges from 1 mw to 10 mw [Ref 5, Table 1] for infrared wavelengths.

Assuming all of the source's output power is detected, the rate is calculated to be an order of magnitude of $10^{15}/\text{sec}$. A rate of this magnitude is impracticable to implement directly.

A combination of two methods is used to increase the feasibility of the implementation. The first approach is a simple time scaling. Thus, the rate calculated above can be equivalently written as $10^9/\mu\text{sec}$ or $10^6/\text{nsec}$. This will not cause the simulation to misrepresent the detector because the signal, itself, is being observed in the scaled time units.

Table 1
Examples of Photodetector Simulation Parameters
for Various Data Rates

Data Rate	Switch Period	Max Elec Emission	Max Simula. Rate	M (e^-/cnt)	C	(q/C)M (V/count)	R (Ohms)
1 MBit	1 μsec	$10^9/\mu\text{sec}$	1000	10^6	10 μF	1.6×10^{-8}	1K
10 MBit	100nsec	$10^8/100\text{nsec}$	1000	10^5	2.0 μF	8.0×10^{-9}	1K
100 MBit	10nsec	$10^7/10\text{nsec}$	1000	10^4	2.0 μF	8.0×10^{-10}	10K
1 GBit	1nsec	$10^6/\text{nsec}$	1000	10^3	16nF	1.0×10^{-8}	1K
10 GBit	100psec	$10^5/100\text{psec}$	1000	10^2	50pF	3.2×10^{-7}	10K

The second method is to have one count represent M electrons emitted by the detector. The counting process is now weighted by the factor M and the factor q/C. Since q/C is very small in magnitude, the M can be easily "absorbed" into the factor q/c without a misrepresentation of the detector.

These two methods are applied to several different data rates (see Table 1). The data rate determines the clock period of the switch. The electron emission rate is then calculated using eqn (21) (source optical power = 2mw) and scaled to the same units of the clock period. A maximum rate for the counting process simulation is determined for a practical implementation. By dividing the actual electron emission rate with the simulation rate, the factor M is found. A capacitance is then chosen such that the factor $(q/C)M$ is a small quantity. With a known capacitance, the value of the resistor is chosen to produce a long RC time constant compared to the clock period (T_s). A long RC time constant is required to support the approximation that the detector can be represented as a Poisson counting process. By using the two approaches described above, a practical and accurate implementation of the photodetector can be conducted.

AGC Algorithm

In this section an algorithm for the AGC simulation will be presented. The algorithm to be developed represents the single loop feedback system which was analyzed in the previous chapter. Using this algorithm the simulated AGC will be driven with constant amplitude inputs to generate a steady-state response curve. This simulated curve is then compared with a theoretical curve to verify the algorithm. The validity of the simulation will also be tested using an amplitude modulated (AM) signal.

Simulation of the AGC. In the preceding chapter an analysis was conducted on a single loop feedback system. From the analysis an equation was developed to mathematically describe the AGC. This mathematical model of the AGC is:

$$y(t) = x(t) G_o e^{-Av(t)} \quad (31)$$

where

$$v(t) = y(t) * h(t)$$

For the simulation the GCP filter is specified to be a simple low pass filter. Thus, the control voltage is given by the convolution integral:

$$v(t) = 1/RC \int_0^t y(\tau) e^{-(t-\tau)/RC} d\tau \quad (40)$$

where

R = filter resistance

C = filter capacitance

Developed from simple circuit analysis, the differential equivalent of eqn (40) is:

$$C dv / dt = [y(t) - v(t)] / R \quad (41)$$

Both equations accurately represent the filter, but eqn (41) will be used to simulate the filter because of its simplicity.

Using numerical methods [Ref 4:189-190] eqn (41) is approximated by:

$$[v(t_{k+1}) - v(t_k)] / \Delta t = [y(t_k) - v(t_k)] / RC \quad (42)$$

or, equivalently:

$$v(t_{k+1}) = y(t_k)(\Delta t/RC) + v(t_k)(1 + \Delta t/RC) \quad (43)$$

where

$t_k = k^{\text{th}}$ sample time

$\Delta t = t_{k+1} - t_k$

Sampling eqn (32) at the same rate produces:

$$y(t_k) = x(t_k) G_o e^{-Av(t_k)} \quad (44)$$

Using these equations, the AGC is easily simulated on the computer. A block diagram of the algorithm is shown in Figure 12.

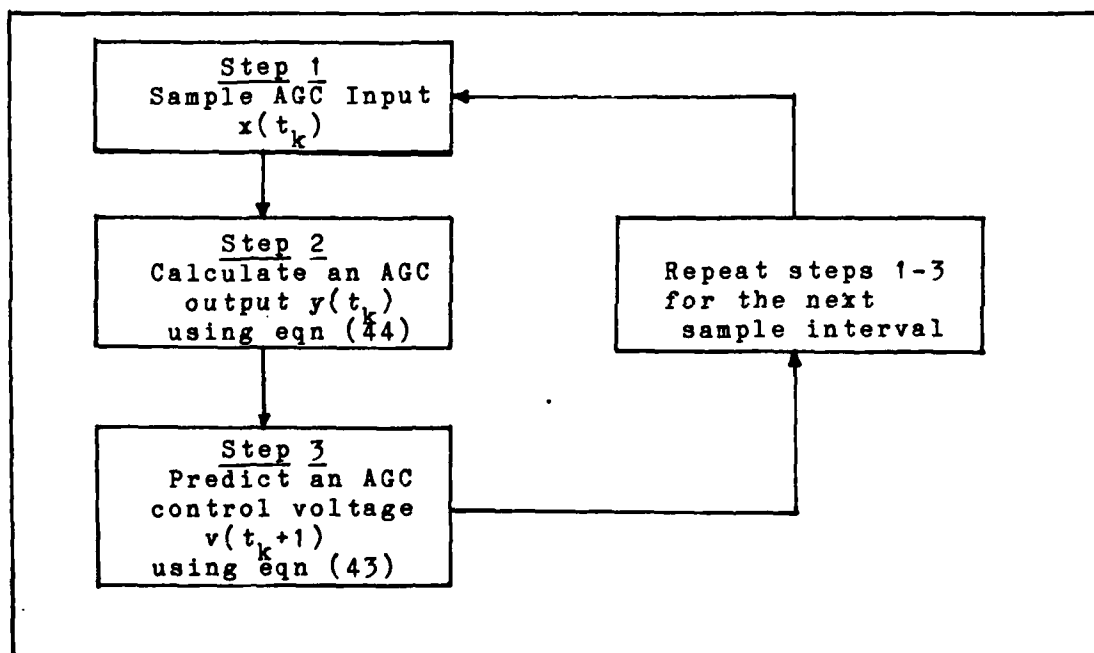


Figure 12. Block Diagram of the AGC Algorithm

Steady-State Response Curve. As mentioned earlier an important characteristic of an AGC is its steady-state response. To generate a response curve, the simulated AGC is driven with constant amplitude inputs. By plotting the AGC response (after transients decay) to these various inputs produces a simulated steady-state response curve (see Figure

13). This is the exact result which would be obtained theoretically for the same AGC parameters.

Test Signal Response. A test signal is used as input to the AGC to verify the accuracy of the simulation. This test signal is an amplitude modulated sine wave defined by:

$$x(t) = (1 + a \sin 2\pi f_L t)(\sin 2\pi f_H t) \quad (45)$$

where

f_H = carrier frequency

f_L = modulation frequency

a = modulation index

The AGC will be designed to reduce the amplitude variations caused by the modulation frequency and to pass the carrier frequency unaffected.

Since the AGC is to reduce amplitude modulations, the GCP must track the envelope of the signal. The GCP will consist of a full wave rectifier and a low pass filter for envelope detection. For the filter to pass only the envelope signal, the RC time constant is required to be within the range [Ref 13:97]:

$$1/f_H \ll R_1 C_1 \ll 1/f_L \quad (46)$$

Since the carrier frequency is not affected by the AGC, an approximate analysis can be conducted by working with the envelopes and neglecting the carrier frequency. The most accurate approximate method [Ref 9:67] is to use the steady-state response curve as shown in Figure 14. The shape of the

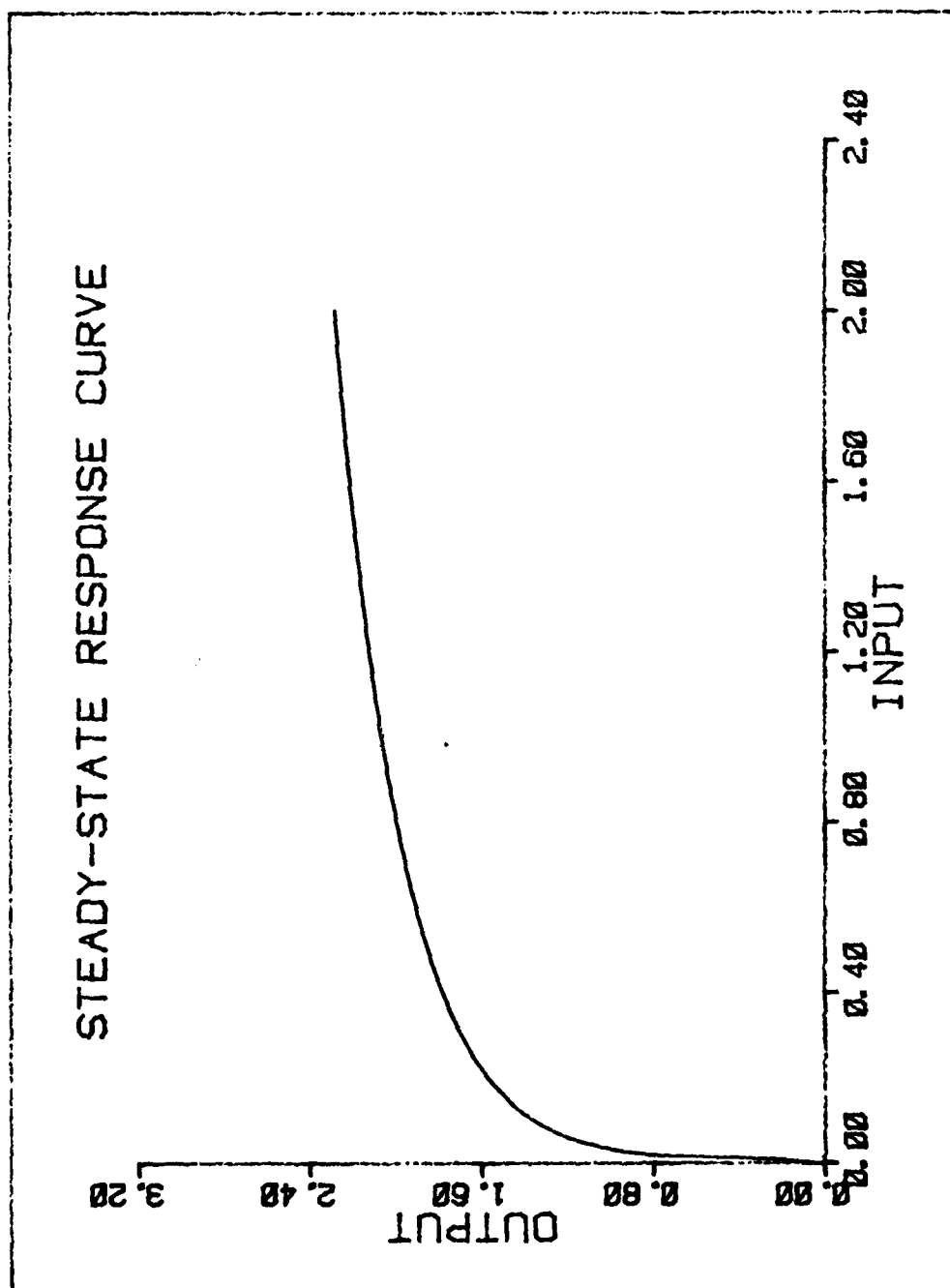


Figure 13. Simulated Steady-State Response Curve
($A=4.0$ and $G=100$)

response curve is determined by the AGC parameters (A and G_o).

The AGC parameters to produce a specific response curve can be computed using eqn's (36) and (37). These equations require knowledge of the range over which the input and output signals vary. The AGC input signal (the test signal) varies between 0.5 volts and 1.5 volts (for a modulation index $a = 0.5$). The AGC output signal will be restricted to the range - 0.9 to 1.1 volts. With these values the AGC parameters A and G_o are calculated to be 4.5 and 100, respectively.

The AGC now can be simulated for comparison with the graphical analysis. The input to the AGC is defined by eqn (45) with $a = 0.5$, $f_L = 0.1/\text{sec}$ and $f_H = 10/\text{sec}$ (see Figure 15). The RC time constant of the low pass filter is 1 sec. The AGC parameters are $A = 6.2$ and $G_o = 100$. The A was increased to take into account a voltage drop across the filter. The AGC output voltage as a result of the simulation is shown in Figure 16.

Receiver Algorithm

The receiver algorithm is simply the integration of the photodetector and the AGC algorithms. With this algorithm the receiver's response to an optical input can be simulated. In this section a method will be developed to compute the parameters to evaluate the performance of the optical receiver.

To analyze the effects of the AGC, the receiver is more appropriately described by the first and second order

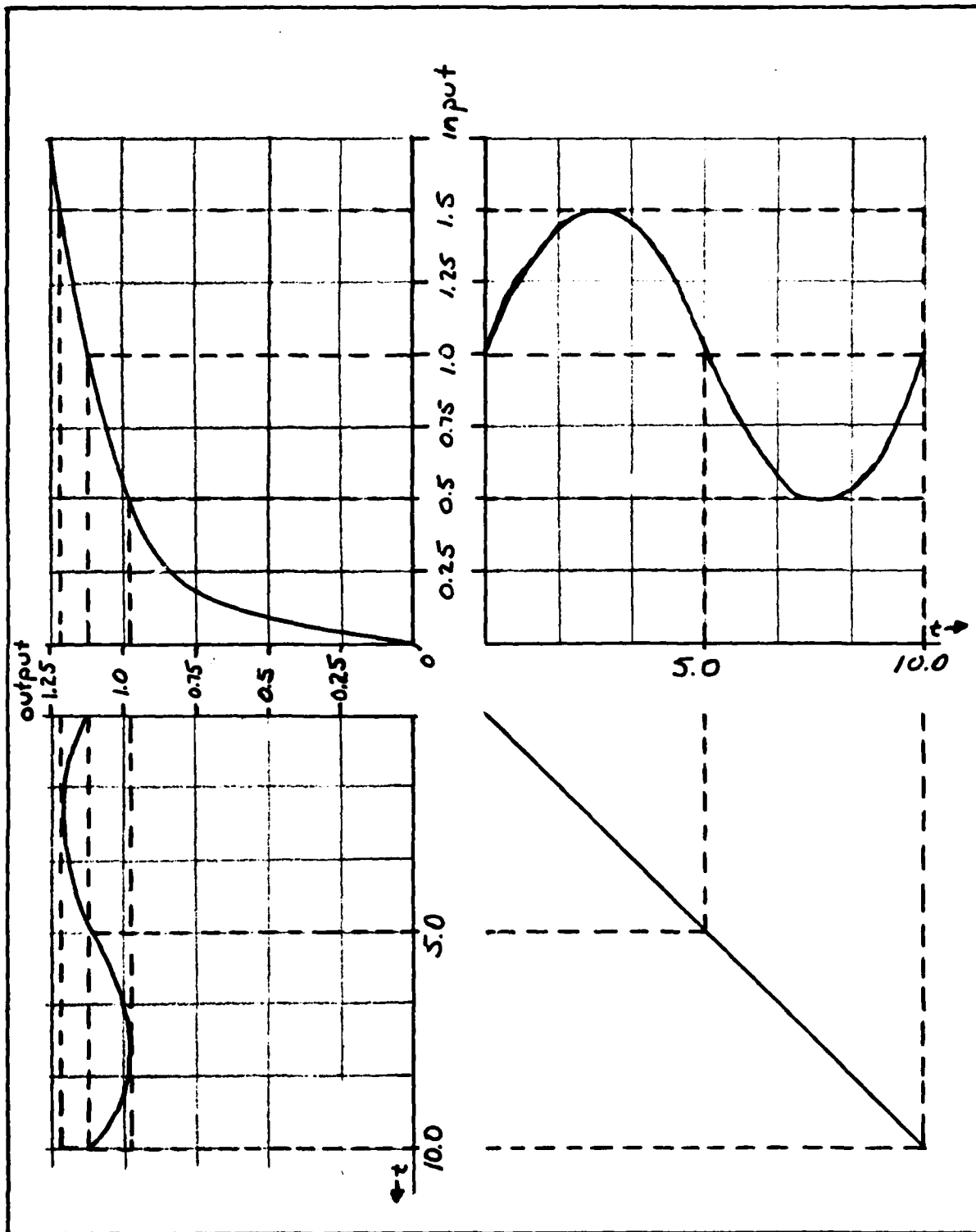


Figure 14. Steady-State Graphical Analysis of the Test Signal

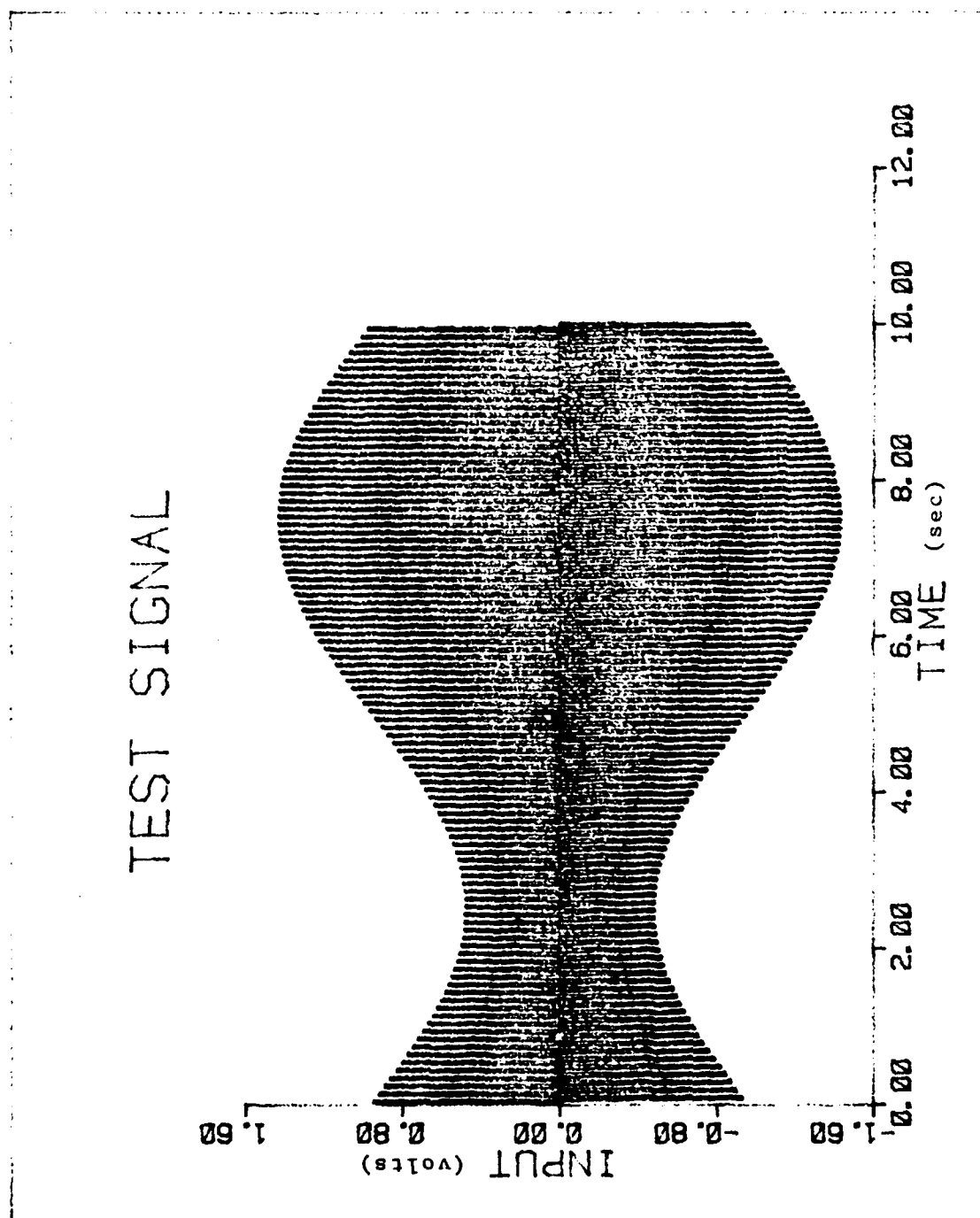


Figure 15. AGC Input Test Signal ($f_1=0.1\text{Hz}$, $f_H=10.0\text{Hz}$ and $a=0.5$)

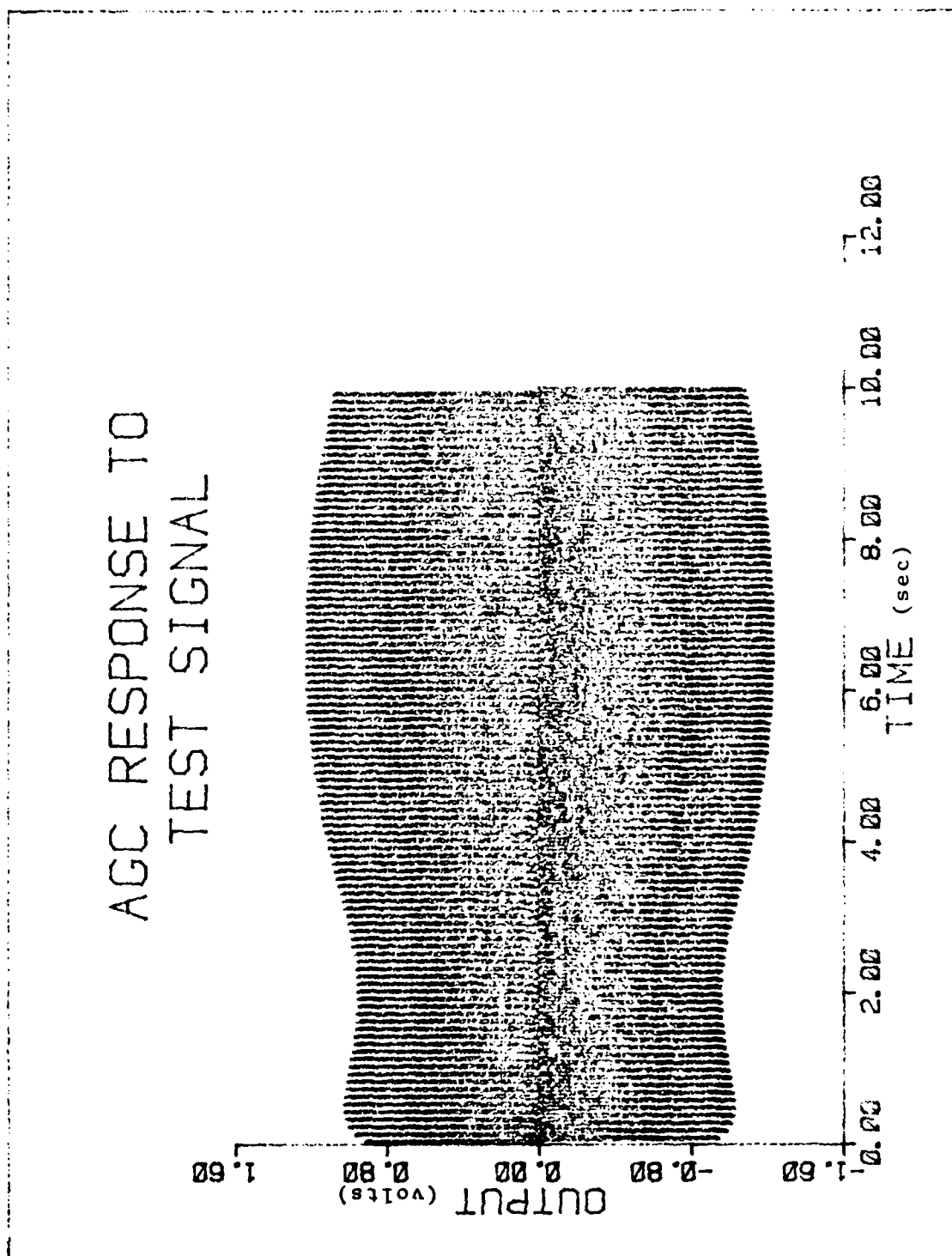


Figure 16. AGC Output with Test Signal Input ($A=6.2$, $G=100$ and $RC=1.0$ sec)

statistics. To generate the statistics, the receiver is simulated several times with the same optical input. After the simulations, the mean of the signal for a sample time t_k is computed by using [Ref 8:245-246]:

$$\overline{s(t_k)} = \left[\sum_{i=1}^N s_i(t_k) \right] / N \quad (46)$$

where

$\overline{s(t_k)}$ = sample mean of the signal at the time t_k

$s_i(t_k)$ = the i^{th} simulation of the signal at time t_k

N = total number of simulations conducted

The signal variance is then obtained by using:

$$\sigma_k^2 = \overline{s^2(t_k)} = \left\{ \sum_{i=1}^N [\overline{s(t_k)} - s_i(t_k)]^2 \right\} / N \quad (47)$$

where

σ_k^2 = sample variance of the signal at time t_k

From these statistics the effects that the AGC has on strength of the signal and the signal fluctuations can be examined.

To study the effects that the AGC has on the detection accuracy, an estimate of the probability of a bit error has to be computed. The decision rule that minimizes the probability of error compares the voltage (r_1) at the end of the first half of a bit period with the voltage (r_2) at the end of the bit period. This decision rule can be applied to both the photodetector output and the AGC output which will be proven in the next chapter. A bit error occurs if $r_1 < r_2$ when a binary one is transmitted, or if $r_1 > r_2$ when a binary zero is transmitted.

For the receiver simulations, the probability of error can be computed by defining a random variable as [Ref 8:265-266]:

$$z_i = \begin{cases} 1 & \begin{cases} \text{if } r_{1i} < r_{2i} \text{ given a binary one transmitted} \\ \text{if } r_{1i} > r_{2i} \text{ given a binary zero transmitted} \end{cases} \\ 1/2 & \text{if } r_{1i} = r_{2i} \\ 0 & \text{otherwise} \end{cases} \quad (48)$$

With this random variable, the probability of error is obtained by using:

$$\text{Pr}_c(\text{error}) = \bar{z} = \left(\sum_{i=1}^N z_i \right) / N \quad (49)$$

where

$\text{Pr}_c(\text{error})$ = computed probability of error

\bar{z} = mean of the random variables (z_i)

The variance of the random variable is defined by:

$$\sigma_z^2 = \left[\sum_{i=1}^N (z_i - \bar{z})^2 \right] / N \quad (50)$$

By using this variance and Tchebycheff's Inequality, the certainty of the estimate of the $\text{Pr}_c(\text{error})$ can be quantified. Tchebycheff's Inequality is given by [Ref Papoulis:259-260]:

$$\text{Pr}\{ |\text{Pr}_A(\text{error}) - \text{Pr}_c(\text{error})| < \epsilon \} = 1 - \sigma_z^2 / (N\epsilon^2) \quad (51)$$

where

$\text{Pr}_A(\text{error})$ = actual probability of error

The probability of error as well as the first and second order statistics will be used to determine the performance of the receiver.

V. Results

In this section an implementation of several optical receivers will be conducted and the effects of the AGC's examined. A receiver with an "instantaneous" AGC (IAGC) will be the first to be analyzed. An IAGC is a special classification of an AGC. The IAGC's are designed to be more sensitive to input changes, whereas the AGC's are designed to respond to the slow fluctuation in the input amplitude (Ref 9: 81). Following the IAGC analysis a receiver containing an AGC will be examined. The last receiver to be analyzed contains a dual AGC, which is (for this study) an IAGC and an AGC cascaded together.

Receiver with an IAGC

Because an IAGC is more sensitive to input changes, it should respond to the changes caused by shot noise as well as the signal fluctuations. The effects that the IAGC has on the photodetector output will be analyzed in this section. This analysis will be accomplished by computing the first and second order statistics along with the probability of error.

Simulation Parameters. To conduct the analysis the receiver models which were developed in the previous chapter will be used. The power densities of the optical pulses being received are arbitrarily chosen to vary over a 20 db range: 0.2w/cm^2 to 2.0w/cm^2 . Using eqn (21) the rate of

photon to electron conversions will vary from 10^{14} to 10^{15} e^- /sec (Area = 1mm^2 , $\eta = 0.1$, and $f_0 = 3.2 \times 10^{14}$). The rate of thermally emitted electrons is generally several orders magnitude smaller than the signal rates and, therefore, was arbitrarily chosen to be 10^{13} e^- /sec. With these counting rates and with a giga bit baud rate, the simulation parameters for the detector are given in table 1.

The AGC parameters, A and G_0 , can be determined by designing the IAGC to limit the output values to a range 20mV to 40mV for inputs that vary between 0.4 μ V to 10.0 μ V. The output range was "arbitrarily" chosen; although tradeoffs were made to keep parameters, A and G_0 , realistic. The input values were obtained from the photodetector's response. The 10.0 μ V is the expected value of the detector at the end of a clock period when the maximum optical signal is being received. The minimum input value was determined by the MAP decision criteria for an on-off keying digital signal. This MAP decision rule, based on the detector output, is defined as (Ref 3:216):

$$X(T_s) = q/C N(T_s) \geq_{D_0}^{D_1} q/C \lambda_S T_s / \ln(1 + \lambda_S / \lambda_D) \quad (52)$$

where

λ_S = rate of photon to electron conversions

λ_D = rate of thermally emitted electrons.

Using the photodetector parameters, $\lambda_D = 10^{13}$ and $\lambda_S = 10^{14}$ (λ_S is the rate for photon to electron conversions correspon-

ding to minimum optical power densities) the optimum decision threshold is computed to be $0.4\mu\text{V}$. Substituting these values into eqns (36) and (37), an A and a G_0 were calculated to be 125 and 6×10^6 , respectively.

The final parameter to be specified is the RC time constant for the AGC feedback filter. As long as the inverse of the RC time constant is large compared to the bandwidth of the signal, the AGC will be able to respond to rapid changes in the input. For the analysis $RC = 0.01\text{nsec}$ will be used.

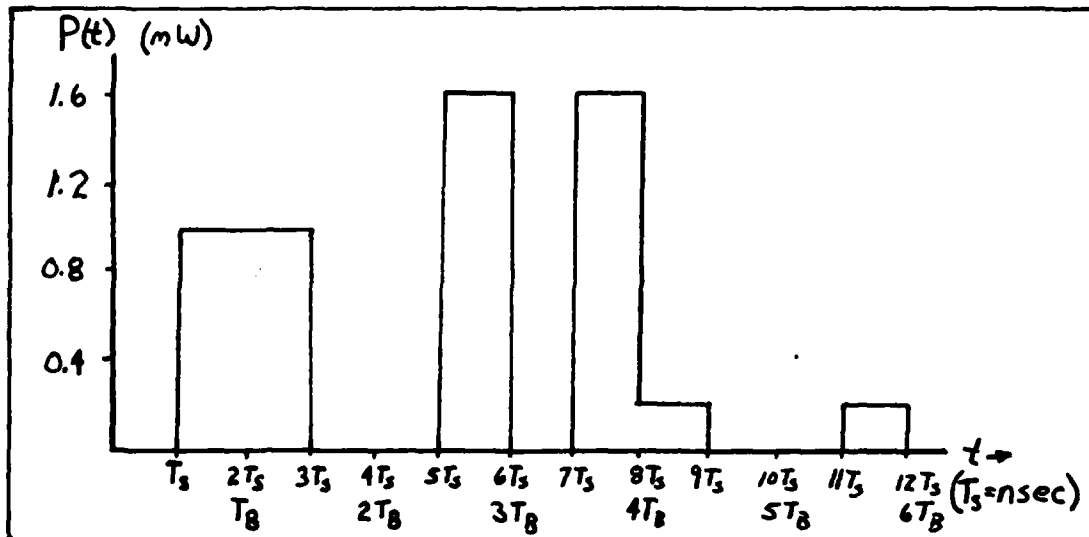


Figure 17. Input Optical Signal for a Receiver with an IAGC

Analysis. With these simulation parameters, the effects of an IAGC in an optical receiver can be studied. For the analysis the received optical signal will be pre-defined (see figure 17). The photodetector detector output for this signal can be easily determined in terms of the first and second order statistics. Using this detector output and the steady-state response curve, the IAGC's response can be predicted

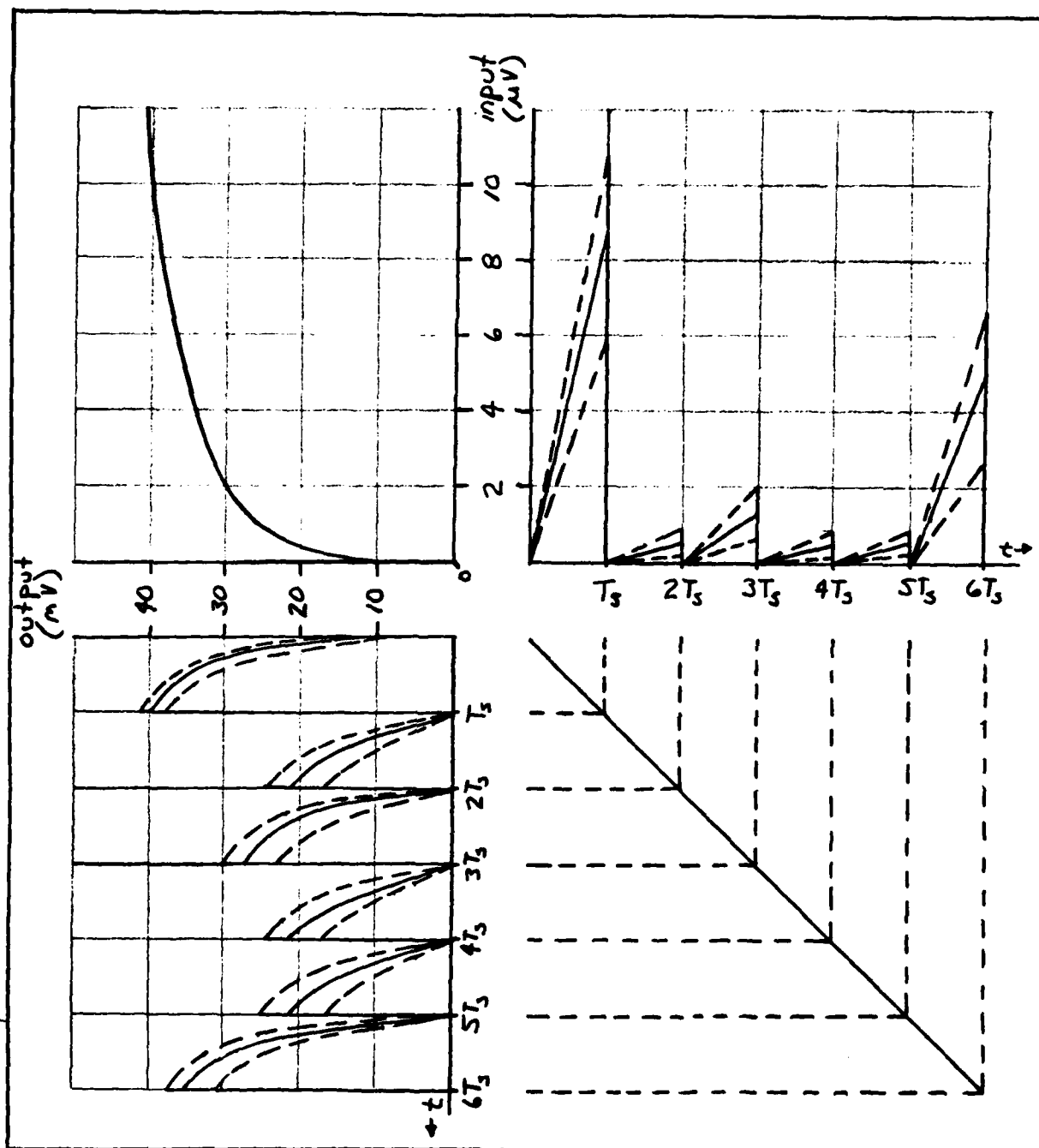


Figure 18. Graphical Analysis of the TAGC Response

(see figure 18).

The AGC response generated from the graphical analysis indicates that the IAGC provides control to the changes in the signal. The relative range over which the signal fluctuates is reduced by the IAGC. This is readily apparent by comparing signal peaks during the intervals at which the optical pulses were received. The IAGC will also reduce the shot noise effects as evident from a decrease in the variance of the signal.

In the process of reducing changes in the signal, the IAGC also distorts the detector signal. From this distorted signal the digital information that was transmitted is to be extracted. Before the addition of the AGC, the decision rule to detect the information was defined as

$$\dot{x}((2i-1)T_s) \underset{D_0}{\overset{D_1}{>}} x((2i)T_s) \quad (53)$$

where

T_s = switch period

$2i T_s = iT_B = i^{\text{th}}$ bit period

$x(t)$ = photodetector output

Since this decision rule is optimal for the photodetector voltage, applying the same decision rule to the AGC output would be appealing. For the particular AGC's being studied, the input-output characteristic (steady state response curve) is a monotonically increasing curve producing a one-to-one input-output relationship. Because of this one-to-one

relationship, the same decision criteria can be used for the AGC output.

The analysis conducted thus far utilized graphical techniques to describe the effects of an AGC. From the graphic analysis, an IAGC's response to the a photodetector input was predicted. The optimum decision rule for this IAGC response was determined to be the same criteria that is used for the detector output. The graphical analysis provides some insight as to what the IAGC response will be, but can not be used to predict the actual response.

To study the dynamic effects of the IAGC requires the use of a computer. Employing the algorithms developed in the preceding chapters, a simulation of the receiver was conducted. The receiver's response to an optical input was obtained using the simulation parameters developed in the first section of this chapter. The statistics of the photodetector's output (see figure 19) as a result of 100 simulations accurately approximates the analytical statistics. And the IAGC's response (see figure 20) to the detector's output was correctly predicted by the graphic analysis.

From these plots, the reduction in the signal variance may not be apparent. Therefore, a signal to noise ratio will be computed. The signal to noise ratio (SNR) is defined as

$$\text{SNR} = (\bar{s}_k)^2 / \overline{s_k^2} \quad (54)$$

where

\bar{s}_k = sample mean at time t_k

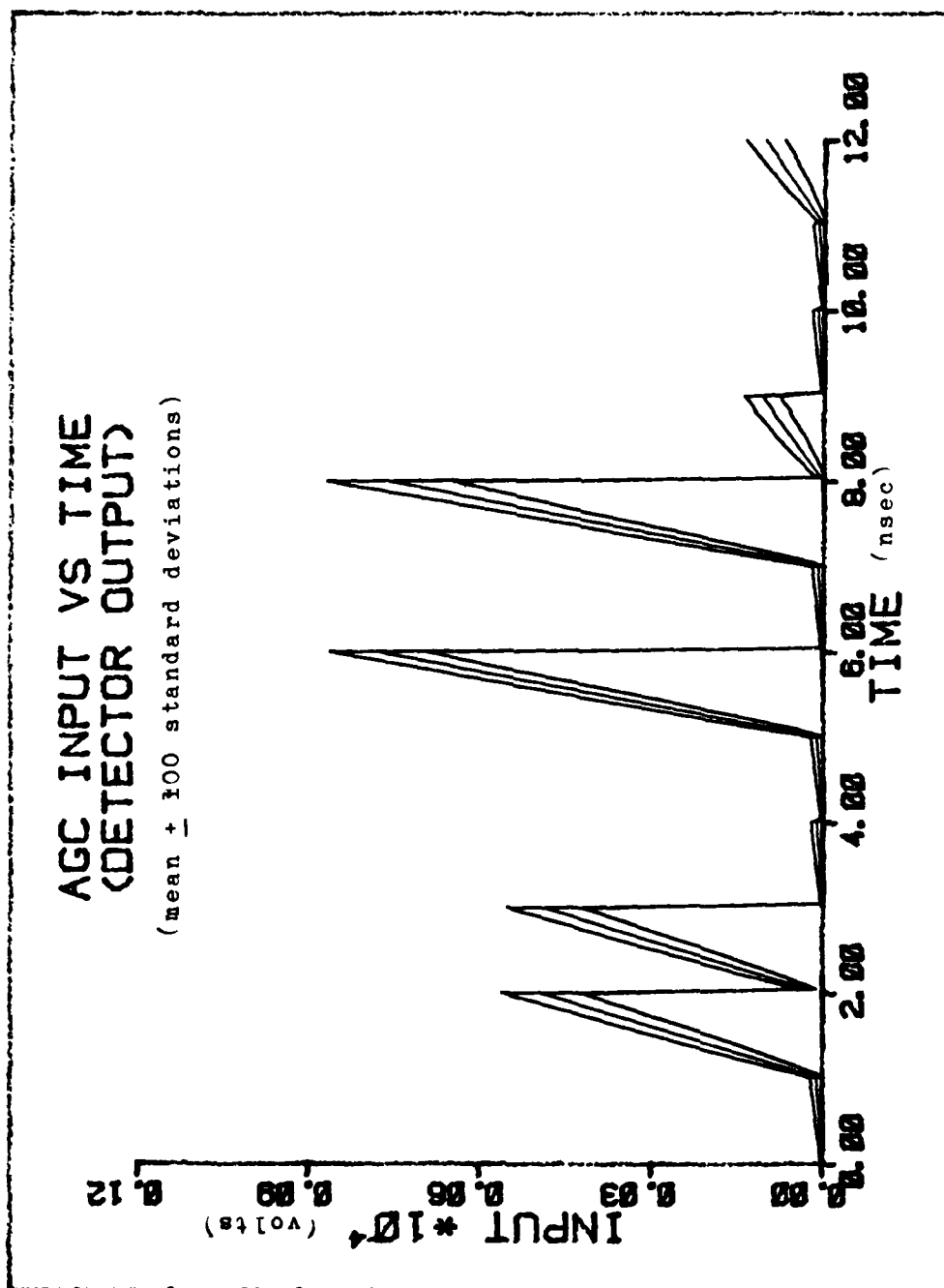


Figure 19. IAGC Input

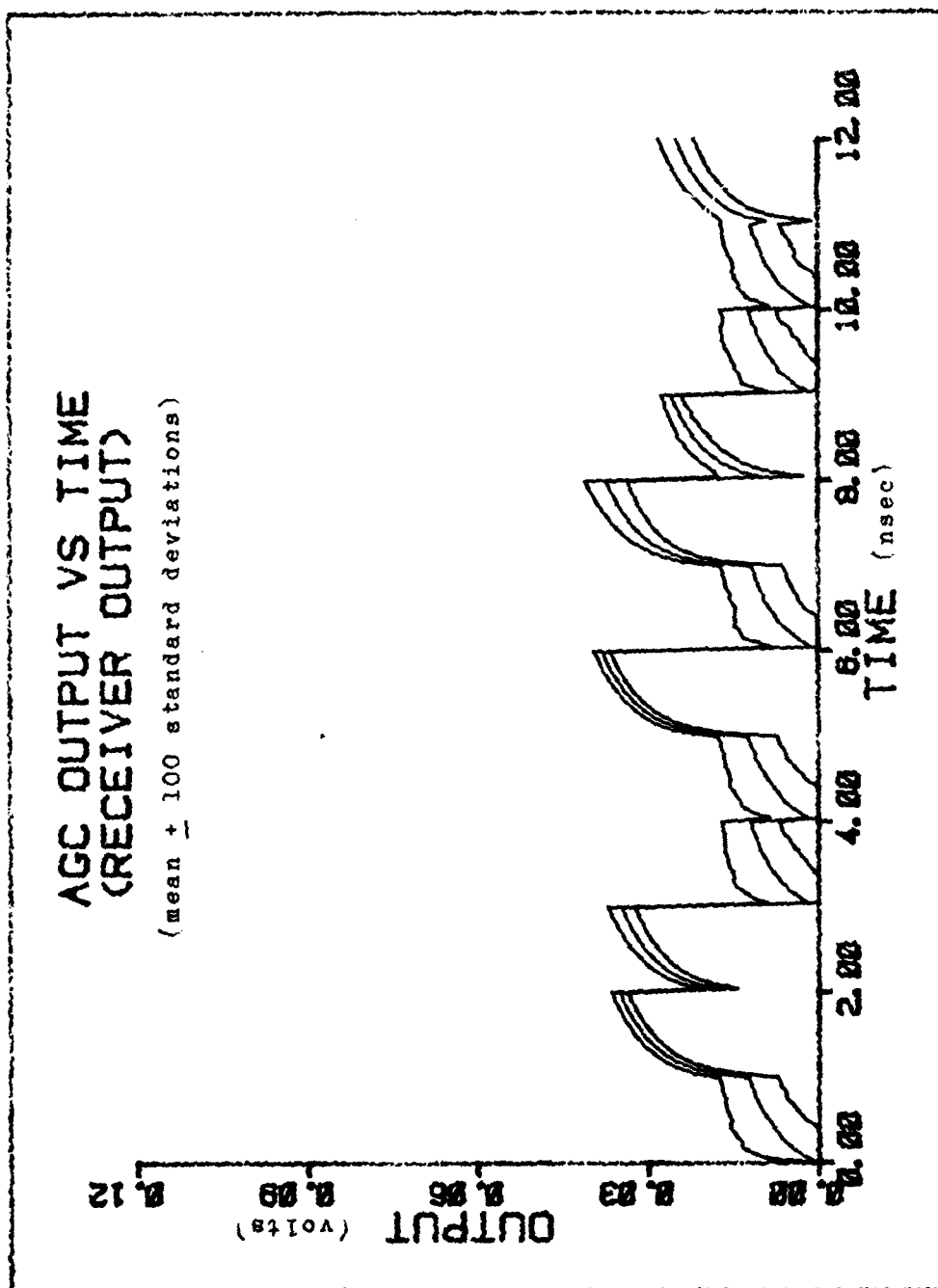


Figure 20. IAGC Output
($G=6 \times 10^5$, $A=125$ and $RC=0.01 \text{ nsec}$)

$\overline{s_k^2}$ = sample variance at time t_k

And an improvement factor (IMP) will be defined as:

$$IMP = SNR_y / SNR_x \quad (55)$$

where

SNR_y = SNR of the AGC output

SNR_x = SNR of the AGC input

An $IMP > 1$ would imply the AGC is reducing the shot noise effects. The IMP is plotted as a function of the input ensemble average (see figure 21) which indicates the IAGC is reducing the signal variance.

Varying the AGC parameters, A and G_o , does not effect the general shape of the IAGC's response. Increasing G_o only provides greater amplification to the photodetector output (see figures A-1 and A-2). Increasing A decreases the amplification but provides better control of the signal fluctuations (see figures A-3 and A-4). Varying the RC time constant, on the other hand, causes transient effects to become noticable (see figures A-5 and A-6). As the RC approaches the switching period, T_g , the IAGC begins to track the time or low frequency components of the signal and becomes less sensitive to input changes. When the reaction time becomes sufficiently slow ($RC \approx T_g$), the AGC loses its classification as an IAGC.

As apparent from the graphical analysis and through the comparisons of the IAGC input-output simulations, the IAGC

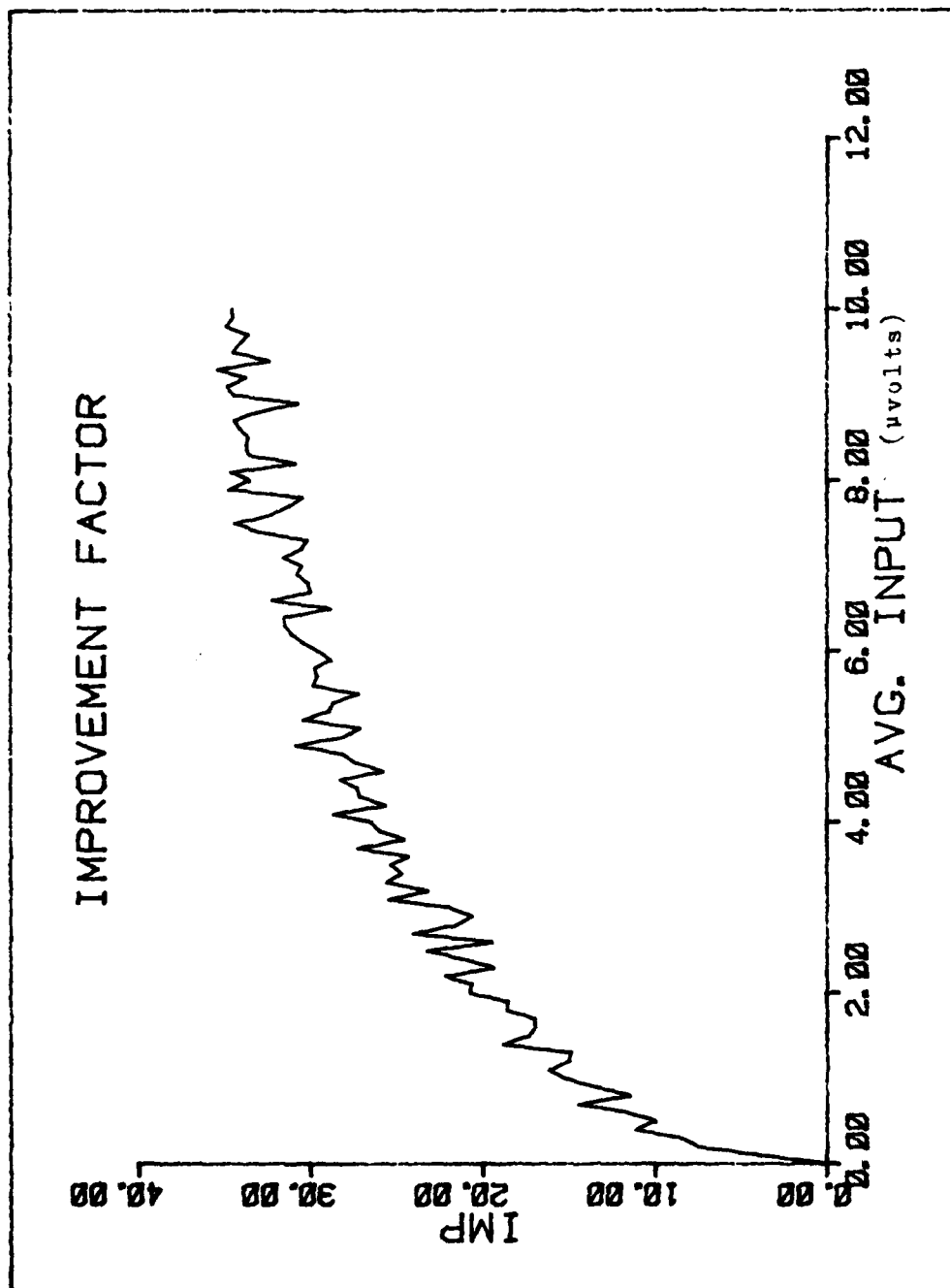


Figure 21. Improvement of SNR by the IAGC

$$(IMP = SNR_{out} / SNR_{in})$$

does reduce the signal variance. By reducing the shot noise effects the IAGC will improve the signal to noise ratio (SNR). At first intuition, an improved SNR would indicate that the probability of error would decrease. For linear systems this would be true, but AGC's have non-linear gain characteristics which also shifts the energy levels.

Detector Pr(error) (with 90% certainty)	IAGC Parameters			IAGC Pr(error) (with 90% certainty)
	G_o	A	RC	
0.052 \pm 0.022	2x10 ⁵	125	0.01	0.050 \pm 0.022
	4x10 ⁵			0.048 \pm 0.022
	6x10 ⁵			0.048 \pm 0.022
	8x10 ⁵			0.047 \pm 0.022
	10x10 ⁵			0.047 \pm 0.022
	6x10 ⁵	75	0.01	0.048 \pm 0.022
		100		0.048 \pm 0.022
		125		0.048 \pm 0.022
		150		0.047 \pm 0.022
		175		0.047 \pm 0.022
	6x10 ⁵	125	0.01	0.048 \pm 0.022
			0.05	0.050 \pm 0.022
			0.1	0.052 \pm 0.025
			0.5	0.083 \pm 0.028
			1.00	0.0 \pm 0.0

Table 2. Estimate of the Probability of a Bit Error for
an Initial Signal (binary one) Using an IAGC

$$(\lambda_S = 5000 \text{ and } \lambda_D = 50000)$$

To analyze the effects of the IAGC on the probability of error, again, requires a simulation of the receiver on the computer. An estimate of the probability of a bit error is shown in Table 2 for the first bit of received information

(binary one). A very weak optical signal and a large dark current were needed to provide a non-zero estimate from the 1000 simulations. From the one-to-one input-output relationship the graphical analysis predicted that the IAGC would have no effect on the probability of error. As long as transients are insignificant, the estimate is virtually unaffected by the IAGC. As the RC time constant increases, the transients become a factor in the detection process causing the probability of error to increase.

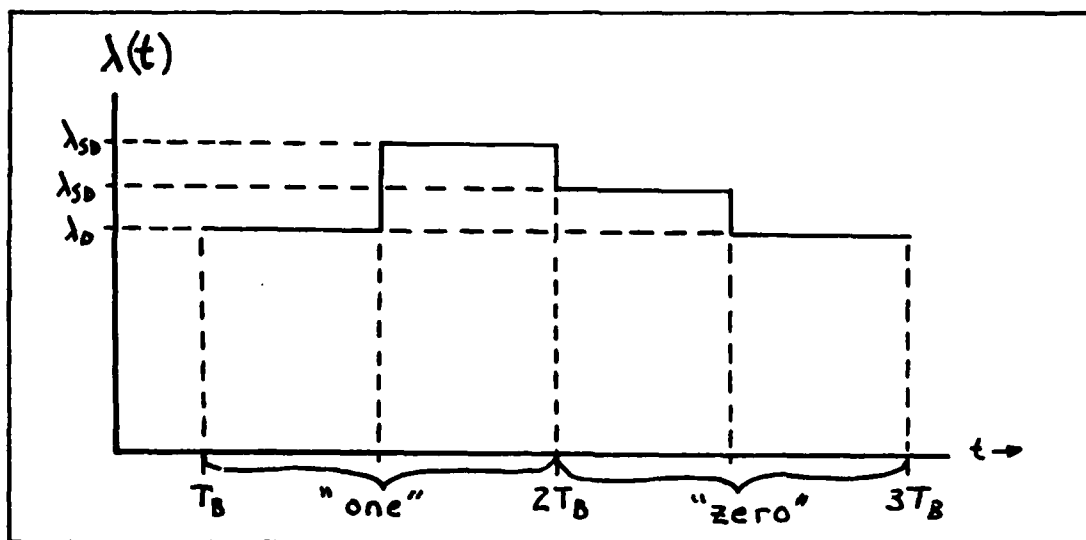


Figure 22. Worst Case Signal

The influence of transients on the detection process is more apparent for the "worst case" signal. This signal assumes a frame interval of strong optical pulses are received followed by a frame interval of pulses from a weak source (see figure 22). The effects of the IAGC for various parameters is shown by Table 3. As expected, increasing the RC time constant slows the IAGC response, thereby, increasing the

probability of a bit error.

Detector Pr(error) (with 90% certainty)	IAGC Parameters			IAGC Pr(error) (with 90% certainty)
	G_o	A	RC	
0.052+0.024	2×10^5	125	0.01	0.062+0.024
	4×10^5			0.062+0.024
	6×10^5			0.064+0.024
	8×10^5			0.064+0.024
	10×10^5			0.064+0.024
	6×10^5	75	0.01	0.062+0.024
		100		0.063+0.024
		125		0.064+0.024
		150		0.064+0.024
		175		0.064+0.024
	6×10^5	125	0.01	0.064+0.024
			0.05	0.067+0.025
			0.1	0.069+0.025
			0.5	0.113+0.031
			1.0	0.204+0.040

Table 3. Estimate of Probability of a Bit Error for
the "Worst Case" Signal Using an IAGC

($\lambda_s = 5000$ and $\lambda_D = 50000$;
for the previous pulse of $\lambda_s = 20000$)

Based on the analysis one can obtain a feel for the effects of the IAGC on average probability of error. As long as the IAGC has a quick response to input charges ($RC \ll T_s$) the probability of a bit error is unaffected. But as RC increases, the bit error increases causing the average probability of error to increase. Although the IAGC does not improve the probability of error, it does provide excellent control to the signal fluctuations, and sufficient amplification of the signal.

Receiver with an AGC

The most common purpose of the AGC's used today is to control slow-time varying fluctuations that are super-imposed on a signal. In this section an analysis is conducted to examine the effects of a common AGC in controlling the optical signal fluctuations.

Simulation Parameters. For the analysis the photodetector parameters will be the same as those used in the previous section. The AGC parameters will be obtained using similar methods but designed to control the fluctuations and to pass the signal unaffected. For the particular signals being analyzed, the fluctuations can be described as a change in the DC component or the time average of the signal between the frame periods (see figure 23). This "DC" signal will be

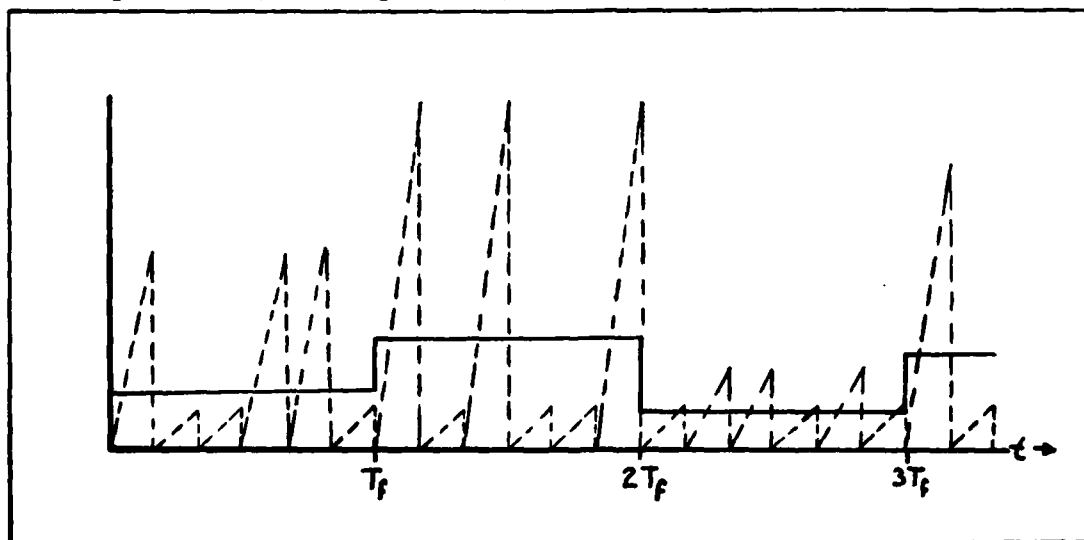


Figure 23. Approximation to Describe Signal Fluctuations

used to compute the AGC parameters and to conduct an approximate analysis of the AGC response.

The AGC will be designed to limit the DC output signal to the range to 2mV to 4mV for an input DC signal that varies between 0.25 μ V and 25 μ V. The input values were obtained by taking the time average of the photodetector's ensemble averaged output. The 0.25 μ V corresponds to the time average of the detector's output during the frame period that a weak optical signal was received and the 25 μ V corresponds to the frame period a strong optical signal was received. The output range was arbitrarily chosen. Using these values in eqn (36) and eqn (37), the AGC parameters, A and G_o , are calculated to be 2×10^3 and 4×10^5 , respectively. The final AGC parameter, the RC time constant, is restricted to the range $T_s < RC < T_f$. This will insure that the AGC will be able to respond to the signal fluctuations and not respond to the signal itself.

Analysis. Using the DC signal, an approximate analysis can be conducted through the graphical techniques (see figure 24). The result of the graphical analysis indicates that the AGC will reduce the range of the DC variations. Since the DC level is directly proportional to the average signal; the reduction in the variation of the DC level would imply that the signal fluctuations will be reduced, assuming the signal is not affected by the AGC. Because of the assumptions (the AGC completely passes the signal and the filter only responds to the DC level of a frame period), this graphical analysis is only able to provide a "loose" approximation to the AGC response.

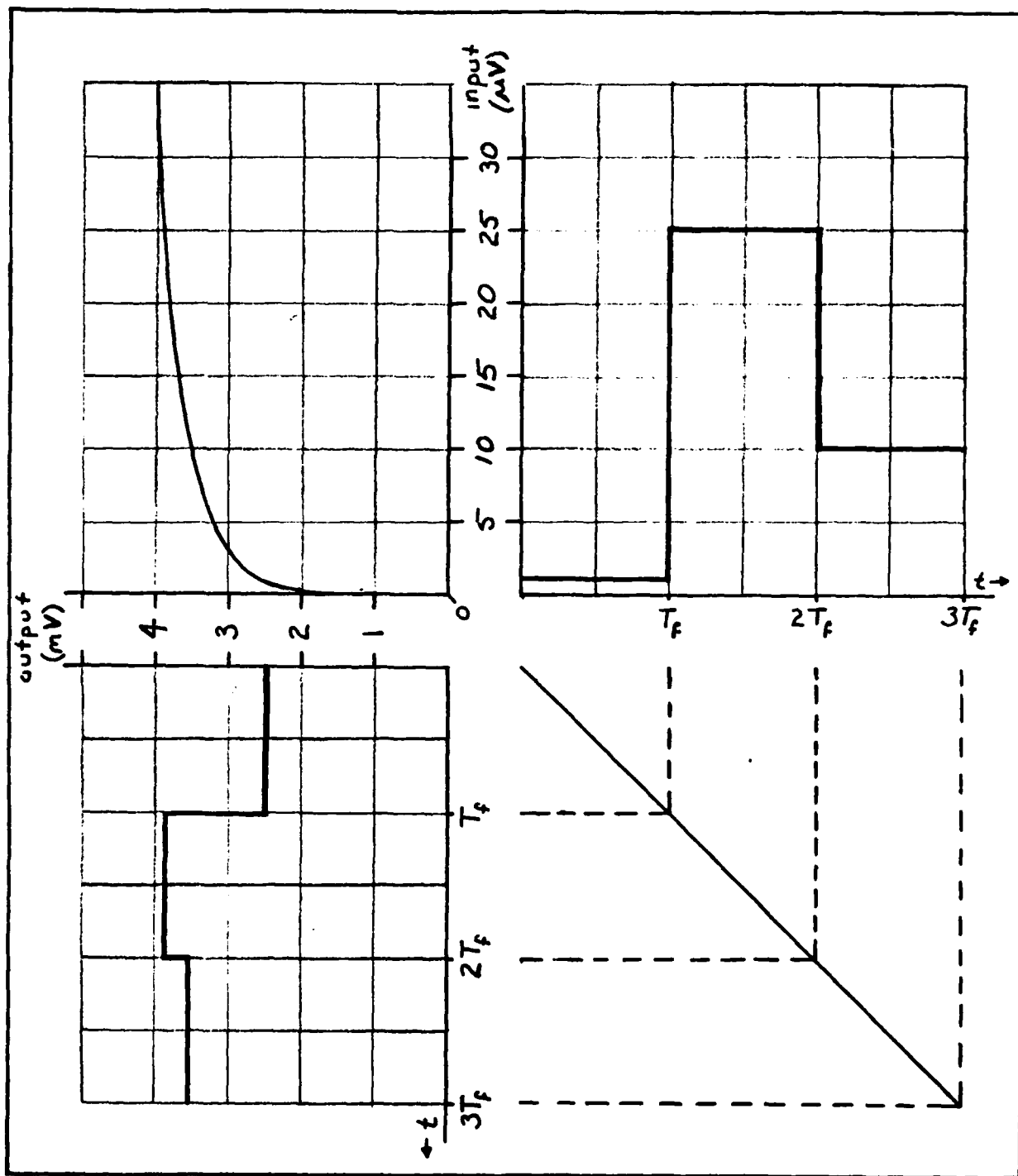


Figure 24. Graphic Analysis of the AGC Response

To obtain an accurate response, the receiver is implemented on the computer. Using the optical signal shown in figure 25, the photodetector's response (see figure 26) as a result of the simulation are analogous to the analytical statistics. Using an $RC = 4.0\text{nsec}$, the AGC output (see figure 27) has very noticable transient effects which distorts the photodetector signal.

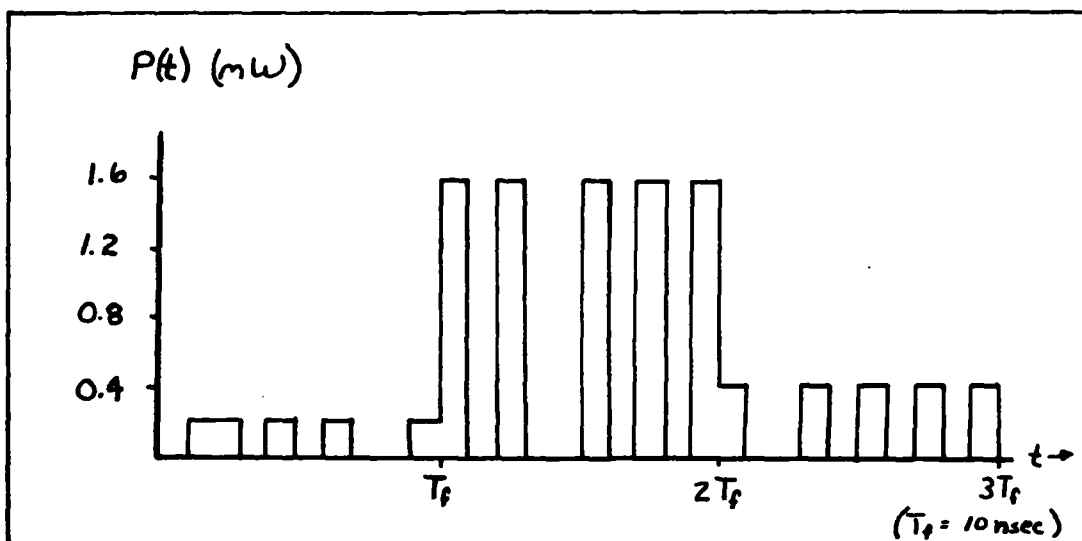


Figure 25. Input Optical Signal for a Receiver with an AGC

The effects of the AGC parameters produce similar results in the performance of the receiver as they did for an IAGC. Increasing the G_0 provides greater amplification (see figures A-7 and A-8), and increasing the A provides better control of the signal fluctuations (see figures A-9 and A-10). Like the IAGC, the RC time constant has the greatest influence on the AGC performance. Increasing RC insures the AGC tracks only the DC component of a frame interval, but this also slows the AGC's response to the changes in the DC level (see figures A-

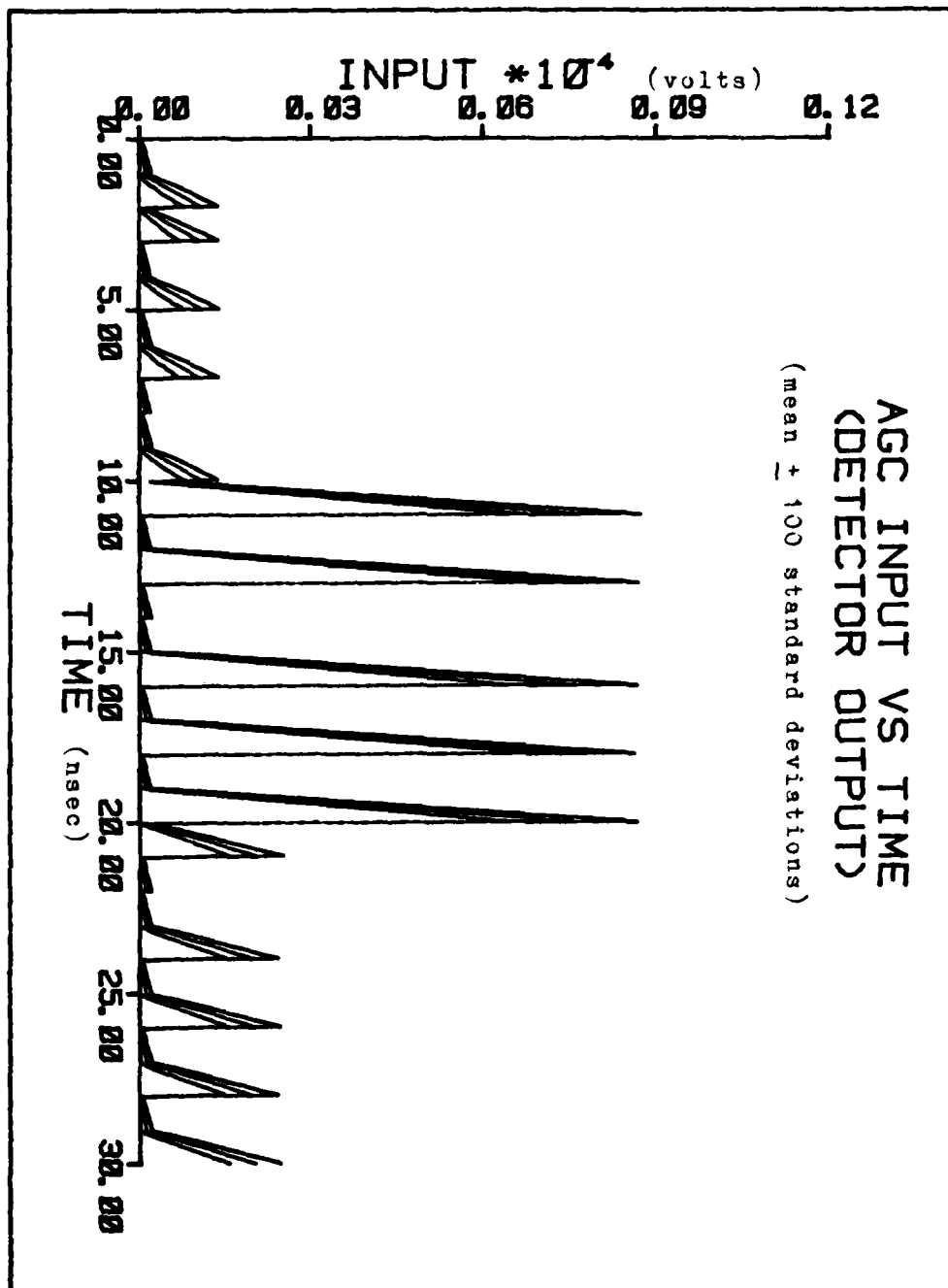


Figure 26. AGC Input

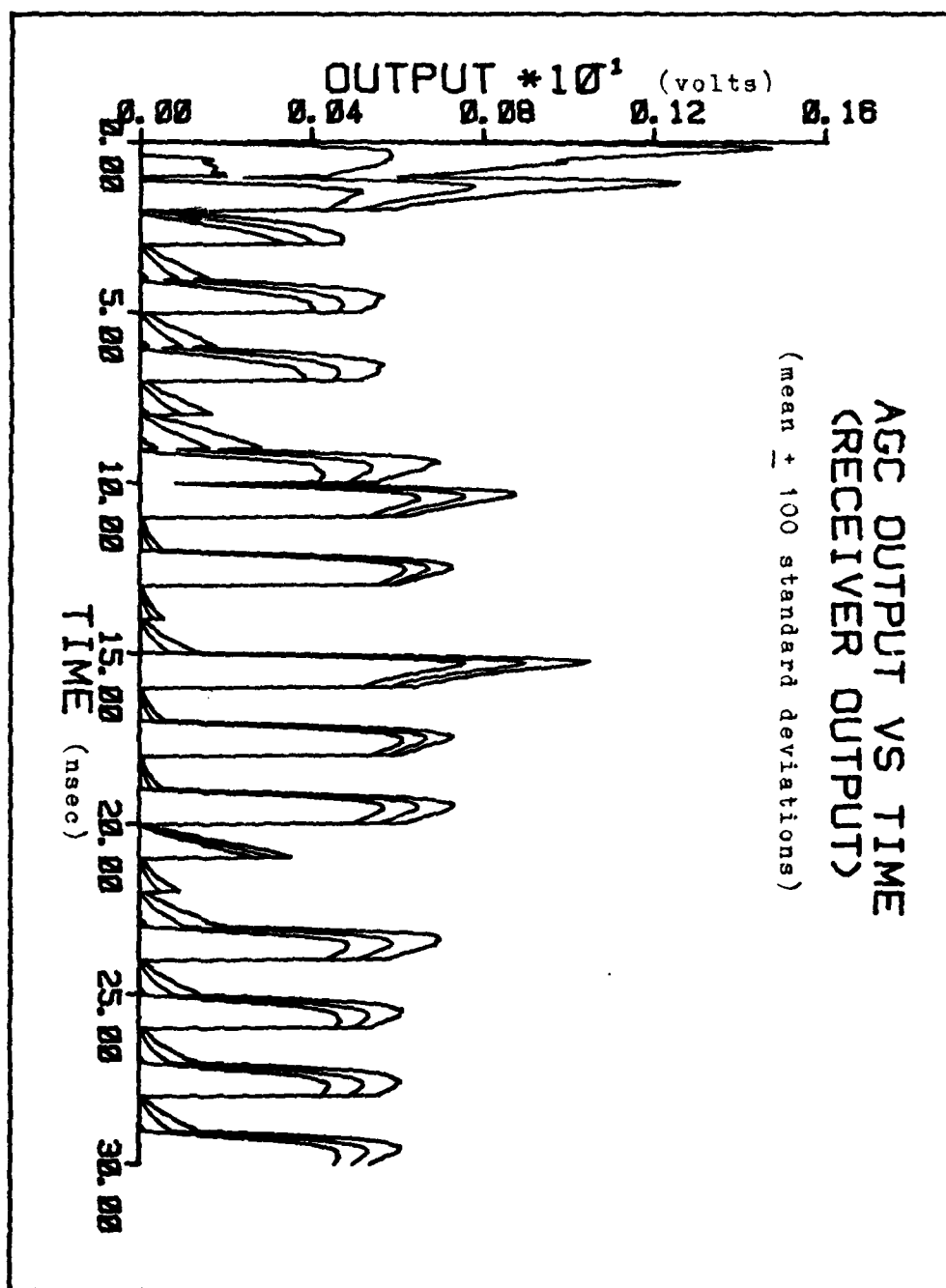


Figure 27. AGC Output
 $(G_o = 4 \times 10^5, A = 2000 \text{ and } RC = 4 \text{ nsec})$

11 and A-12) introducing transients. Decreasing RC increases the AGC's reaction to DC charges but unfortunately also causes the AGC to respond to the signal. Decreasing RC below T_s causes the AGC to be classified as an IAGC.

Detector Pr(error) (with 90% certainty)	AGC Parameters			AGC Pr(error) (with 90% certainty)
	G_o	A	RC	
0.0±0.0	1×10^5	2000	4.0	0.657±0.047
	2×10^5			0.240±0.042
	4×10^5			0.079±0.027
	6×10^5			0.061±0.024
	8×10^5			0.055±0.023
	4×10^5	1600	4.0	0.033±0.018
		1800		0.049±0.022
		2000		0.079±0.027
		2200		0.158±0.036
		2400		0.298±0.046
	4×10^5	2000	2.0	0.072±0.026
			4.0	0.079±0.027
			6.0	0.156±0.036
			8.0	0.218±0.042
			10.0	0.241±0.043

Table 4. Estimate of the Probability of a Bit Error for the "Worst Case" Signal Using an AGC

($\lambda_s = 10000$ and $\lambda_D = 50000$;
for the previous pulse of $\lambda_s = 20000$)

The effects of the AGC on probability of error should ideally be neglectible, because an AGC is to pass the signal undistorted. But because of the transients, the AGC causes the probability of error to increase as evident from Table 4 (for the "worst case" signal given in figure 22). Note, the

signal rate λ_s is larger in this analysis than in the IAGC analysis. As apparent from comparing Tables 3 and 4, the AGC has a greater detrimental effect on the average probability of error even though it is designed not affect the signal.

Receiver with a Dual AGC

The analysis of the AGC's conducted thus far was limited simple AGC configurations. In this section a simulation of a dual AGC (two simple AGC's cascaded together) will be conducted. The compound AGC configuration will consist of an IAGC followed by a common AGC. Because the IAGC has a quick response, it will be able to control the large signal fluctuations without affecting the probability of error. The AGC will be able to provide further amplification of the signal and provide greater control of the fluctuations. Since the IAGC significantly decreases the dynamic range of the signal fluctuation, the transient effect of the AGC on the probability of error will be minimal.

The IAGC to be used in this compound configuration will be the same as the IAGC that was studied in the first section. The IAGC output is then used as an input to the AGC. The AGC now designed to track the changes in the DC component of the IAGC output instead of the photodetector's output. Using the same method as developed in the previous section the AGC parameters are computed to be $A=0.5$, $G_o=3200$ and $RC=4.0\text{ nsec}$.

Simulating this receiver produces an output shown in figure 28, where the detector output is given in figure 26.

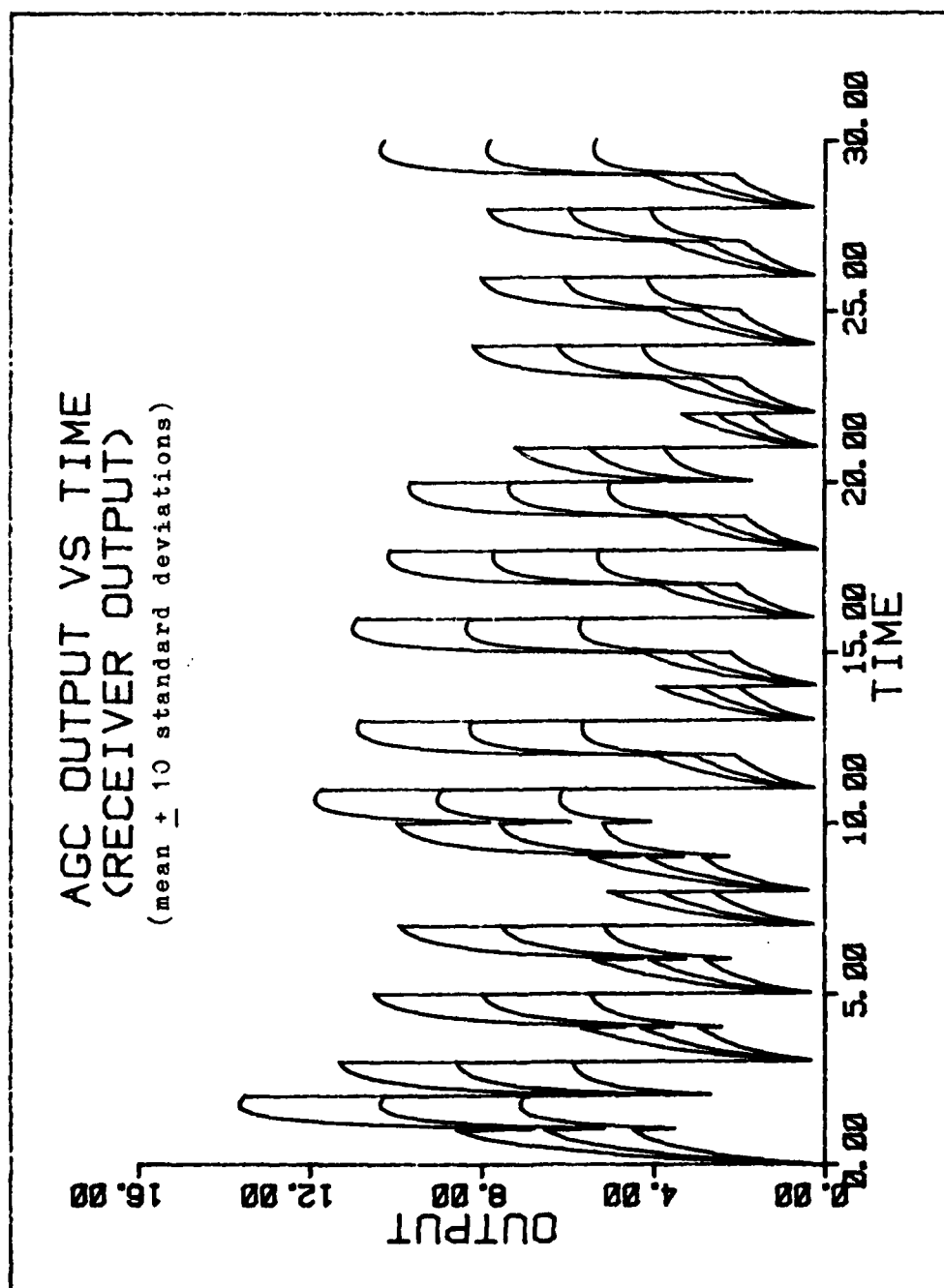


Figure 28. Dual AGC Output

As evident from figure 28 the dual AGC is able to provide control to the signal fluctuations and to provide ample gain to the detector output. Since the dual AGC is two simple AGC's cascaded together varying the parameters should produce the same effects as they did for each of the separate AGC's. Because of the time constraints, the plots of the dual AGC output for various parameters could not be generated.

The effects that the dual AGC has on probability of error is shown in Table 5 and Table 6. Through comparisons of Table 5 with Table 4, the probability of error is generally better than the AGC alone. This is expected because the IAGC is able to reduce the signal fluctuations, thereby, reducing detection errors caused by the slow AGC response. Although comparing Table 6 with Table 3, the AGC's slow response does still have a detrimental effect on detection accuracy.

Detector Pr(error) with 90% certainty	IAGC Parameters			AGC Parameters			Dual AGC Pr(error) with 90% certainty
	G_0	A	RC	G_0	A	RC	
0.0+0.0	2×10^5						0.027+0.0162
	4×10^5						0.008+0.0089
	6×10^5	125	0.01	3200	0.5	4	0.003+0.0055
	8×10^5						0.003+0.0055
	10×10^5						0.003+0.0055
	6×10^5	75 100 125 150 175	0.01	3200	0.5	4	0.003+0.0055 0.003+0.0055 0.003+0.0055 0.007+0.0083 0.013+0.0113
	6×10^5	125	0.01 0.05 0.1 0.5 1.0	3200	0.5	4	0.003+0.0055 0.006+0.0077 0.008+0.0089 0.163+0.0369 0.550+0.0497
	6×10^5	125	0.01	2400 2800 3200 3600 4000	0.5	4	0.027+0.0122 0.007+0.0083 0.003+0.0055 0.003+0.0055 0.003+0.0055
	6×10^5	125	0.01	3200	0.40 0.45 0.50 0.55 0.60	4	0.000+0.0000 0.003+0.0055 0.003+0.0055 0.014+0.0117 0.057+0.0232
	6×10^5	125	0.01	3200	0.5	2 4 6 8 10	0.043+0.0203 0.003+0.0055 0.000+0.0000 0.000+0.0000 0.000+0.0000
	6×10^5	125	0.01	3200	0.5		
(λ _S =10000 and λ _D =50000; for previous pulse of λ _S =20000)							

Table 5. Estimate of the Probability of a Bit Error for
the "Worst Case" Signal Using a Dual AGC

Detector Pr(error) with 90% certainty	IAGC Parameters			AGC Parameters			Dual AGC Pr(error) with 90% certainty
	G_0	A	RC	G_0	A	RC	
0.063+0.024	2x10 ⁵ 4x10 ⁵ 6x10 ⁵ 8x10 ⁵ 10x10 ⁵	125	0.01	3200	0.5	4	0.309+0.0462 0.169+0.0375 0.103+0.0304 0.070+0.0255 0.055+0.0228
	6x10 ⁵	75 100 125 150 175	0.01	3200	0.5	4	0.053+0.0224 0.065+0.0247 0.103+0.0304 0.155+0.0362 0.213+0.0409
	6x10 ⁵	125	0.01 0.05 0.1 0.5 1.0	3200	0.5	4	0.103+0.0304 0.107+0.0309 0.135+0.0342 0.396+0.0489 0.782+0.0413
	6x10 ⁵	125	0.01	2400 2800 3200 3600 4000	0.5	4	0.245+0.0430 0.158+0.0346 0.103+0.0304 0.069+0.0253 0.055+0.0228
	6x10 ⁵	125	0.01	3200	0.40 0.45 0.50 0.55 0.60	4	0.013+0.0113 0.040+0.0196 0.103+0.0346 0.229+0.0420 0.456+0.0498
	6x10 ⁵	125	0.01	3200	0.5	2 4 6 8 10	0.330+0.0471 0.103+0.0304 0.039+0.0194 0.021+0.0143 0.017+0.0129
($\lambda_S=5000$ and $\lambda_D=50000$; for previous pulse of $\lambda_S=20000$)							

Table 6. Estimate of the Probability of a Bit Error for
the "Worst Case" Signal Using a Dual AGC

VI. Conclusions and Recommendations

Conclusions.

The purpose of this paper was to analyze the effects of an AGC in an optical receiver. The particular optical signal, which was studied, was a Manchester coded digital signal with varying optical power densities. The optical signal was converted into an electrical signal by a photodetector. Inserted after this detector was an AGC with the intent of improving the performance of the receiver. The criteria to assess the AGC's effects on the receiver's performance were:

- 1) amplification of the detector signal
- 2) control of the signal fluctuations
- 3) improve the detection accuracy.

Using this criteria three specific AGC's were analyzed.

From the analysis, an AGC which has a quick response was determined to be the most suitable for the optical receiver. Although a quick AGC response causes distortion of the photodetector output, the decision criteria was not effected by the addition of the AGC's. Of the three AGC's examined, the IAGC had the fastest reaction to input changes (as long as $RC \ll T_g$). The IAGC was able to provide amplification of the signal and to control signal fluctuations, but it had no significant effect on the probability of error. Because of their slow response, the other AGC's that were studied caused an

increase in probability of error. The IAGC was able to provide amplification of the signal and control signal fluctuations, but it had no significant effect on the probability of error. Thus, an AGC in an optimal receiver is not capable of improving the probability of error. Although this is not the result which is desired, it is an intuitively pleasing result. Having a device (which controls the signal amplitude) improve the accuracy of PPM detection would not have been anticipated.

Although the AGC will not improve the detection accuracy, it can be used to amplify the signal and to control the signal fluctuations. For signals with a wide dynamic range of fluctuations, using an AGC in the receiver may be more applicable than a constant gain amplifier. Since the AGC had non-linear gain characteristics, it can be use to provide ample gain to a weak signal to simplify the detection process. And during the reception of a strong signal the AGC will automatically reduce the gain to prevent saturation of the decision circuitry. Therefore, circuit limitations may require the use of an AGC, even though an AGC will not improve the probability of error.

Recommendations

Because of the numerous possible AGC configurations and time constraints, only three AGC's were examined, therefore the analysis could be expanded to investigate other AGC models. Since the AGC's can not improve the detection accuracy, the study should be focused on minimizing an increase

in the probability of error, while maintaining that the AGC still provide sufficient amplification of the signal and control of the fluctuations.

Other photodetector models could also be analyzed. In this paper the photodetector was modelled as a weighted Poisson counting process. This required a large RC time constant (compared to the signal bandwidth) and the implementation of a switch. Using a large RC time constant caused the signal information to be lost and an impracticable switch had to be implemented to obtain the information sent. Therefore, a more accurate photodetector model could be investigated by eliminating the switch, which would require the RC time constant in the detector model to be reduced.

The analysis could also be expanded to examine other optical signals and channels. A study of optical signals which are transmitted through the atmosphere may be more adaptable to AGC control. The atmospheric turbulence will cause the signal to incur continuous time varying fluctuations, unlike the discrete fluctuations caused in the fiber optic system which was analyzed. With the continuous time-varying fluctuations the AGC will not be required to have a quick response. This will enable the use of AGC's which are commonly used today.

in the probability of error, while maintaining that the AGC still provide sufficient amplification of the signal and control of the fluctuations.

Other photodetector models could also be analyzed. In this paper the photodetector was modelled as a weighted Poisson counting process. This required a large RC time constant (compared to the signal bandwidth) and the implementation of a switch. Using a large RC time constant caused the signal information to be lost and an impracticable switch had to be implemented to obtain the information sent. Therefore, a more accurate photodetector model could be investigated by eliminating the switch, which would require the RC time constant in the detector model to be reduced.

The analysis could also be expanded to examine other optical signals and channels. A study of optical signals which are transmitted through the atmosphere may be more adaptable to AGC control. The atmospheric turbulence will cause the signal to incur continuous time varying fluctuations, unlike the discrete fluctuations caused in the fiber optic system which was analyzed. With the continuous time-varying fluctuations the AGC will not be required to have a quick response. This will enable the use of AGC's which are commonly used today.

Bibliography

1. Davenport, William B. Jr. Probability and Random Processes. New York: McGraw-Hill Book Company, 1970.
2. Deffebach, H. L. and W. O. Frost. A Survey of Digital Baseband Signalling Techniques. Alabama: George C. Marshall Space Flight Center, June 1971.
3. Gagliardi, Robert M. and Sherman Karp. Optical Communications. New York: Wiley-Interscience Publication, 1976.
4. Hornbeck, Robert W. Numerical Methods. New York: Quantum Publishers, Inc., 1975.
5. Kleekamp, Charles and Bruce Metcalf. Designer's Guide to Fiber Optics-Parts 1-4. Summary of Optical Fiber Systems. Boston: Cahners Publishing Company, 1978.
6. Melsa, James L. and David L. Cohn. Decision and Estimation Theory. New York: McGraw-Hill Book Company, 1978.
7. Oliver, B. M. "Automatic Volume Control as a Feedback Problem," Proceedings of the IRE, 36:466-473 (April 1948).
8. Papoulis, Athanasios. Probability, Random Variables and Stochastic Processes. New York: McGraw-Hill Book Company, 1965.
9. Senior, Edwin W. Automatic Gain Control Theory for Pulsed and Continuous Signals. A Comprehensive Study of AGC's. Stanford: Stanford Electronic Laboratories, June 1967. (AD 825 380).
10. Snyder, Donald. Random Point Process. New York: Wiley-Interscience Publication, 1975.
11. Solymar, Laszlo and Donald Walsh. Lectures on the Electrical Properties of Materials (Second Edition). Oxford: Oxford University Press, 1979.
12. Williams, N. A. F. "Automatic Gain Control Systems," Wireless World, 83:60-1 (September 1977).
13. Ziemer, R. E. and W. H. Tranter. Principles of Communications. Boston: Houghton Mifflin Company, 1976.

Appendix A

Graphs of Various AGC Responses

This appendix contains plots of the AGC response to a given optical input for various AGC parameters. The plots are presented in pairs in which one AGC parameter is varied between the pair. This will enable the reader to compare the effects that the parameter has on the photodetector output.

The photodetector output for the first six graphs is given in Figure 19 and the last six in figure 26. Each graph contains a plot of the mean \pm 100 standard deviations, which is a result of 100 simulations.

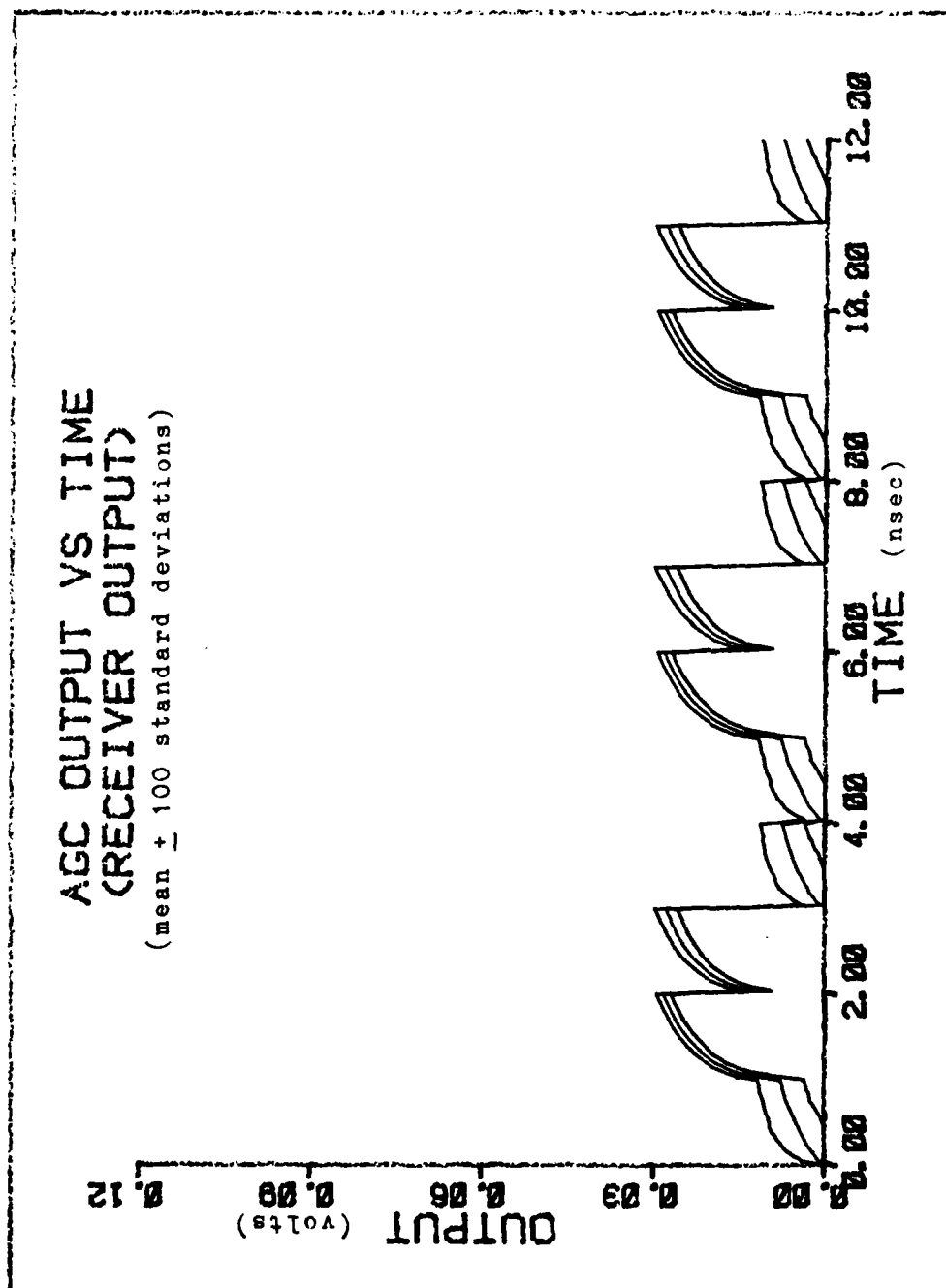


Figure A-1. IAGC Output with $G_0 = 2 \times 10^5$

($A=125$ and $RC=0.01 \text{ nsec}$)

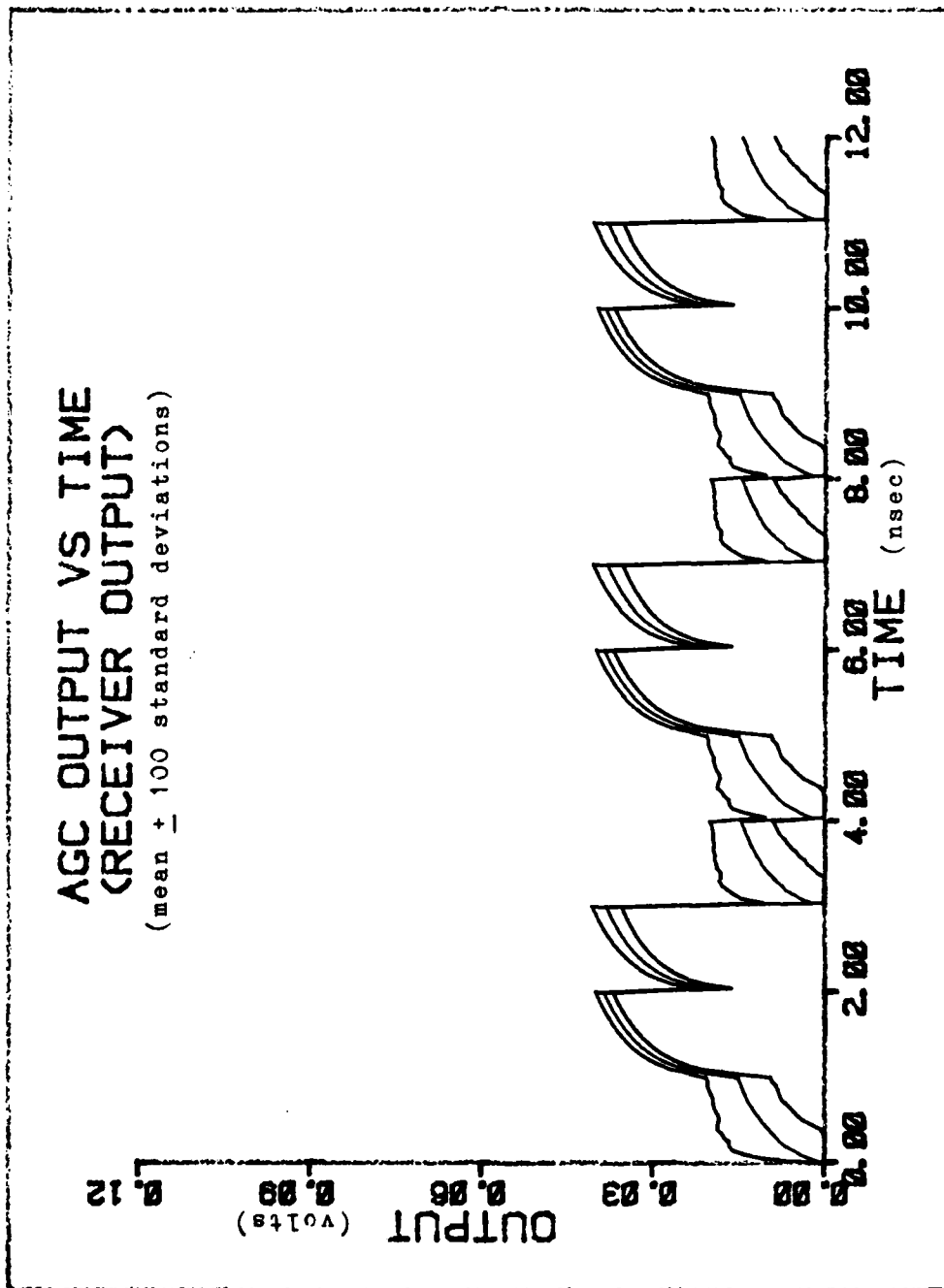


Figure A-2. IAGC Output with $G_o = 10 \times 10^5$

($A=125$ and $RC=0.01\text{nsec}$)

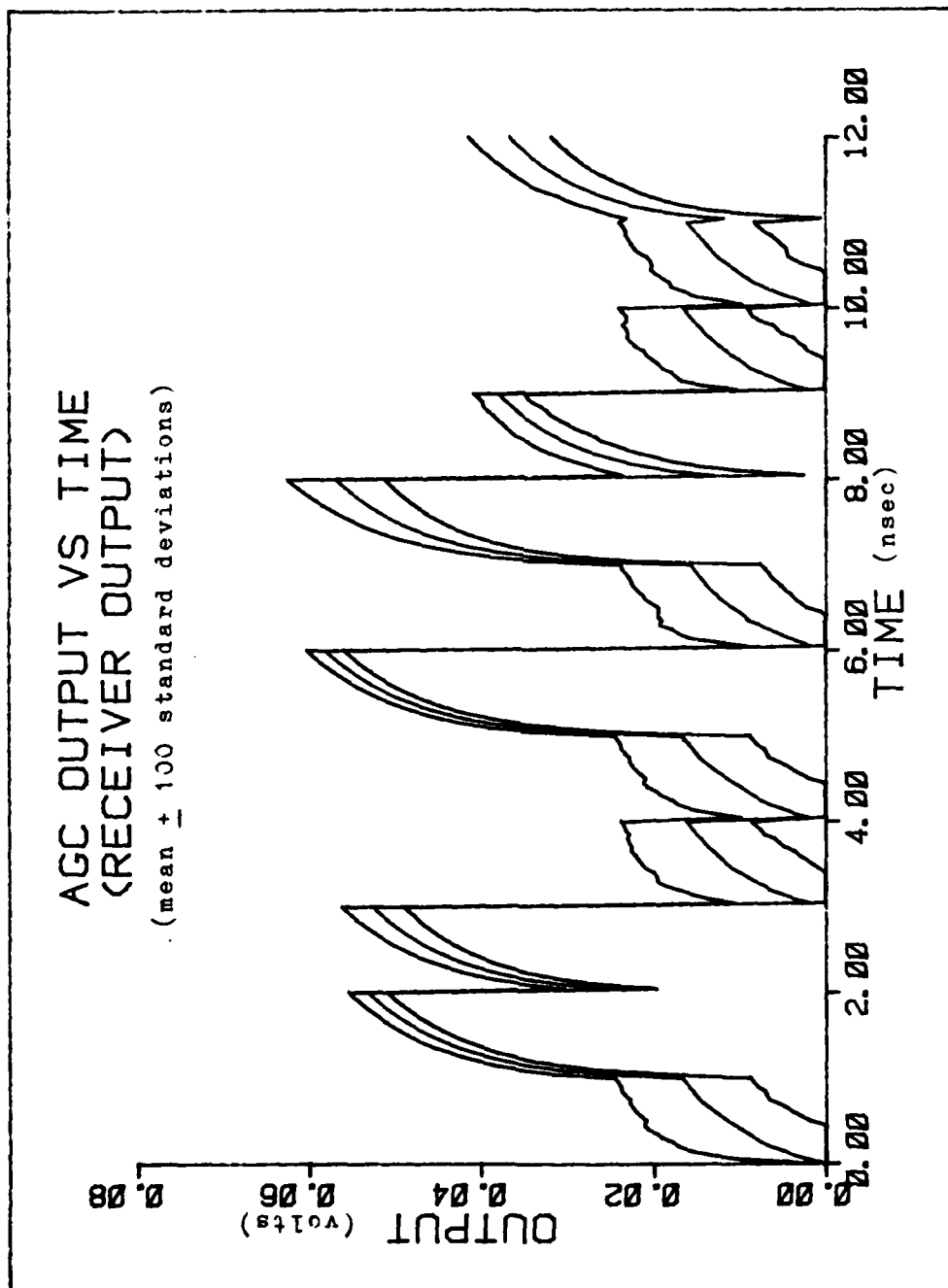


Figure A-3. IAGC with $A=75$

($G_0=6 \times 10^6$ and $RC=0.01 \text{ nsec}$)

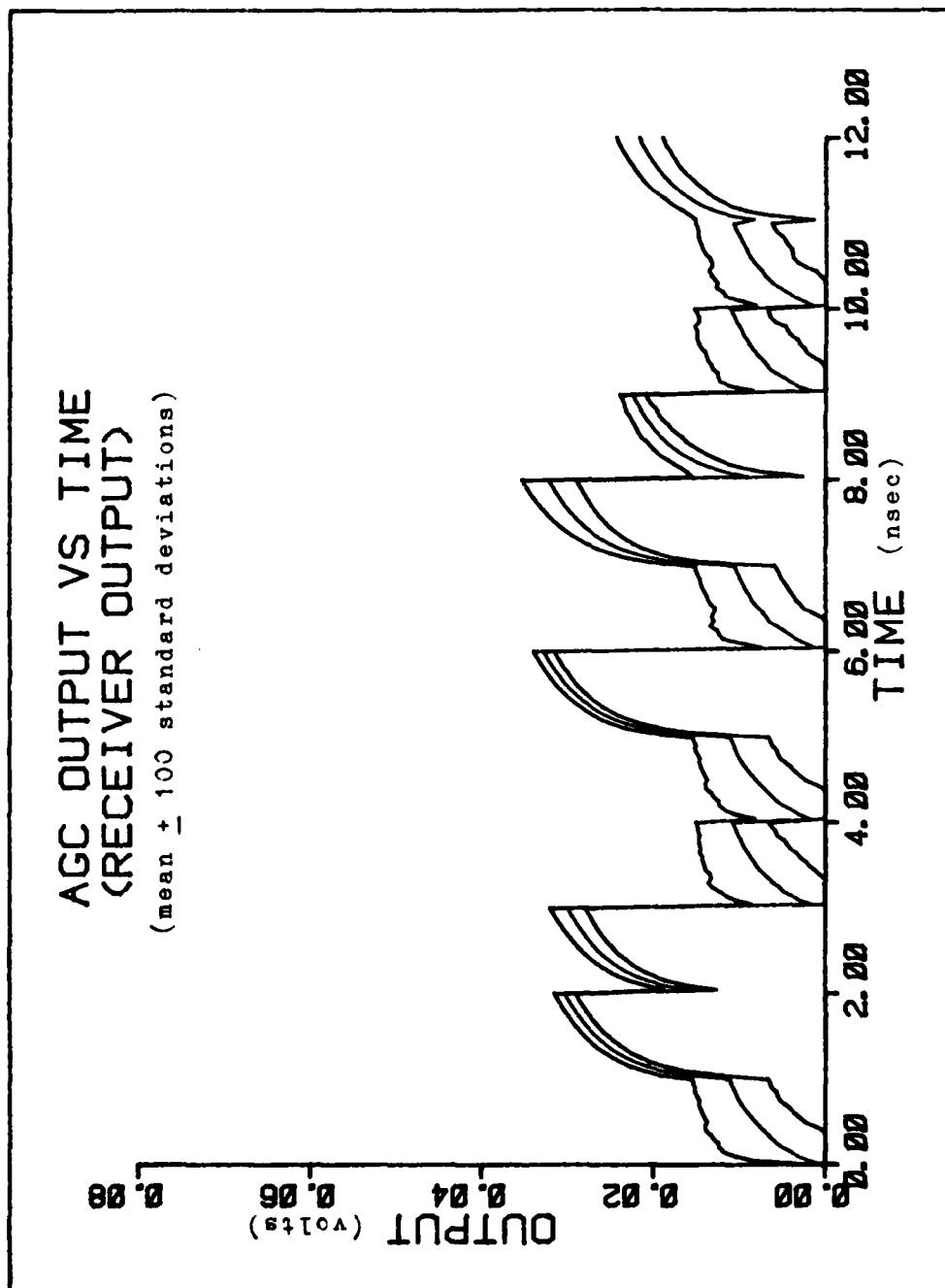


Figure A-4. IAGC Output with $A=150$
 $(G_o=6 \times 10^5 \text{ and } RC=0.01 \text{ nsec})$

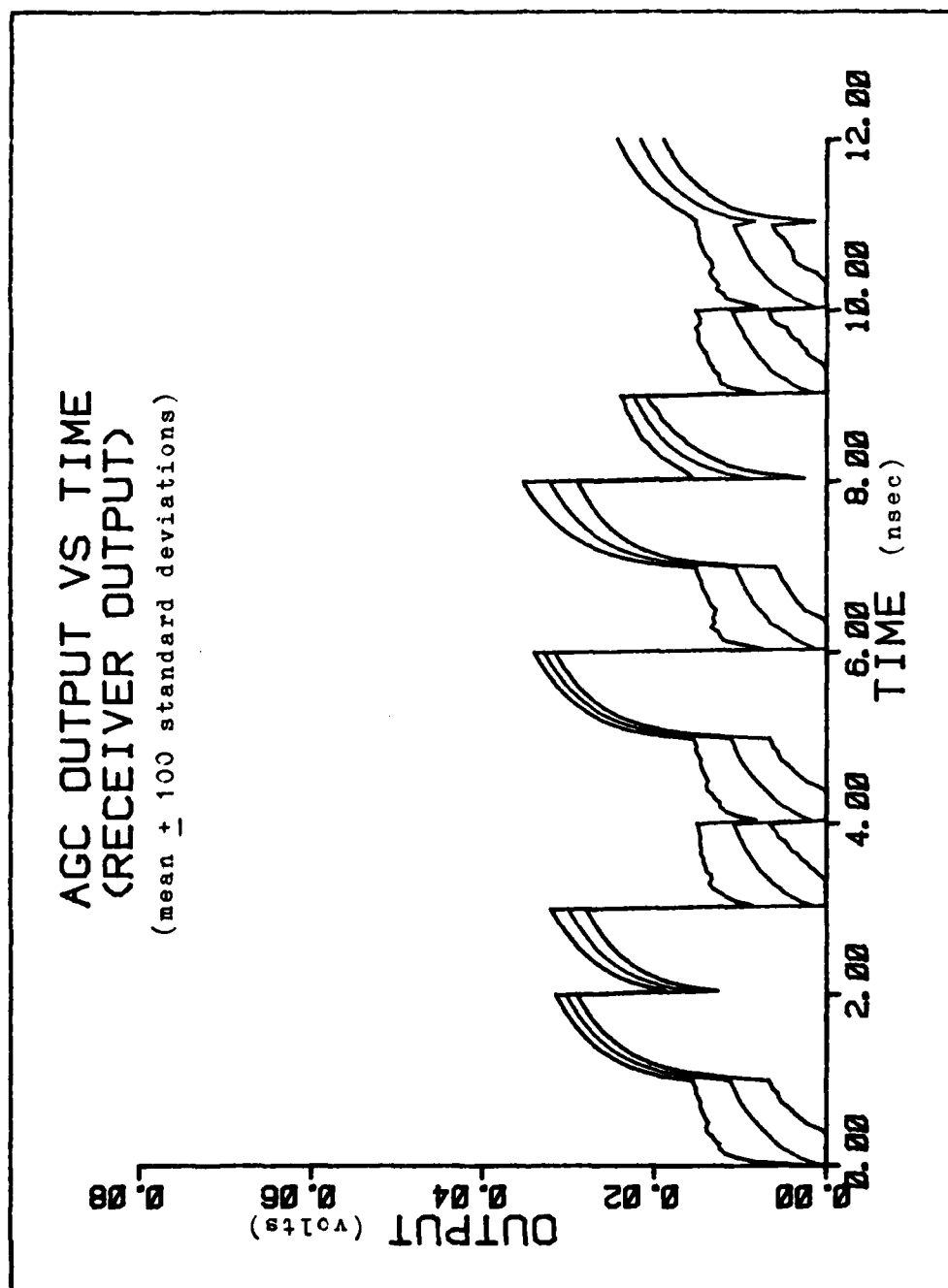


Figure A-4. IAGC Output with $A=150$
 $(G_0=6 \times 10^5 \text{ and } RC=0.01 \text{ nsec})$

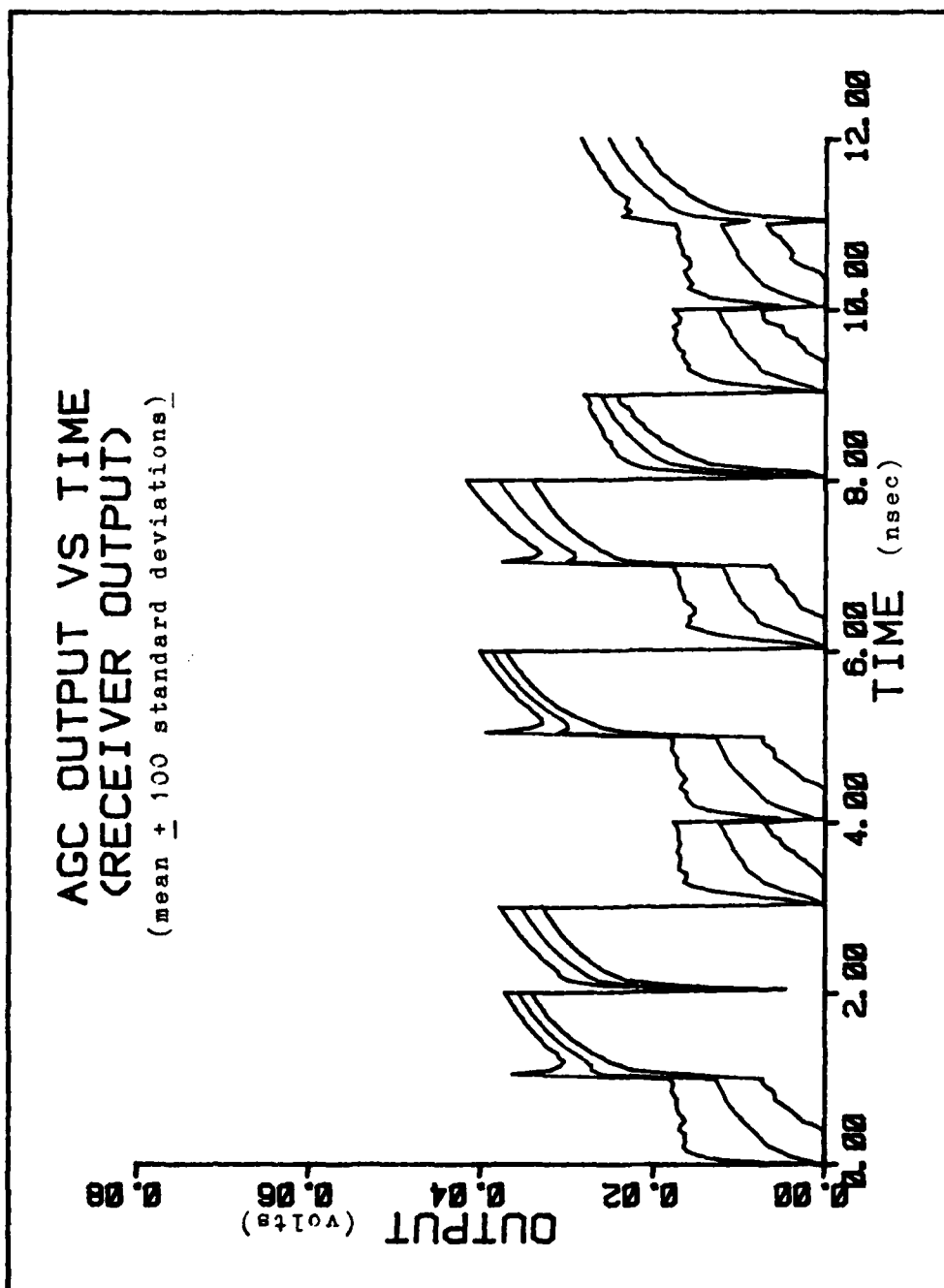


Figure A-5. IAGC Output with $RC=0.1\text{nsec}$

($G_0=6 \times 10^5$ and $A=125$)

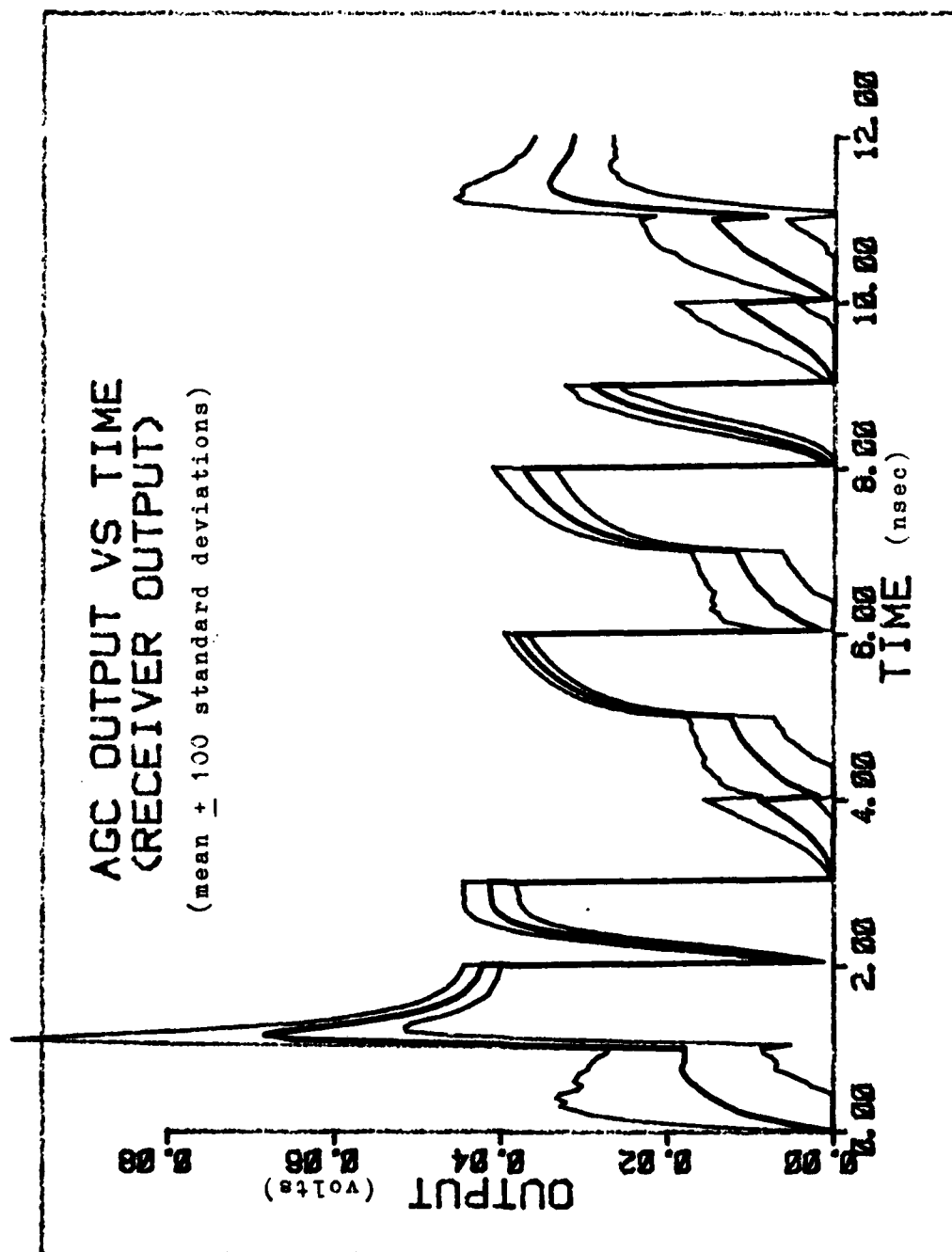


Figure A-6. IAGC Output with $RC=1.0\text{ nsec}$

($G_o=6 \times 10^5$ and $A=125$)

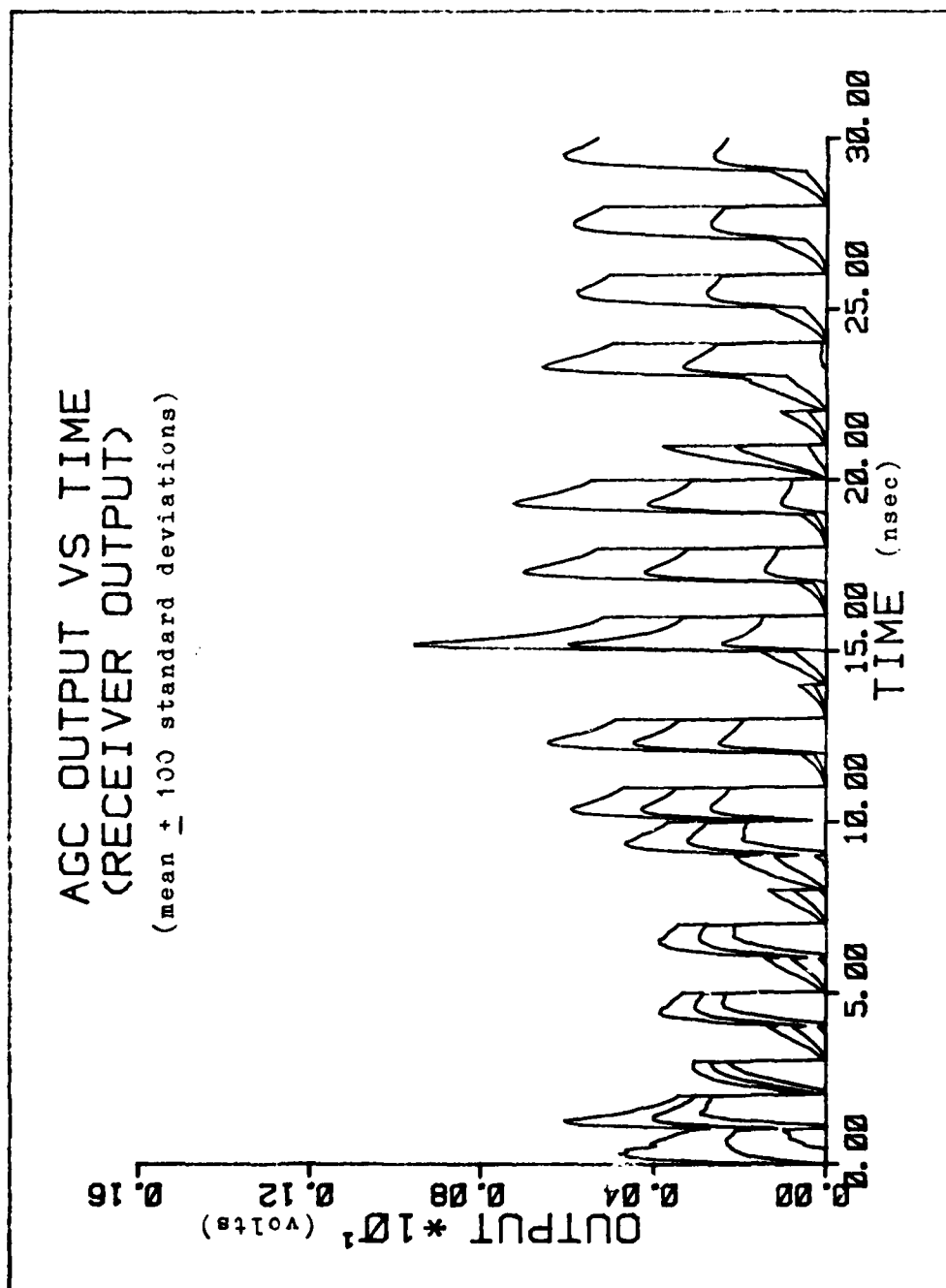


Figure A-7. AGC Output with: $G_o = 1 \times 10^5$

($A=2000$ and $RC=4.0\text{nsec}$)

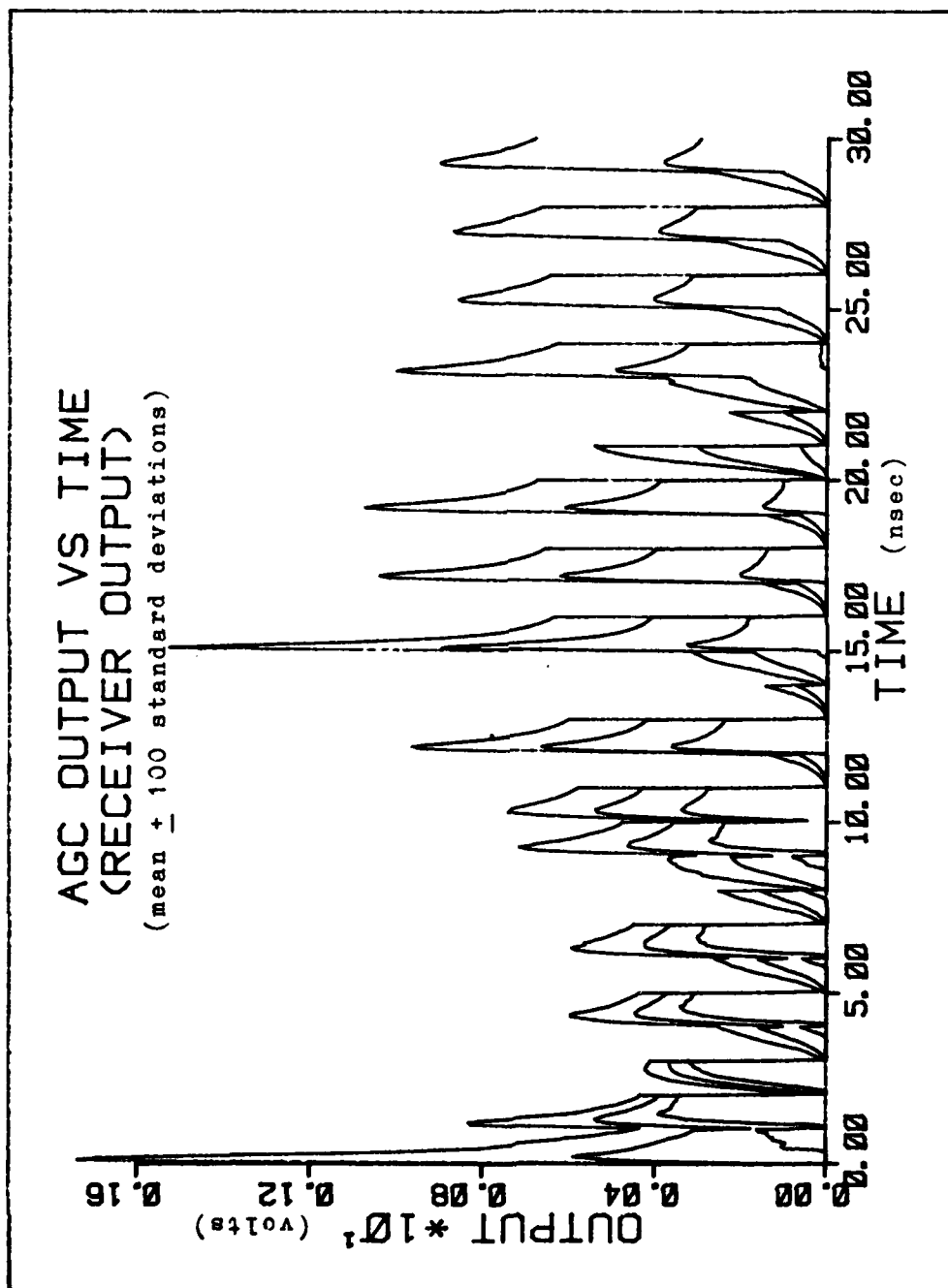


Figure A-8. AGC Output with $G_0 = 8 \times 10^5$
($A=2000$ and $RC=4.0\text{nsec}$)

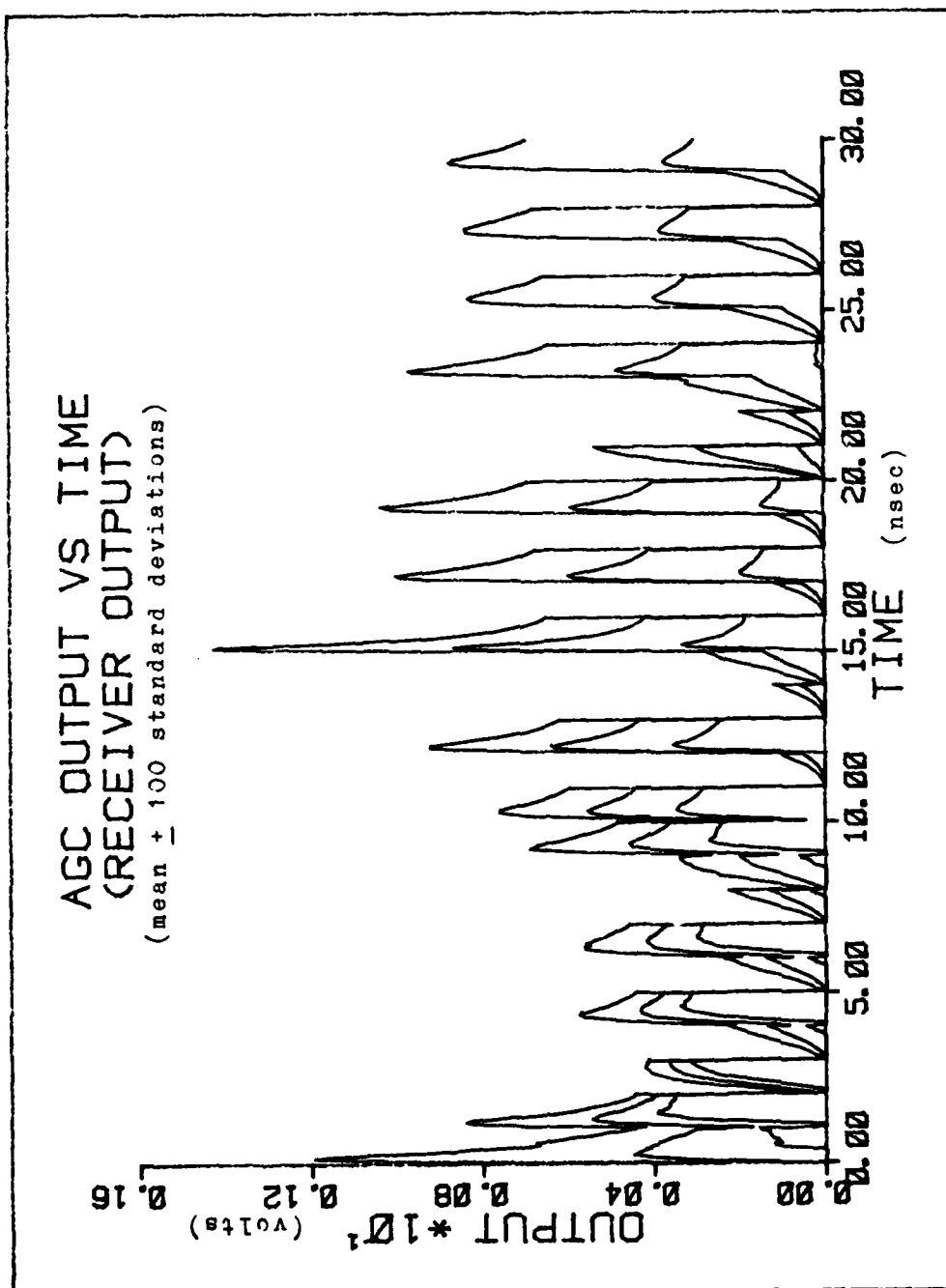


Figure A-9. AGC Output with $A=1800$

($G_0=4 \times 10^5$ and $RC=4.0 \text{ nsec}$)

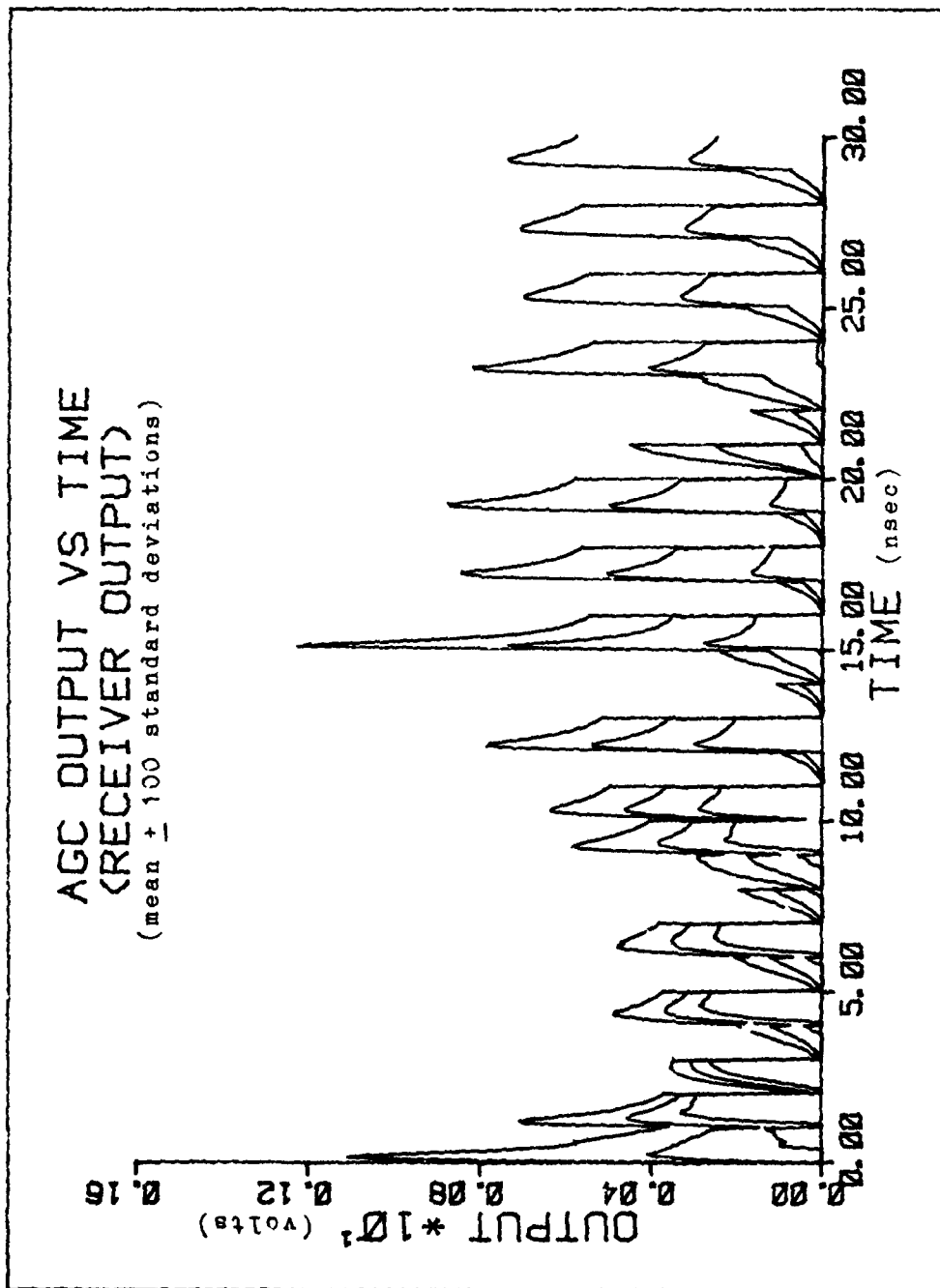


Figure A-10. AGC Output with $A=2200$

($G_0=4 \times 10^5$ and $RC=4.0 \text{ nsec}$)

AD-A124 696

IMPROVED SIGNAL CONTROL: AN ANALYSIS OF THE EFFECTS OF
AUTOMATIC GAIN CON..(U) AIR FORCE INST OF TECH
WRIGHT-PATTERSON AFB OH SCHOOL OF ENGI... K L FISHER
DEC 82 AFIT/GEO/EE/82D-3

2/2

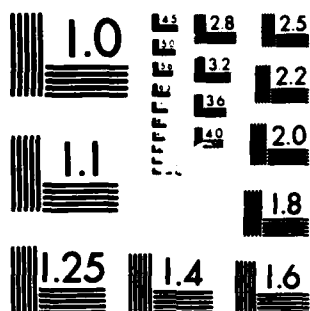
UNCLASSIFIED

F/G 17/2

NL



END
DATE
FILMED
DTIC



MICROCOPY RESOLUTION TEST CHART
NATIONAL BUREAU OF STANDARDS-1963-A

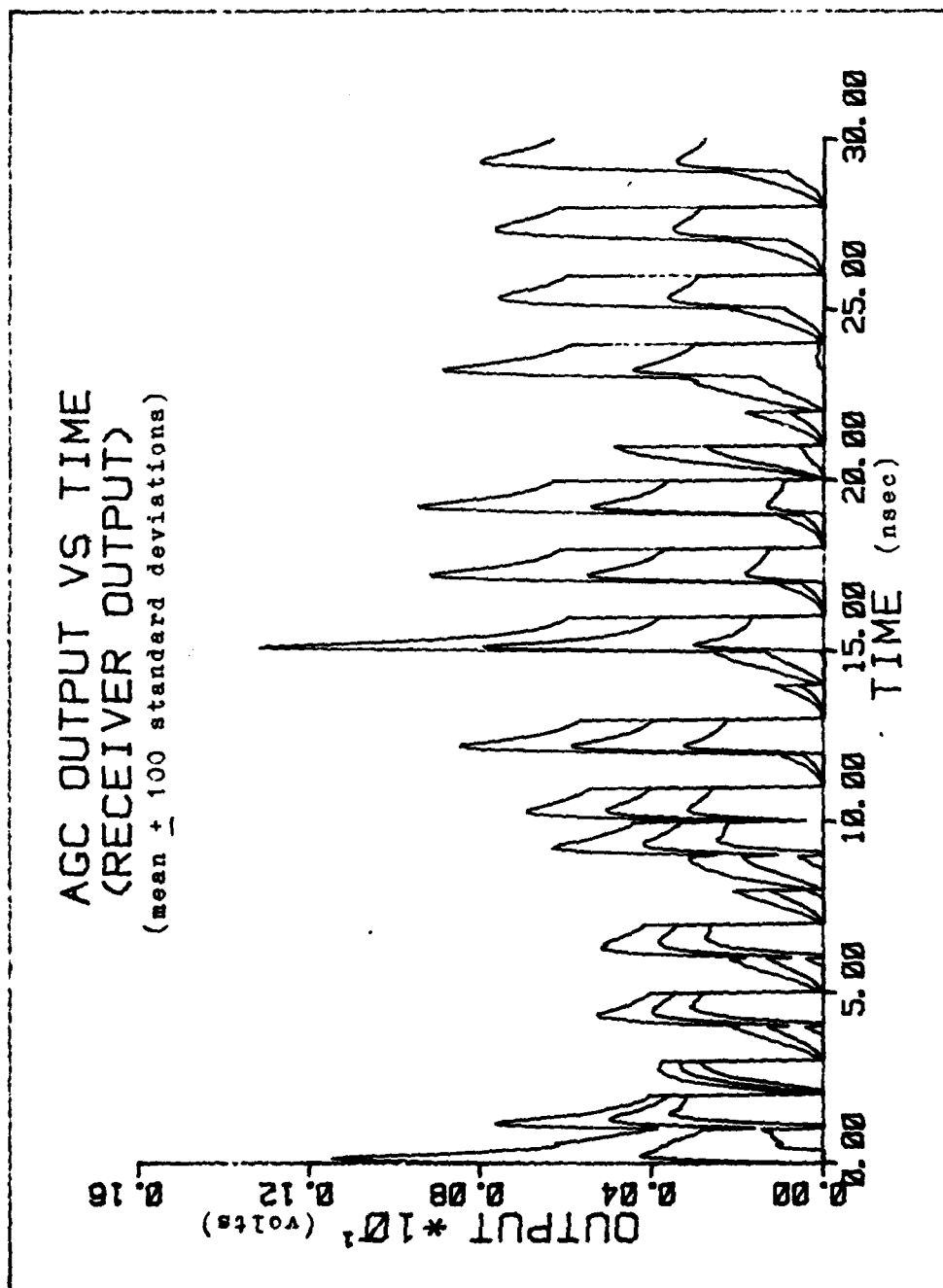


Figure A-11. AGC Output with $RC=2.0\text{nsec}$

($G_0=4 \times 10^5$ and $A=2000$)

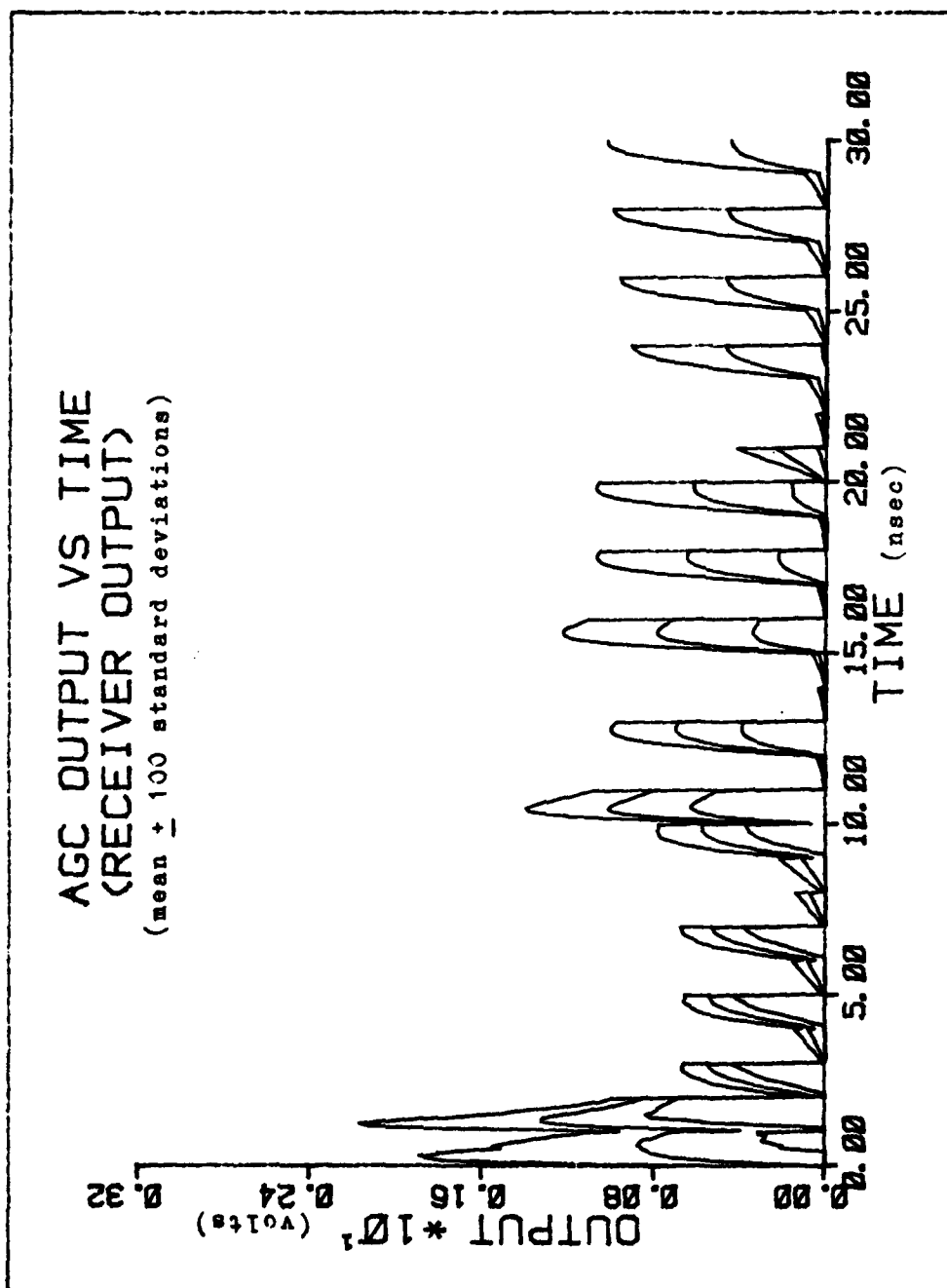


Figure A-12. AGC Output with $RC=8.0\text{nsec}$

($G_o=4 \times 10^5$ and $A=2000$)

Appendix B

Computer Program

This appendix contains the program which was used to generate the data for the plots and the tables provided in this report. The program is written in FORTRAN IV programming language and implemented on the CDC 6600 computer system. The uniform random number generator subroutine is not presented here. This routine was obtained from the IMSL library which was available at AFIT.

```

100=  PROGRAM DUAL(INPUT,OUTPUT,TAPE5=INPUT,TAPE6=INPUT,TAPE1,
110=  *TAPE2,TAPE3,TAPE4,TAPE7,TAPE8)
120=  DIMENSION X1(100),Y1(100),V1(100),T1(100),T2(100),R(2),XLAMDA(31)
130=  *,YT(100),XT(100),Y2(100),V2(100)
140=  DOUBLE PRECISION DSEED
150=  INTEGER COUNT1,COUNT2
160=C
170=C
180=C
190=C  *** INITIAL SEED FOR RANDOM NUMBER GENERATION ***
200=C
210=  DSEED=92751
220=C
230=C
240=C  *** NUMBER OF SIMULATIONS OF A GIVEN OPTICAL SIGNAL ***
250=C
260=  NRUN=100
270=C
280=C
290=C  *** INPUT OPTICAL SIGNAL GIVEN IN TERMS OF THE SIMULATION RATES **
300=C  *** THESE RATES WERE ARBITRARILY CHOSEN BY THE PROGRAMER ***
310=C
320=  XLAMDA(1)=0.0
330=  XLAMDA(2)=100.0
340=  XLAMDA(3)=100.0
350=  XLAMDA(4)=0.0
360=  XLAMDA(5)=100.0
370=  XLAMDA(6)=0.0
380=  XLAMDA(7)=100.0
390=  XLAMDA(8)=0.0
400=  XLAMDA(9)=0.0
410=  XLAMDA(10)=100.0
420=  XLAMDA(11)=800.0
430=  XLAMDA(12)=0.0
440=  XLAMDA(13)=800.0
450=  XLAMDA(14)=0.0
460=  XLAMDA(15)=0.0
470=  XLAMDA(16)=800.0
480=  XLAMDA(17)=0.0
490=  XLAMDA(18)=800.0
500=  XLAMDA(19)=0.0
510=  XLAMDA(20)=800.0
520=  XLAMDA(21)=200.0
530=  XLAMDA(22)=0.0
540=  XLAMDA(23)=0.0
550=  XLAMDA(24)=200.0
560=  XLAMDA(25)=0.0
570=  XLAMDA(26)=200.0
580=  XLAMDA(27)=0.0
590=  XLAMDA(28)=200.0
600=  XLAMDA(29)=0.0
610=  XLAMDA(30)=200.0

```



```

630=C      *** SIMULATION RATE OF THE THERMALLY EMITTED ELECTRONS ***
640=C
650=      DARK=10.0
660=C
670=C
680=C
690=C      *** (Q/C)*M = CONST1 - WEIGHTING FACTOR FOR THE COUNTING PROCESS
700=C      TO PRODUCE AN ACCURATE REPRESENTATION OF THE DETECTOR ***
710=C
720=      CONST1=1.0E-8
730=C
740=C
750=C
760=C
770=C      *****
780=C      *** AGC PARAMETERS ***
790=C      *****
800=C
810=C      *** AGC PARAMETERS FOR THE FIRST AGC (IAGC) ***
820=C
830=      RC=0.01
840=      G=600000.0
850=      A=125.0
860=C
870=C
880=C      *** AGC PARAMETERS FOR THE SECOND AGC (COMMON AGC) ***
890=C
900=      RC2=10.0
910=      A2=0.5
920=      G2=3200.0
930=C
940=C
950=C
960=C
970=C
980=C      *****
990=C      *** TIME PARAMETERS (UNITS ARE RELATED TO THE BAUD RATE) ***
1000=C      *****
1010=C
1020=C
1030=C      *** PERIOD OF THE SWITCH (CLOCKING PERIOD) ***
1040=C      *** THIS PERIOD = 1/2 THE BIT PERIOD ***
1050=C
1060=      PERIOD=1.0
1070=C
1080=C      *** COMPUTER SAMPLING INTERVAL ***
1090=C
1100=      DELTA=0.001
1110=C
1120=C
1130=C      *** NUMBER OF CLOCK PERIODS TO SIMULATED ***
1140=C
1150=      NPER=4

```

..

```

1170=C
1180=C *** NUMBER OF SAMPLES PER CLOCK PERIOD ***
1190=C
1200= NSAMP=INT((PERIOD+0.0000001)/DELTA)
1210=C
1220=C
1230=C *** THE J-TH SAMPLE AT WHICH THE STASTICS ARE COMPUTED ***
1240=C
1250= JSAMP=50
1260=C
1270=C
1280=C *** THE BIT PERIOD AT WHICH PROB(ERROR) IS COMPUTED ***
1290=C
1300=C CLOCK PERIOD FOR THE FIRST HALF OF THE BIT PERIOD
1310= NPER1=5
1320=C CLOCK PERIOD FOR THE SECOND HALF OF THE BIT PERIOD
1330= NPER2=6
1340=C
1350=C
1360=C
1370=C
1380=C
1390=C *****
1400=C *** INITIALIZE PARAMETERS ***
1410=C *****
1420=C
1430=C
1440= DO 10 K=1,NRUN
1450= T1(K)=0.0
1460= T2(K)=0.0
1470= X1(K)=0.0
1480= V2(K)=0.0
1490= V1(K)=0.0
1500=10 CONTINUE
1510=C
1520=C
1530=C
1540=C
1550=C *** BEGIN SIMULATION ***
1560=C
1570= DO 400 I=1,NPER
1580=C
1590=C
1600= JTH=1
1610= COUNT1=0
1620= COUNT2=0
1630=C
1640=C
1650=C *** SIMULATE ONE CLOCK PERIOD ***
1660=C
1670= DO 300 J=1,NSAMP
1680=C
1690= TIME=DELTA*FLOAT(J)

```

..

```

1710=C      *** COMPUTE THE DETECTOR VOLTAGE, AGC OUTPUT VOLTAGE, AGC
1720=C      CONTROL VOLTAGE FOR EACH RUN ***
1730=C
1740=C      DO 100 K=1, NRUN
1750=C
1760=C
1770=C      *****
1780=C      *** GENERATION OF A COUNTING PROCESS TO SIMULATE AN IDEAL DETECTOR
1790=C      *****
1800=C
1810=C      IF (XLAMDA(I).EQ.0.0) GOTO 30
1820=C      COUNT1=0
1830=C
1840=C      T1(K) IS THE TIME AT WHICH M ELECTRONS ARE EMITTED FROM THE
1850=C      IDEAL PHOTODECTOR AS A RESULT OF THE INCIDENT OPTICAL SIGNAL
1860=C
1870=C      IF(T1(K).GT.TIME) GOTO 30
1880=C      GGUBS - IMSL UNIFORM NUMBER GENERATOR SUBROUTINE
1890=C      CALL GGUBS(DSEED,2,R)
1900=C      GENERATE A NEW SEED
1910=C      DSEED=R(2)*123457.0
1920=C
1930=C      CONVERT UNIFORM NUMBER INTO A EXPONENTIAL RANDOM NUMBER
1940=C      TAU1=-ALOG(R(1))/XLAMDA(I)
1950=C      INCREMENT COUNT; ONE COUNT IS EQUIVALENT TO M PHOTON TO
1960=C      ELECTRON CONVERSIONS
1970=C      COUNT1=COUNT1+1
1980=C      TIME AT WHICH M PHOTON TO ELECTRON CONVERSIONS OCCUR
1990=C      T1(K)=T1(K)+TAU1
2000=C      GOTO 20
2010=C      CONTINUE
2020=C      INITIALLY ONE COUNT TO MANY IS GENERATED
2030=C      IF((J.EQ.1).AND.(COUNT1.NE.0)) COUNT1=COUNT1-1
2040=C
2050=C      *****
2060=C      *** GENERATION OF COUNTING PROCESS TO ADD DARK CURRENT EFFECTS ***
2070=C      *****
2080=C
2090=C
2100=C      THESE PARAMETERS ARE SIMILAR TO THOSE DESCRIBED IN THE
2110=C      IDEAL SIMULATION
2120=C
2130=C      IF(DARK.EQ.0.0) GOTO 50
2140=C      COUNT2=0
2150=C      IF(T2(K).GT.TIME) GOTO 50
2160=C      CALL GGUBS(DSEED,2,R)
2170=C      DSEED=R(2)*123457.0
2180=C      TAU2=-ALOG(R(1))/DARK
2190=C      COUNT2=COUNT2+1
2200=C      T2(K)=T2(K)+TAU2
2210=C      GO TO 40
2220=C      CONTINUE
2230=C      IF((J.EQ.1).AND.(COUNT2.NE.0)) COUNT2=COUNT2-1

```

..

```

2240=C *****
2250=C *** PHOTODETECTOR SIMULATION ***
2260=C *****
2270=C
2280= X1(K)=CONST1*FLOAT(COUNT1+COUNT2)+X1(K)
2290=C
2300=C
2310=C
2320=C *****
2330=C *** DUAL AGC SIMULATION ***
2340=C *****
2350=C
2360=C
2370=C IAGC OUTPUT VOLTAGE
2380= Y1(K)=X1(K)*G*EXP(-(A*V1(K)))
2390=C IAGC CONTROL VOLTAGE
2400= V1(K)=(Y1(K)-V1(K))*DELTA/RC+V1(K)
2410=C AGC OUTPUT VOLTAGE
2420= Y2(K)=Y1(K)*G2*EXP(-(A2*V2(K)))
2430=C AGC CONTROL VOLTAGE
2440= V2(K)=(Y2(K)-V2(K))*DELTA/RC2+V2(K)
2450=100 CONTINUE
2460=C
2480=C
2490=C
2500=C
2510=C *****
2520=C *** COMPUTE STATISTICS ***
2530=C *****
2540=C
2550=C
2560=C CALCULATE STATISTICS FOR EVERY J-TH SAMPLE
2570=C
2580= IF(JTH.NE.JSAMP) GOTO 200
2590= JTH=0
2600= SUM1=0.0
2610= SUM2=0.0
2620= SUM3=0.0
2630= SUM4=0.0
2640= SUM5=0.0
2650= SUM6=0.0
2660=C
2670=C
2690=C
2700=C *** COMPUTE MEAN ***
2710=C
2720= DO 60 K=1,NRUN
2730= SUM1=SUM1+X1(K)
2740= SUM2=SUM2+Y2(K)
2750=60 CONTINUE
2760=C
2770= XMN=SUM1/FLOAT(NRUN)
2780= YMN=SUM2/FLOAT(NRUN)

```

```

2800=C      *** COMPUTE VARIANCE ***
2810=C
2820=      DO 70 K=1,NRUN
2830=      SUM3=SUM3+(XMN-X1(K))**2
2840=      SUM4=SUM4+(YMN-Y1(K))**2
2850=70     CONTINUE
2860=C
2870=      XVAR=SUM3/FLOAT(NRUN)
2880=      YVAR=SUM4/FLOAT(NRUN)
2890=C
2900=C
2910=C
2920=C
2930=C      *** COMPUTE SIGNAL TO NOISE RATIOS ***
2940=C
2950=      SNRX=XMN**2/XVAR
2960=      SNRY=YMN**2/YVAR
2970=C
2980=C
2990=C
3000=C      *** IMPROVEMENT FACTOR ***
3010=C
3020=      IMP=SNRY/SNRX
3030=C
3040=C
3050=C
3060=C
3070=C
3080=C      *** WRITE ONTO TAPE NEEDED DATA ***
3090=C
3100=      WRITE(1,*) XMN,XVAR
3110=      WRITE(7,*) YMN,YVAR
3120=C
3130=C
3140=200    CONTINUE
3150=C
3160=      IF(JSAMP.GT.1) JTH=JTH+1
3170=C
3180=C
3190=300    CONTINUE
3200=C
3210=C      *****
3220=C      *** COMPUTE THE PROBABILITY OF ERROR ***
3230=C      *****
3240=C
3250=C
3260=C
3270=C
3280=C
3290=      IF(NPER.NE.NPER1) GOTO 72
3300=      DO 71 JK=1,NRUN
3310=      XT(JK)=X1(JK)
3320=      YT(JK)=Y2(JK)
3330=71     CONTINUE
3340=C
3350=72     CONTINUE

```

..

```

3390=C      *** THIS ROUTINE WILL ONLY COMPUTE THE PR(ERROR)
3400=C      FOR A BINARY "ONE" ***
3410=C
3420=      IF(NPER.NE.NPER2) GOTO 75
3430=      SUM1=0.0
3440=      SUM2=0.0
3450=      SUM3=0.0
3460=      SUM4=0.0
3470=C
3480=C
3490=      DO 74 JK=1,NRUN
3500=      IF(X1(JK).GT.XT(JK)) SUM1=SUM1+1.0
3510=      IF(X1(JK).EQ.XT(JK)) SUM2=SUM2+0.5
3520=      IF(Y2(JK).GT.YT(JK)) SUM3=SUM3+1.0
3530=      IF(Y2(JK).EQ.YT(JK)) SUM4=SUM4+0.5
3540=74     CONTINUE
3560=C
3570=C
3580=C      COMPUTE A PROBABILITY OF ERROR FOR THE INPUT
3590=      PRX=(SUM1+SUM2)/FLOAT(NRUN)
3600=C
3610=C      COMPUTE A PROBABILITY OF ERROR FOR THE OUTPUT
3620=      PRY=(SUM3+SUM4)/FLOAT(NRUN)
3630=C
3650=C
3660=C
3670=C      COMPUTE THE VARIANCE OF THE INPUT PR(ERROR)
3680=      PRXVAR=(SUM1*(1.0-PRX)**2+SUM2*(0.5-PRX)**2)/FLOAT(NRUN)
3690=      PRXVAR=PRXVAR+(1.0-PRX)*PRX**2
3700=C
3710=C      COMPUTE THE VARIANCE OF THE OUTPUT PR(ERROR)
3720=      PRYVAR=(SUM3*(1.0-PRY)**2+SUM4*(0.5-PRY)**2)/FLOAT(NRUN)
3730=      PRYVAR=PRYVAR+(1.0-PRY)*PRY**2
3740=C
3750=C
3760=75     CONTINUE
3770=C
3790=C
3800=C
3810=C      *** RE-INITIALIZE PARAMETERS ***
3820=C
3830=      DO 80 K=1,NRUN
3840=      X1(K)=0.0
3850=      T1(K)=0.0
3860=      T2(K)=0.0
3870=80     CONTINUE
3880=C
3890=C
3900=400    CONTINUE
3910=C
3950=      STOP
3960=      END
3970=*EOR

```

..

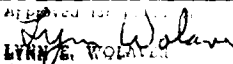
VITA

Kirk Lee Fisher was born 8 December 1959 in New Columbia, Pennsylvania. He graduated from High School in 1977 and attended the Pennsylvania State University from which he received a Bachelor of Science in Electrical Engineering in May 1981. During the first two years he attended the Hazelton Branch Campus and upon entering University Park Campus he accepted a scholarship through the Air Force Reserve Officer Training Corps. In June of 1981 he entered the School of Engineering at the Air Force Institute of Technology to obtain a Master's of Science. He is a member Eta Kappa Nu, Tau Beta Pi and Institute of Electrical and Electronics Engineers.

Permanent Address: Box 393 RD # 1
New Columbia, Pennsylvania
17856

UNCLASSIFIED

SECURITY CLASSIFICATION OF THIS PAGE (When Data Entered)

REPORT DOCUMENTATION PAGE		READ INSTRUCTIONS BEFORE COMPLETING FORM
1. REPORT NUMBER AFIT/GEO/EE/82D-3	2. GOVT ACCESSION NO. AD-A124696	3. RECIPIENT'S CATALOG NUMBER
4. TITLE (and Subtitle) IMPROVED SIGNAL CONTROL: AN ANALYSIS OF THE EFFECTS OF AUTOMATIC GAIN CONTROL FOR OPTICAL SIGNAL DETECTION		5. TYPE OF REPORT & PERIOD COVERED MS Thesis
7. AUTHOR(s) Mark L. Fisher		6. PERFORMING ORG. REPORT NUMBER
9. PERFORMING ORGANIZATION NAME AND ADDRESS Air Force Institute of Technology (AFIT-EN) Wright-Patterson AFB, Ohio 45433		8. CONTRACT OR GRANT NUMBER(s)
11. CONTROLLING OFFICE NAME AND ADDRESS		10. PROGRAM ELEMENT, PROJECT, TASK AREA & WORK UNIT NUMBERS
14. MONITORING AGENCY NAME & ADDRESS (if different from Controlling Office)		12. REPORT DATE Dec, 1982
		13. NUMBER OF PAGES 93
		15. SECURITY CLASS. (of this report) UNCLASSIFIED
		15a. DECLASSIFICATION/DOWNGRADING SCHEDULE
16. DISTRIBUTION STATEMENT (of this Report) Approved for public release; distribution unlimited		
17. DISTRIBUTION STATEMENT (of the abstract entered in Block 20, if different from Report)		
18. SUPPLEMENTARY NOTES <div style="text-align: right;">  LYNN E. WOLAN Dean for Research and Professional Development Air Force Institute of Technology (AFIT) Wright-Patterson AFB OH 45433 </div> <div style="text-align: right; font-size: 1.5em;">4 JAN 1983</div>		
19. KEY WORDS (Continue on reverse side if necessary and identify by block number) Automatic Gain Control Optical Communication Signal Detection Fiber Optics		
20. ABSTRACT (Continue on reverse side if necessary and identify by block number) <p>This paper is to analyze the effects of an automatic gain control (AGC) in an optical receiver system. The intent of using an AGC is to improve the performance of the receiver.</p> <p>The received signal is Manchester encoded and contains fluctuations caused by transmission attenuation. In the conversion from an optical signal to an electrical signal, the photodetector produces shot noise. The purpose of the AGC</p>		

DD FORM 1473 EDITION OF 1 NOV 65 IS OBSOLETE

UNCLASSIFIED

SECURITY CLASSIFICATION OF THIS PAGE (When Data Entered)

UNCLASSIFIED

SECURITY CLASSIFICATION OF THIS PAGE(When Data Entered)

will be to amplify the photodetector signal, control signal fluctuations, reduce shot noise, and improve detection accuracy.

Using this criteria, the effects of the AGC in the receiver was examined. But because of the non-linearities associated with an AGC, an analytical analysis can not be conducted. Therefore, the receiver was simulated on the computer. This paper describes the models and algorithms used to analyze the receiver. Through the simulations, the receiver's performance with an AGC is compared to the performance without an AGC.

Because of the limited time for the analysis, only three specific AGC's were examined. The first AGC studied is classified as an instantaneous AGC (IAGC) followed by an analysis of a common AGC. The final AGC to be investigated is a dual AGC which is an AGC cascaded to an IAGC.

UNCLASSIFIED

SECURITY CLASSIFICATION OF THIS PAGE(When Data Entered)

nal
ac-

the
ies
con-
com-
l to
er's
hout

hree
las-
ysis
dual

END

DATE
FILMED

3-83

DTIC

(Date Entered)